

Pseudo-local Dirac Observables in Effective Theories of Quantum Gravity

Diploma thesis by
Alexander Schenkel

Supervised by PD Dr. Thorsten Ohl



Institut für Theoretische Physik und Astrophysik,
Universität Würzburg, D-97074 Würzburg, Germany

May 21, 2008

Zusammenfassung

In unserer Arbeit haben wir einen Ansatz von Giddings *et al.* [1] aufgegriffen, um Observablen in effektiven Quantengravitationstheorien zu definieren und zu untersuchen. In der oben genannten Arbeit wurde gezeigt, dass die lokalen Observablen der Feldtheorie keine sinnvollen Größen in Quantengravitationstheorien sind, man aber durch Integration über die gesamte Raumzeit sinnvolle Observablen konstruieren kann. Diese integrierten Observablen sind zwar invariant unter den Eichsymmetrien der Gravitation, d.h. den lokalen Koordinatentransformationen, aber sie sind offensichtlich nicht lokal.

Der zweite Schritt ist es nun, geeignete Variablen des Systems als Uhr- und Maßstabvariablen zu verwenden, um relativ zu ihnen Lokalität beschreiben zu können. Diese Variablen müssen ebenfalls in geeigneten Zuständen vorliegen, damit man sie zur Lokalisierung verwenden kann. Durch diesen Begriff der relationalen Lokalität erkennt man, dass die Lokalisierung von Observablen ein dynamisches Problem darstellt, und somit unverweigerlich über die Gravitationswechselwirkung auf die Geometrie zurückwirkt. Je präziser wir die Observablen auf der Raumzeit auflösen möchten, desto höhere Energien sind notwendig, und desto mehr Rückwirkung entsteht.

Wir werden in dieser Arbeit im Rahmen der perturbativen Quantengravitation die Rückwirkung der dynamischen Lokalisierung auf die Geometrie untersuchen. Diese Theorien liefern eine intrinsische Grenze an die Lokalität, welche durch den Zusammenbruch der Störungsreihe gegeben ist. Diese Untersuchungen geben zwar keine Auskunft über die Lokalisierung in nichtperturbativen Quantengravitationstheorien, sie geben jedoch Aufschlüsse über die sogenannte semiklassische Lokalität. Doch genau diese semiklassische Interpretation der Lokalität über eine fixierte Hintergrundgeometrie ist zur Zeit notwendig, da die meisten Hochenergieexperimente Streuexperimente sind, für deren Interpretation durch heutige Theorien man noch einen fixierten Hintergrund benötigt. Somit ist die semiklassische Lokalität auch die Grenze, bis zu welcher wir heute die lokale Physik verstehen können.

Wir werden im folgenden zuerst kurz in die Grundlagen der effektiven Quantengravitation und deren Beschreibung auf fixierten Hintergründen eingehen. Es werden die Konzepte von relationalen Dirac-Observablen und den damit zusammenhängenden Uhr- und Maßstabvariablen eingeführt. Danach werden wir zwei explizite quantenfeldtheoretische Modelle untersuchen, welche solche integrierten Observablen beinhalten, die in geeigneten lokalisierten Wellenpaket-Zuständen von skalaren Uhr- und Maßstabvariablen dynamisch lokalisiert werden können. Diese Observablen werden als pseudo-lokal bezeichnet, da sie aus nichtlokalen Operatoren unter der Anwendung geeigneter lokalisierter Zustände entspringen. Es werden die Grenzen der Lokalisierung mithilfe dieser beiden Modelle untersucht und diese miteinander verglichen.

Am Ende widmen wir uns der Frage, welche Effekte stärker den Zusammenbruch der perturbativen Quantengravitation beeinflussen, die klassischen oder die quantentheoretischen Geometrieeffekte. Hierzu werden wir die pseudo-lokale Selbstgravitation zweier sich kreuzender skalarer Wellenpakete sowohl klassisch als auch quantenfeldtheoretisch bestimmen und miteinander vergleichen.

Contents

1	Introduction	1
2	Physical and mathematical basics	4
2.1	Notation and conventions	4
2.2	Riemannian geometry	5
2.3	Basics in cohomology	5
2.4	Classical dynamical systems	6
2.5	Constrained systems and BRST formalism	7
2.6	Canonical quantization	9
2.6.1	Generalities	9
2.6.2	Fock representation	10
2.6.3	Quantum BRST formalism	11
2.7	LSZ formalism for in-out matrix elements	12
2.8	Schwinger-Keldysh formalism for in-in matrix elements	13
3	Effective theory of quantum general relativity (QGR)	15
3.1	QGR as low-energy effective theory	15
3.2	Pseudo-local observables in QGR from clock and rod variables	16
3.3	QGR with fixed background	17
3.4	Gauge transformations with fixed background	18
3.5	Graviton expansion of geometric quantities and the Einstein-Hilbert action	20
3.6	Dynamical localization of pseudo-local operators on semiclassical fixed backgrounds	21
4	Canonical BRST formulation of linearized QGR on a flat background	22
4.1	Hamiltonian and constraint algebra	22
4.2	Algebraically generated gauge transformations	23
4.3	BRST charge and minimal BRST invariant Hamiltonian	24
4.4	Exact functionals for extending the Hamiltonian	24
4.5	Equations of motion and gauge fixing conditions	25
4.6	Canonical transformation to suitable ghost variables	26
4.7	Covariant expression of the BRST charge	27
4.8	Auxiliary Fock space representation	28
4.9	Graviton propagator in harmonic gauge	29
4.10	Cohomology of the one graviton subspace	29
4.11	Structure of the physical multi-graviton space	31
4.12	Equivalence to Gupta-Bleuler method	33
5	Pseudo-local matter observables with matter clocks and rods	34
5.1	Definition of the theory and observables	34
5.2	Feynman rules	36
5.3	Tree-level localization	38
5.4	One loop corrections and counterterms	39

5.5	Bremsstrahlung corrections	42
5.6	Effective vertices	44
5.7	On-shell Ward identity	45
5.8	Results and interpretation	47
5.8.1	IR cutoff independence of the results	47
5.8.2	Relative NLO contributions for S -type localization	47
5.8.3	Relative NLO contributions for T -type localization	50
5.8.4	Physical implications to the problem of dynamical localization	52
6	Pseudo-local Yang-Mills observables with matter clocks and rods	54
6.1	Definition of the theory and observables	54
6.2	Feynman rules	57
6.3	One loop corrections and counterterms	58
6.4	Graviton and Yang-Mills Bremsstrahlung	60
6.5	Effective vertices	60
6.6	Results and comparison to the pure scalar model	63
6.6.1	IR cutoff independence of the results	63
6.6.2	Relative NLO contributions for S -type localization	64
6.6.3	Relative NLO contributions for T -type localization	66
6.6.4	Implications to localization and comparison to the pure scalar model	68
7	Pseudo-local geometry observables with matter clocks and rods	69
7.1	Definition of the pseudo-local curvature observable	69
7.2	Classical computation	70
7.3	Quantum computation	71
7.4	Comparison between the quantum and classical results and outlook	73
8	Conclusions	75
A	General gauge fixed BRST invariant equations of motion	77
B	BRST invariant states for effective quantum gravity coupled to classical matter	79
C	Renormalization of graviton induced tadpoles	82
D	Colored processes, gluon Bremsstrahlung and IR finiteness in Yang-Mills theory	84
E	Localized wave packet states	87
E.1	Gaussian wave packets	87
E.2	Scattering of wave packets	89
F	Implementation of gravitons in FeynArts and FormCalc	91

Chapter 1

Introduction

The understanding of space and time was revolutionized by Einstein with the development of the general theory of relativity. This theory is different from most of the others, since it does not only give some new dynamics or interactions, but also posits the nature as a whole to be invariant under a new kind of spacetime symmetry, the diffeomorphisms of the spacetime manifold. Because of this symmetry, nature has to be described in a background independent way, which means that we do not introduce a background on which we describe dynamics, but we have to describe geometry together with its matter content as a whole.

The assumption of diffeomorphism invariance of the whole system has striking consequences. For example every dynamical degree of freedom introduced to the system will interact with the geometry through gravitational interactions, since any kind of energy is a source of gravity. Moreover this interaction can not be screened, such that it is always present.

Another effect which directly follows from diffeomorphism invariance is that parameterizing the theory, that is using parameter coordinates, does not work anymore, since the diffeomorphisms are a gauged symmetry and hence these parameter coordinates are unphysical. Because of this we can not use the “local” observables we know from local field theory any longer and have to think about other observables, which are gauge invariant under the symmetries of the system.

In particular, if we want to construct a diffeomorphism invariant framework based on local field theory, we have somehow to “remove” the dependence on the parameter spacetime from “local” observables. One way to achieve this is to integrate over the whole parameter spacetime and therefore mapping “local” observables to nonlocal ones [1]. This technique can be understood as a kind of group averaging over the group of spacetime diffeomorphisms, with the natural invariant measure $d\mu = d^4x\sqrt{-g}$.

At this point a very serious problem occurs. Since one can show that every diffeomorphism invariant observable must not depend on parameter spacetime [1] we have either observables constant over spacetime or integrated ones, which includes the S -matrix, if it exists. With none of them the description of local physics is possible at a first sight. This fact would have serious consequences since we are definitely local observers and measure local quantities in experiments. And the main purpose of a theory is to predict measurable quantities. Is therefore general relativity no physical theory?

The answer is no, since there is an elegant and very natural way out of this problem by defining relational observables [1]. The main idea of this approach is to choose some dynamical variables as clocks and rods and measure space and time with respect to them. This approach is even very natural in classical general relativity, since there one always talks about space and time with respect to some ideal clock located at some preferred position, e.g. an ideal clock at the desk in my office. We now just have to specify the measurement of “reading the clock” in order to talk about time. It was already Einstein and later also DeWitt who have noticed the fact that “*the description of the flow of time requires a self-consistent inclusion of the actual dynamical degrees of freedom that register this flow*” [1], which means that time has to emerge from the dynamical theory itself and is no external parameter.

In the case of quantum general relativity the definition of relational observables is a sensible approach too, see e.g. [1, 2] and references therein. For relational quantum observables it is also very important that only the interplay between specially prepared quantum states and specially chosen operators leads

to a sensible definition of “locality”. These special operators, which in specially prepared states can be interpreted as “local” ones are from now on called pseudo-local.

Since the clock and rod variables are dynamical variables, i.e. some matter fields or part of the metric field, the localization of pseudo-local observables is a dynamical problem. If we take the clock and rod variables to be some matter fields, we could for example think about localizing some observables with particle excitations of these fields. More specifically we could localize some spacetime point x if we generate a two particle wave packet state with wave packets only overlapping in a region around x .

It now becomes clear that any kind of localization has to be an excitation of the ground state and therefore will cause backreaction on the geometry through the gravitational interaction. This fact has dramatic consequences on the limits on localization, since the theory will have some “internal cutoff” to localization, which is an effect quite natural in quantum gravity.

In order to interpret locality we will assume that the state of the universe is sufficiently semiclassical to separate off a background geometry. In this case the concept of locality is understood. If we now localize with a higher and higher precision the state will become more and more non-semiclassical, for example a black hole, because backreaction will be very strong. If the state is so far from semiclassicality that a background can not be extracted anymore, we loose the interpretation of locality. We interpret this transition from a semiclassical to a non-semiclassical state as the limit on localization, since at this stage we loose our conceptional understanding of locality.

The framework in which we will study the dynamical process of localization will be quantum field theory on a fixed background. Here the assumption of a semiclassical quantum state is used in order to separate off the background and describe only the fluctuations on it dynamically. This effective approach to quantum gravity has the advantage that we can describe the dynamics with methods from perturbative quantum field theory on fixed backgrounds. In this formalism the breakdown of the theory can come from two different sources. First, quantum geometry effects could enter such that no classical background can be extracted any longer. But second, also classical curvature effects would lead to the breakdown of the theory defined on a fixed background, since we do not include the classical dynamics of the classical background and neglect classical geometry changes. The question which effects will be stronger will be further discussed at the end of this work.

Another totally different point of view on the breakdown of perturbative gravity is the following. Since most present small scale experiments are performed by scattering of particles, our understanding of small scale physics relies on scattering theory, which today necessarily requires a fixed background. Hence the breakdown of the perturbation theory including gravitons reflects the breakdown of the understanding of locality in today’s picture. In other words, a full theory of quantum gravity with the possibility to enter smaller scales does not necessarily improve our understanding of locality, because we do not know yet how to interpret the scattering experiments testing these small scales. This motivates the investigation of the perturbative limits on locality.

This work is devoted to the investigation of the localization of a certain class of pseudo-local observables on a flat background. We will restrict ourselves to bosonic matter fields, where by matter we mean every nongravitational field, including photons for example. The reason for that is that fermions would require a reformulation of metric variable gravity into vielbein and connection variables, which would unnecessarily complicate the technical part of our work. We assume that the basic features of dynamical localization can also be studied in bosonic theories.

In chapter 2 we will introduce the necessary mathematical basics in geometry and (constraint) quantization. We will keep this chapter rather short because we assume the reader to be familiar with these topics.

In chapter 3 we give a short introduction to effective quantum gravity and possible Dirac observables in it. In particular we will describe how in situations when the universe is in a suitable semiclassical state we can separate off a background and describe only metric fluctuations dynamically. Furthermore we will show that even if a background is fixed there remains a residual gauge symmetry for the gravitons.

In chapter 4 we perform the canonical quantization of linearized gravity using BRST methods in Fock space. We will work out the physical Hilbert space for the gravitons using cohomology methods and determine the physical graviton polarizations.

In chapter 5 we investigate a definite model on Minkowski background which gives rise to pseudo-local observables of a scalar field which are localized with respect to other scalar fields through matter three

point interactions [1]. For a suitable localization we have to prepare tight wave packets for the clock and rod field, which include high energy and momentum states. Higher energies will lead to more and more graviton loop contributions to the process of localization, such that at a certain ratio of loop corrections the theory breaks down. This energy scale where the theory breaks down will be interpreted as the limit on localization. The inverse scale therefore will be the smallest length scale up to which we can use our semiclassical picture of locality, using the above defined clocks and rods.

As a kind of crosscheck to the results of chapter 5 we investigated in chapter 6 a model with a Yang-Mills gauge field coupled to scalar matter field in the presence of gravitons on a flat background. This theory contains a three point interaction vertex as well, so that there exist similar pseudo-local observables as in chapter 5. We have performed the same analysis as for the pure scalar model in order to find out if there is some universality of the results.

In chapter 7 we will approach the question what kind of effect is dominant to the breakdown of perturbative quantum gravity, the quantum or the classical geometry effects. We will investigate the self-gravitation of two crossing wave packets in perturbative quantum and classical gravity and compare the results.

Finally chapter 8 concludes this work by a compact summary of the results.

Additional (interesting) insights gained throughout this work as well as rather lengthy expressions and calculations were put into the appendix. It also contains the instruction how one can modify FeynArts and FormCalc [3] in order to include gravitons.

Chapter 2

Physical and mathematical basics

2.1 Notation and conventions

This chapter is devoted to introducing the necessary conventions used throughout this work. The Minkowski metric is given by $\eta_{\mu\nu} = \eta^{\mu\nu} = \text{diag}(1, -1, -1, -1)$. Greek indices α, β, \dots are used to label indices of Riemann or Minkowski tensors. Latin indices i, j, k, \dots are used to label spacelike indices of tensors. We have the identity $v^i = -v_i$ for any 3-vector \mathbf{v} , and the positive definite Euclidean scalar product is defined between vectors with either both upper or both lower indices, i.e. $(v, w)_{\text{euclid}} := v^i w^i = v_i w_i = -v^i w_i$. We use Einstein's summation convention, but sometimes write explicitly the sums when it helps to avoid confusion. The symmetrization and antisymmetrization of a tensor T is given by round and square brackets respectively

$$T_{(\mu\nu)} := \frac{1}{2}(T_{\mu\nu} + T_{\nu\mu}) \quad (2.1)$$

$$T_{[\mu\nu]} := \frac{1}{2}(T_{\mu\nu} - T_{\nu\mu}) . \quad (2.2)$$

We sometimes write partial/covariant derivatives as comma/semicolon operation in order to get more compact expressions. The following definitions apply to the derivatives of some field V

$$V_{,\mu} := \partial_\mu V \quad \text{and} \quad V_{;\mu} := D_\mu V . \quad (2.3)$$

When we work on a general 4-dimensional manifold \mathcal{M} , we always assume that it is globally hyperbolic, i.e. the manifold can be topologically decomposed as $\mathcal{M} = \mathbb{R} \times \Sigma$, where Σ is a spacelike 3-dimensional submanifold. A spacetime point is denoted by $x \in \mathcal{M}$, and its spacelike part in boldface letters by $\mathbf{x} \in \Sigma$. The smearing of an operator density $O(\mathbf{x})$ on Σ by a function $f : \Sigma \rightarrow \mathbb{C}$ is defined by

$$O(f) := \int_{\Sigma} d^3x \sqrt{-g_{\Sigma}} f(\mathbf{x}) O(\mathbf{x}) , \quad (2.4)$$

if not stated otherwise. Here g_{Σ} is the subspace metric on Σ .

Working on Minkowski space $\mathcal{M}^4 := (\mathbb{R}^4, \eta)$, we use as wave packets the positive frequency square integrable functions $\mathcal{L}^2(\mathcal{M}^4)$ solving the Euler Lagrange equations together with the covariant scalar product

$$(f, g)_{\text{cov}} := i \int d^3x (f^*(x) \partial_t g(x) - \partial_t f^*(x) g(x)) =: i \int d^3x f^*(x) \overleftrightarrow{\partial}_t g(x) . \quad (2.5)$$

We will use natural units, i.e. $\hbar = c = 1$.

2.2 Riemannian geometry

In this section we will introduce the general definitions in differential and Riemannian geometry we use throughout this work. We assume the reader to be familiar with these ideas and therefore state the definitions and formulas without explanation. For further information see e.g. [4].

The basic object in the following is a m -**dimensional differential manifold** \mathcal{M} , which is a topological space with a collection of charts $\{(U_i, \phi_i)\}$ such that $\bigcup U_i = \mathcal{M}$ and ϕ_i homeomorphisms between U_i and a subset of \mathbb{R}^m . Having overlapping sets, i.e. $U_i \cap U_j \neq \emptyset$, the chart exchanges $\phi_i \circ \phi_j^{-1}$ should be bijective and smooth.

Given some smooth map between two manifolds $f : \mathcal{M} \rightarrow \mathcal{N}$ there exists a natural functor to an induced map between the tangential spaces and a cofunctor to a map between the cotangential spaces, called the **pushforward** and **pullback**, respectively. The coordinate representation of these maps are given by the Jacobian or inverse Jacobian matrix of the map f .

A **diffeomorphism** $f : \mathcal{M} \rightarrow \mathcal{N}$ is defined as a homeomorphism between \mathcal{M} and \mathcal{N} with the property that its chart representation is infinitely differentiable, i.e. C^∞ .

A $(0, 2)$ tensor field g on \mathcal{M} is called a **pseudo-Riemannian metric** if it satisfies (i.) $g_p(U, V) = g_p(V, U)$ for any point $p \in \mathcal{M}$ and $U, V \in T_p(\mathcal{M})$ and (ii.) if $g_p(U, V) = 0$ for any $U \in T_p(\mathcal{M})$ then $V = 0$. Here $T_p(\mathcal{M})$ denotes the tangential space in the point $p \in \mathcal{M}$.

Using the coordinate representation of the metric and assuming a torsion-free manifold we can give expressions for the **connection** symbols (here Christoffel symbols), the **Riemann tensor** and the **Ricci tensor**. They are given by

$$\Gamma_{\mu\nu}^\alpha := \frac{1}{2}g^{\alpha\beta}(g_{\mu\beta,\nu} + g_{\nu\beta,\mu} - g_{\mu\nu,\beta}) \quad (2.6)$$

$$R_{\mu\nu\beta}^\alpha := \Gamma_{\mu\beta,\nu}^\alpha - \Gamma_{\mu\nu,\beta}^\alpha + \Gamma_{\nu\lambda}^\alpha \Gamma_{\beta\mu}^\lambda - \Gamma_{\mu\nu}^\lambda \Gamma_{\lambda\beta}^\alpha \quad (2.7)$$

$$R_{\mu\nu} := R_{\mu\nu\alpha}^\alpha = \Gamma_{\mu\lambda,\nu}^\lambda - \Gamma_{\mu\nu,\lambda}^\lambda + \Gamma_{\nu\lambda}^\sigma \Gamma_{\sigma\mu}^\lambda - \Gamma_{\mu\nu}^\sigma \Gamma_{\lambda\sigma}^\lambda, \quad (2.8)$$

where $g^{\alpha\beta}$ is the inverse metric, i.e. the $(2, 0)$ tensor satisfying $g^{\alpha\beta}g_{\beta\gamma} = \delta_\gamma^\alpha$.

The unique metric compatible **covariant derivative**, i.e. $D_\mu g_{\alpha\beta} = 0$, is given by the following abstract expression

$$D_\mu := \partial_\mu + \omega_\mu, \quad (2.9)$$

where ω is an abstract connection, which can be expressed through a sum of Christoffel symbols when acting on a tensor expression on the right. For example the covariant derivative of a vector and covector field is given by

$$D_\mu A^\nu := \partial_\mu A^\nu + \Gamma_{\mu\alpha}^\nu A^\alpha \quad (2.10)$$

$$D_\mu B_\nu := \partial_\mu B_\nu - \Gamma_{\mu\nu}^\alpha B_\alpha, \quad (2.11)$$

and for general (p, q) tensor fields it is given by using Leibniz's rule for the abstract connection ω .

Working on a (pseudo)-Riemannian manifold there is a natural diffeomorphism invariant **volume element** given by

$$\int d\mu := \int d^m x \sqrt{|g|}. \quad (2.12)$$

2.3 Basics in cohomology

Since we will later use some terminology of the theory of cohomology we will briefly give the required definitions, without going too much into details.

For our purpose cohomology is the investigation of some nilpotent linear operation $d_i : V_i \rightarrow V_{i+1}$ (not necessarily an automorphism) between some vector spaces V_i . By nilpotency we mean that acting with the operator twice on an element is zero, i.e. $d_{i+1}(d_i v) = 0 \forall v \in V_i$.

This fact leads to the following natural classification of those elements in $v \in V_i$ with $d_i v = 0$:

1. v is called a **cocycle** or **closed**, if $d_i v = 0$
2. v is called a **coboundary** or **exact**, if there exists a $w \in V_{i-1}$ with $v = d_{i-1} w$

Note that every exact vector is closed by using the nilpotency.

A natural question which always arises in such context is the following: Is every closed vector $v \in V_i$ exact? This information is contained in the so called i -th cohomology group defined by the factor space

$$H^i := \text{Ker}(d_i) / \text{Im}(d_{i-1}), \quad (2.13)$$

where Ker is the kernel and Im is the image of the operator.

At this point it makes sense to give some examples of physical importance. Assume as space V_i the space of i -forms on a manifold and as $d_i = d$ the exterior derivative. It holds $d^2 = 0$ because of antisymmetrization and therefore we have a system to which we can apply cohomology. The Lemma of Poincaré, see e.g. [4], in particular states that every cohomology group is trivial in the case $\mathcal{M} = \mathbb{R}^m$. One physical implication for example is the fact that on \mathbb{R}^3 every rotation-free vector field is given by the gradient of some scalar field.

In our case cohomology is used to classify physical operators and states in the presence of BRST symmetry. Physical quantities must be BRST closed, but are non-unique since the addition of exact quantities does not change physics. Therefore the physical information is encoded in cohomology groups.

2.4 Classical dynamical systems

In this chapter we give the basics of classical dynamical systems in order to define some notation. We do not distinguish between finite dimensional systems and infinite dimensional ones. A dynamical system, for our purpose, is defined as follows.

Definition 1. A dynamical system is a topological manifold Γ (with an even or infinite number of dimensions), the so called phase space, together with a symplectic 2 form Ω and some given dynamical function $H : \Gamma \rightarrow \mathbb{R}$, sometimes called the Hamiltonian.

A symplectic 2 form is a non degenerate 2 form that is closed, i.e. the outer derivative vanishes $d\Omega = 0$.

In such a system the algebra of all smooth functions from the phase space to complex numbers contains the observables of the theory. This algebra has some extra structure coming from the symplectic form Ω and is defined as follows.

Definition 2. A Poisson algebra is the associative and involutive \star -algebra $(\mathcal{A}_{\text{poisson}}, \cdot)$ of all smooth functions from the phase space to complex numbers together with an antisymmetric bilinear map $\{\cdot, \cdot\} : \mathcal{A}_{\text{poisson}} \times \mathcal{A}_{\text{poisson}} \rightarrow \mathcal{A}_{\text{poisson}}$ called the Poisson bracket, which satisfies the Jacobi identity and Leibniz rule. The multiplication operation in this algebra is defined by pointwise multiplication of the functions, i.e. $(f \cdot g)(x) := f(x)g(x)$ for all $x \in \Gamma$, and therefore is commutative.

The nice thing about the symplectic form defined above is that it gives a natural definition of the Poisson bracket by

$$\{A, B\} := \Omega^{ab} \partial_a A \partial_b B, \quad (2.14)$$

where Ω^{ab} is the inverse of the symplectic form, which exists because of the nondegeneracy of Ω .

The dynamics of the system is given by the one parameter group defined from the Hamilton vector field of the Hamiltonian, which is given by

$$X_H := \{\cdot, H\} : \mathcal{A}_{\text{poisson}} \rightarrow \mathcal{A}_{\text{poisson}}. \quad (2.15)$$

But we can also generate other flows by defining the Hamilton vector fields of the corresponding conserved charges of the flow. The infinitesimal change of an observable O by the group action of some conserved charge G with parameter ϵ is given by

$$\delta_\epsilon O := \epsilon \{O, G\}. \quad (2.16)$$

At least locally the symplectic form can always be expressed in position and momentum variables as [4]

$$\Omega := dq_a \wedge dp^a \quad (2.17)$$

which leads to the following Poisson bracket

$$\{A, B\} = \sum_a \frac{\partial A}{\partial q^a} \frac{\partial B}{\partial p^a} - \frac{\partial B}{\partial q^a} \frac{\partial A}{\partial p^a}, \quad \forall A, B \in \mathcal{A}_{\text{poisson}}. \quad (2.18)$$

The translation of this result to the field theoretic case is straightforward by identifying $q^a \rightarrow \phi(\mathbf{x})$, $p^a \rightarrow \pi(\mathbf{x})$ and $\sum_a \rightarrow \int d^3x \sqrt{-g_\Sigma}$.

Finally we give the fundamental Poisson brackets between position and momentum variables for infinite dimensional systems. They are given by

$$\{\phi(f), \phi(g)\} = \{\pi(f), \pi(g)\} = 0 \quad (2.19)$$

$$\{\phi(f), \pi(g)\} = \int d^3x \sqrt{-g_\Sigma} f(\mathbf{x}) g(\mathbf{x}). \quad (2.20)$$

2.5 Constrained systems and BRST formalism

A constrained dynamical system is defined to be a dynamical system together with a set of constraints $\{\chi^a : \chi^a \in \mathcal{A}_{\text{poisson}} \text{ and } \chi^a \approx 0 \text{ for all } a = 1, \dots, m\}$, where m is the number of constraint(densitie)s and \approx denotes a weak equality, which is defined as follows

Definition 3. *Two functions $F(q, p), G(q, p) \in \mathcal{A}_{\text{poisson}}$ are called weakly equal, i.e. $F \approx G$, if they coincide on the constraint surface. They are called strongly equal, i.e. $F = G$, if they coincide on the whole phase space. In particular, weakly vanishing functions can have nontrivial Poisson brackets on the reduced phase space.*

In this work we assume all constraints to be first class, i.e. the Poisson bracket of two constraints or one constraint and the Hamiltonian is given by a linear combination of only the constraints. Second class constraints do not appear in this work and therefore do not have to be defined. The interested reader is referred to [5, 6].

Since we have first class constraints, we can in general write

$$\{\chi^a, \chi^b\} := U^{abc} \chi^c \quad (2.21)$$

$$\{H, \chi^a\} := V^{ab} \chi^b, \quad (2.22)$$

where U^{abc} and V^{ab} are assumed to be constants.

We assume that the set of constraints generates gauge transformations by their Hamilton vector fields, which is given in most first class constraint systems, in particular in all the systems of physical relevance known to us. But as a remark, there are also systems which violate this so called ‘‘Dirac conjecture’’, which is discussed in [6].

The gauge transformations are therefore induced by a linear combination of the constraints with some parameters ϵ^a , which acts on an observable O by

$$\delta_\epsilon O = \{O, \chi^a[\epsilon^a]\}, \quad (2.23)$$

where $\chi^a[\epsilon^a] = \sum_a \epsilon^a \chi^a$ in the case of finite dimensional systems and the sum of smeared constraints $\chi^a[\epsilon^a] = \sum_a \chi^a(\epsilon^a)$ in the field theoretic case.

In the presence of gauge symmetries we do not expect the whole Poisson algebra $\mathcal{A}_{\text{poisson}}$ to be physical observables, since it contains elements which change under gauge transformations and therefore are unphysical. The physical observables should be invariant under all gauge transformations. This idea can be used to define physical observables in the following way [5].

Definition 4. *The physical observables, sometimes called Dirac observables, are exactly the observables that have weakly vanishing Poisson brackets with all constraints. They form a Poisson sub-algebra of $\mathcal{A}_{\text{poisson}}$ called the physical observable algebra $\mathcal{A}_{\text{phys}}$.*

The reason why $\mathcal{A}_{\text{phys}}$ is a sub-algebra of the Poisson algebra is because if some observables have vanishing Poisson brackets with the constraints, the finite sums and products also have vanishing Poisson brackets by using the properties of definition 2. This sub-algebra is a Poisson algebra in its own right, since the Jacobi identity guarantees that it is closed under Poisson brackets.

In the following we will discuss a certain method for investigating constrained systems, the BRST method, which provides a powerful tool especially for investigations of Yang-Mills theories [7, 8]. The advantage of this method is that it naturally can be applied to perturbative quantum gauge field theories. In this part we will follow [7] and refer to this work for further information and details. Furthermore we restrict ourselves to bosonic phase space variables and therefore fermionic ghost variables.

The first step of this method is to introduce a phase space extension by fermionic variables η^a , called the ghost variables, together with their conjugate momenta $\bar{\eta}^a$ for every constraint χ^a , $a = 1, \dots, m$. The spin of the ghost variables has to be chosen such that the smeared constraints $\chi^a[\eta^a]$ are scalars. In general this results in a violation of the spin statistics theorem, which is not problematic if we can show that ghosts do not show up in the physical world. Since fermionic degrees of freedom are described by using Grassmann numbers, we have to define a generalized Poisson bracket, the so called graded Poisson bracket, which is given by [7]

$$\{A, B\}_{\text{gr}} := \frac{\partial^r A}{\partial z^a} C^{ab} \frac{\partial^l B}{\partial z^b}, \quad (2.24)$$

where $z = (q, p, \eta, \bar{\eta})$ are the coordinates of the phase space and $C^{ab} = \{z^a, z^b\}_{\text{gr}}$ are the fundamental brackets which have to be defined. l and r indicates the derivative from the left or right, which is different for Grassmann numbers. A natural definition of the fundamental brackets is so that they later, in quantum theory, are given by commutators for bosons and anticommutators for fermions. Hence a possible choice is that the ordinary bosonic coordinates q and p have the same graded brackets as normal Poisson brackets and the brackets for the ghost coordinates are given by

$$\{\bar{\eta}^a, \eta^b\}_{\text{gr}} = -\delta^{ab} \quad (2.25)$$

$$\{\eta^a, \bar{\eta}^b\}_{\text{gr}} = -\delta^{ab} \quad (2.26)$$

$$\{\bar{\eta}^a, \bar{\eta}^b\}_{\text{gr}} = \{\eta^a, \eta^b\}_{\text{gr}} = \{\eta^a, \text{bv}\}_{\text{gr}} = \{\bar{\eta}^a, \text{bv}\}_{\text{gr}} = 0, \quad (2.27)$$

where bv denotes some bosonic variable. In the following we will omit the subscript gr and assume every Poisson bracket to be graded.

For a consistent formalism we have to define the behavior of the ghost variables under complex conjugation. A possible definition, according to [7], is given by

$$\eta^{a*} = \eta^a \quad (2.28)$$

$$\bar{\eta}^{a*} = -\bar{\eta}^a. \quad (2.29)$$

Fundamental in the BRST formulation of a constrained system is the definition of the generator of BRST transformations which is given by

$$\Omega_{\text{BRST}} := \chi^a[\eta^a] - \frac{1}{2} \eta^b \eta^a U^{abc} \bar{\eta}^c. \quad (2.30)$$

It can be shown that Ω_{BRST} is a fermionic, real and nilpotent generator, i.e. $\{\Omega_{\text{BRST}}, \Omega_{\text{BRST}}\} = 0$, which generates gauge transformations with ghosts as ‘‘parameters’’ acting on bosonic variables [7].

With this new symmetry we can systematically define **strongly** BRST invariant observables O_{BRST} out of weakly gauge invariant observables O by the extension

$$O_{\text{BRST}} = O + (-)^{\epsilon(O)} \eta^a V_O^{ab} \bar{\eta}^b + \{\Omega_{\text{BRST}}, \Psi\}, \quad (2.31)$$

where $\epsilon(O)$ denotes the Grassmann parity of the observable O and Ψ is a general function of the variables of the form

$$\Psi := \psi_{(1)}^a[\bar{\eta}^a] + \text{higher powers of ghosts} \quad (2.32)$$

and V_O^{ab} is defined by

$$\{O, \chi^a\} := V_O^{ab} \chi^b \quad (2.33)$$

which holds true, since O was defined to be a Dirac observable, i.e. $\{O, \chi^a\} \approx 0$.

Furthermore one can show that [7]

$$O_{\text{BRST}}|_{\eta^a=\bar{\eta}^a=0} \approx O|_{\eta^a=\bar{\eta}^a=0} \quad (2.34)$$

and

$$\{O_{\text{BRST}}^{(1)}, O_{\text{BRST}}^{(2)}\}|_{\eta^a=\bar{\eta}^a=0} \approx \{O^{(1)}, O^{(2)}\}|_{\eta^a=\bar{\eta}^a=0}. \quad (2.35)$$

Hence the BRST invariant extension of an observable is well defined, since in the final result it is equivalent to the canonical method, at least at classical level.

The main advantage of BRST symmetry does not lie in its classical formulation, but in its quantization. The extra term Ψ introduced in (2.31) can be used to fix the gauge and therefore change the equations of motion of the unphysical parts. This can be used to modify the equations of motion in order to perform the Fock quantization, see e.g. [7] for quantum electrodynamics. Furthermore the BRST generator Ω_{BRST} together with the strongly BRST invariant Hamiltonian will be used to define the physical states, i.e. the physical Hilbert space of the theory, and their dynamics.

2.6 Canonical quantization

Throughout this work we will quantize our theories by using canonical quantization. This chapter is devoted to remind the reader of the basics of canonical quantization from an algebraic point of view [9]. We will give the necessary conventions and formulas for Fock space representations, since we will use them heavily in the following. Finally we will introduce the BRST method applied to constrained quantum theories [7].

2.6.1 Generalities

Since Heisenberg's uncertainty principle shows us that physics at small distances has some inherent complementarity in measuring certain observables, we have to think about how one can integrate these facts into a redefinition of dynamical systems. The most natural method for implementing complementarity is to perform a deformation of the classical Poisson algebra into a noncommutative algebra [10], the so called quantum algebra, since complementarity can only hold in noncommutative algebras. Measurements in the quantum algebra are described by acting with appropriate states (positive functionals) on its elements.

Practically one does not generate the quantum algebra by deformation but by relating some elementary classical observables of the system to some abstract operators and generate the quantum algebra as the free associative algebra from them [9]. The information about the classical system is transferred to the quantum algebra by defining commutation relations among the elementary observables of the form that for two elementary quantum observables \hat{A}, \hat{B} the identity $[\hat{A}, \hat{B}] = i\hbar\{A, B\}$ holds true. We also encode reality conditions into the quantum algebra by defining an involution \star in the quantum algebra with the property that $\hat{A}^* = \hat{A}^\star$.

If the classical phase space of the theory is a linear space, a natural choice of elementary observables are the position variables q^a and momentum variables p^a . Since the Poisson brackets close in the vector space $S := \text{Span}\{1, q^a, p^a\}$ it is sufficient to quantize S and identify the free generated associative algebra, with imprinted commutation relations, as quantum algebra. More precisely we generate the free associative

\star -algebra from S and factor out the ideal generated by the relations coming from reality conditions and commutation relations. The generalization to field theory is straightforward.

For completeness and to fix the convention we give the fundamental commutation relations in the case of a theory with linear phase space for infinite dimensional systems. They are given by

$$[\hat{\phi}(f), \hat{\phi}(g)] = [\hat{\pi}(f), \hat{\pi}(g)] = 0 \quad (2.36)$$

$$[\hat{\phi}(f), \hat{\pi}(g)] = i\hbar \int d^3x \sqrt{-g_\Sigma} f(\mathbf{x}) g(\mathbf{x}) \hat{1}. \quad (2.37)$$

From now on we omit the hat above operators if it does not cause confusion, and we set $\hbar = 1$.

The next step is to find representations of the abstract quantum algebra discussed above as operator algebras on Hilbert spaces. We will only consider the case of field theories, since finite dimensional systems will not occur in the following. The problem with representing quantum algebras on Hilbert spaces is that in general one can only construct the Hilbert spaces for free quantum field theories, except for some special cases. Therefore, in the following we will constrain ourselves to representations of free field theories. Interacting quantum field theories are for our purpose sufficiently well defined by defining the asymptotic free Hilbert space to be the Hilbert space of the theory and representing the operators in the interaction picture [11], since we just treat them perturbatively. Other problems in field theory, like the nonvalidity of Stone and von Neumann's theorem and others are not considered in this work.

2.6.2 Fock representation

In this section we will present the basics of Fock space representations using the example of a free real scalar field ϕ on 4 dimensional Minkowski space in order to give the main ideas and to fix the notation.

The starting point for constructing a Fock space is noting that there exists an isomorphism \mathcal{I}_{t_0} between the classical phase space of the theory at some time t_0 and the solution space of the Euler Lagrange equations. This can be seen as follows. Given a phase space point $(\phi(\mathbf{x}), \pi(\mathbf{x}))$ at a time t_0 it can be used as initial conditions to solve the Euler Lagrange equations for the field $\phi(x)$ by identifying $\pi(\mathbf{x}) = \dot{\phi}(x)|_{t=t_0}$. Thus we have enough initial conditions to solve the second order differential equations. The inverse map $\mathcal{I}_{t_0}^{-1}$ is also well defined, since given a solution $\phi(x)$ to the Euler Lagrange equations we can define $\mathcal{I}_{t_0}^{-1}(\phi(x)) = (\phi(t_0, \mathbf{x}), \dot{\phi}(t_0, \mathbf{x}))$.

The main idea now is to perform a quantization of the solutions $\phi(x)$ and construct a one particle Hilbert space from them, which is the basic ingredient for the Fock space.

If the theory has linear Euler Lagrange equations, which is the case in free field theories as in our example, we can write the most general solution of them in terms of Fourier decomposition as

$$\phi(x) = \int \widetilde{d^3k} (a_{\mathbf{k}} e^{-ikx} + a_{\mathbf{k}}^* e^{ikx}), \quad (2.38)$$

where $a_{\mathbf{k}}$ is the Fourier coefficient and $\widetilde{d^3k} = \frac{d^3k}{(2\pi)^3 2k^0}$. There has been an explicit distinction between positive and negative frequency solutions, which can be done in the case of a free scalar field and is very essential for further investigations.

Now we perform the quantization by assigning every $a_{\mathbf{k}}$ an operator with the properties that

$$[a_{\mathbf{k}}, a_{\mathbf{p}}] = [a_{\mathbf{k}}^\dagger, a_{\mathbf{p}}^\dagger] = 0 \quad (2.39)$$

$$[a_{\mathbf{k}}, a_{\mathbf{p}}^\dagger] = (2\pi)^3 2k^0 \delta(\mathbf{p} - \mathbf{k}), \quad (2.40)$$

where a^\dagger is the adjoint operator of a defined by quantizing a^* .

It can be shown that using the isomorphism \mathcal{I}_{t_0} we can recover the fundamental commutation relations (2.36) of the ordinary variables.

The Fock vacuum $|0\rangle \in \mathcal{H}_{\text{Fock}}$ can be defined by a state with the property

$$a_{\mathbf{k}}|0\rangle = 0 \quad \forall \mathbf{k} \in \mathbb{R}^3. \quad (2.41)$$

Given this definition we can define the one particle wave packet creation operators by

$$a_f^\dagger := -(f^*, \phi)_{\text{cov}} = -i \int d^3x f(x) \overleftrightarrow{\partial}_t \phi(x) \quad (2.42)$$

where $f(x)$ is some wave packet with only positive frequency parts on Minkowski space \mathcal{M}^4 .

The one particle Hilbert space \mathcal{H}_1 can now be constructed out of the $\mathcal{L}^2(\mathcal{M}^4)$ space with the scalar product $(f, g)_{\text{cov}}$, which can be shown to induce a positive definite norm for solutions to the Euler Lagrange equations with either positive or negative frequency. It is given as follows

$$\mathcal{H}_1 := \{a_f^\dagger|0\rangle : f \in \mathcal{L}^2(\mathcal{M}^4) \wedge f \text{ is pos. freq. solution to E-L eq.}\}, \quad (2.43)$$

with a scalar product given by $\langle f|g\rangle = (f, g)_{\text{cov}}$, which can be seen by using the commutators (2.39).

In analogy, the n particle Hilbert space can be constructed by acting with n wave packet creation operators on the vacuum and therefore is given by

$$\mathcal{H}_n := \bigotimes_s^n \mathcal{H}_1, \quad (2.44)$$

where s denotes the symmetrized tensor product. The scalar product on \mathcal{H}_n is induced by the one particle scalar product by using the commutators (2.39). Finally the Fock space is given by

$$\mathcal{H}_{\text{Fock}} := \mathbb{C}|0\rangle \oplus \bigoplus_{n=1}^{\infty} \mathcal{H}_n, \quad (2.45)$$

with the naturally induced scalar product from its summands.

This Hilbert space naturally supports a representation of the quantum algebra generated by the elementary observables ϕ and π , since they can be expressed in terms of the creation and annihilation operators $a_{\mathbf{k}}^\dagger$ and $a_{\mathbf{k}}$ by means of Fourier transformation.

2.6.3 Quantum BRST formalism

In this section we assume that we deal with a constrained quantum field theory with bosonic field variables A and fermionic ghosts η . We also assume that the phase space of the theory is a linear space so that we can perform quantization by quantizing the linear functions of the phase space variables.

We assume that we have found some pre-Hilbert space that is a vector space, not necessarily complete, in which the norm may not be positive definite, on which we can represent the field operators together with their (anti-)commutation relations. A natural candidate for this pre-Hilbert space is the product of some pre-Hilbert space for A called \mathcal{V}_A and some pre-Hilbert space for the ghosts and antighosts \mathcal{V}_η given by $\mathcal{V} = \mathcal{V}_A \otimes \mathcal{V}_\eta$. In order to find these (pre-) Hilbert spaces we have the freedom to manipulate the classical equations of motion by adding BRST invariant terms to the Hamiltonian so that even Fock representations can exist.

Like in the Dirac programme of quantization we now want to represent the gauge transformations, which are here extended to the BRST transformations, on the pre-Hilbert space \mathcal{V} and use their action on the auxiliary states in order to define physical states. Therefore we need to represent Ω_{BRST} as a hermitian, nilpotent operator on \mathcal{V} , which has to be checked explicitly to exist in every theory under consideration. As a remark, there exist theories in which the operator ordering prevents this representation, like in the case of string theories with a nonmatching number of dimensions.

Having a representation of Ω_{BRST} , we can use the condition that physical states should be BRST invariant, which is given by the action of the BRST generator

$$\Omega_{\text{BRST}}|\text{phys}\rangle = 0. \quad (2.46)$$

The problem with this definition is that not every state satisfying (2.46) can be interpreted as a physical state, since all states $|\psi\rangle \in \text{Im}(\Omega_{\text{BRST}}) := \{|\psi\rangle : \exists|\phi\rangle \in \mathcal{V}, |\psi\rangle = \Omega_{\text{BRST}}|\phi\rangle\}$ will satisfy this equation

too, but have zero norm, because of the nilpotency of Ω_{BRST} . Hence they can not be interpreted as physical states, which have to be normalized to some finite positive value.

A possible and sensible physical Hilbert space would be the completion of the factor space given by

$$\mathcal{H}_{\text{phys}} := \overline{\text{Ker}(\Omega_{\text{BRST}})/\text{Im}(\Omega_{\text{BRST}})}, \quad (2.47)$$

on which the physical observable algebra, i.e. the algebra of BRST invariant observables can be represented. A natural representation of this algebra can be induced from the representation on the pre-Hilbert space \mathcal{V} by

$$\mathcal{O}[|\psi\rangle] := [\mathcal{O}|\psi\rangle], \text{ for } |\psi\rangle \in \text{Ker}(\Omega_{\text{BRST}}), \quad (2.48)$$

which is well defined since $[\mathcal{O}, \Omega_{\text{BRST}}] = 0$ and hence the action of \mathcal{O} can be shifted from the physical Hilbert space $\mathcal{H}_{\text{phys}}$ to the pre-Hilbert space \mathcal{V} . The state $[|\psi\rangle] \in \mathcal{H}_{\text{phys}}$ denotes the equivalence class to which the state $|\psi\rangle \in \mathcal{V}$ belongs.

The scalar product on $\mathcal{H}_{\text{phys}}$ can be naturally induced by the scalar product on \mathcal{V} by

$$([|\psi\rangle], [|\phi\rangle])_{\text{phys}} := \langle \psi | \phi \rangle \quad (2.49)$$

which is well defined, since every state in $\text{Im}(\Omega_{\text{BRST}})$ has vanishing scalar product with a state in $\text{Ker}(\Omega_{\text{BRST}})$, so that it does not depend on the representative of the equivalence class we choose on the r.h.s. of (2.49). The positive definiteness of the norm induced by the scalar product on $\mathcal{H}_{\text{phys}}$ has to be checked for the system under consideration. For the case of Yang - Mills theories this was done by Kugo and Ojima [12] using BRST cohomology methods.

In a perturbative treatment of interacting gauge theories it would be somehow nicer if we could avoid working in the factor space $\mathcal{H}_{\text{phys}}$ explicitly and work consistently in the pre-Hilbert space instead, since the states in the auxiliary Hilbert space are easier to handle. The good thing about the BRST approach is that we can do so. For the S -matrix the identity

$$\langle [\psi] | S [|\phi\rangle] \rangle = \langle \psi | S | \phi \rangle, \text{ for } |\psi\rangle, |\phi\rangle \in \text{Ker}(\Omega_{\text{BRST}}) \quad (2.50)$$

holds true, since $S = \exp(-i \int_{-\infty}^{\infty} dt H_{\text{BRST}})$ is a physical operator. So we can specify our initial and final states by some representative of the equivalence classes with some subsidiary condition, e.g. that it contains no ghosts and no unphysical polarizations, and calculate S -matrix elements from them. In intermediate steps of the time evolution, i.e. in loop diagrams, we can use representatives in which ghosts and unphysical polarizations are **both** contained and therefore simplify polarization sums as usual.

2.7 LSZ formalism for in-out matrix elements

In this section we will give the necessary formulae for a perturbative investigation of in-out matrix elements in interacting quantum field theories on flat spacetime. Their derivation can be found in nearly every introductory textbook on quantum field theory, e.g. [11].

The basic observables we are interested in are matrix elements of some time ordered operator $O := T\{\prod_i O_i\}$ between asymptotic states. Let f_a and g_b be wave packets for all a, b then these matrix elements are given by

$$\begin{aligned} \langle f_1, \dots, f_n; \text{out} | O | g_1, \dots, g_m; \text{in} \rangle &= (iZ^{-\frac{1}{2}})^{n+m} \\ &\times \prod_{a,b} \left(\int d^4x_a d^4y_b f_a^*(x_a) g_b(y_b) (\square_{x_a} + m^2)(\square_{y_b} + m^2) \right) \langle 0; \text{out} | T\{\phi(x_1) \dots \phi(y_m) O\} | 0; \text{in} \rangle \\ &+ \text{nonconnected terms}, \quad (2.51) \end{aligned}$$

where Z denotes the wave function renormalization, m the mass of the particle, and the nonconnected terms will vanish if $(f_a, g_b)_{\text{cov}} = 0$ for all a, b .

The operators O_i we are interested in will be given by integrated local operators $O_i(x)$, i.e.

$$O_i := \int d^4x O_i(x) \quad (2.52)$$

and therefore do not depend on x . It is natural to write the general formula (2.51) in Fourier space as

$$\langle f_1, \dots, f_n; \text{out} | O | g_1, \dots, g_m; \text{in} \rangle = \int \prod_{a,b} \frac{d^4p_a}{(2\pi)^4} \frac{d^4k_b}{(2\pi)^4} \prod_{a,b} \mathcal{B}(f_a, p_a)^* \mathcal{B}(g_b, k_b) \tilde{G}(p_1, \dots, k_m), \quad (2.53)$$

where $\mathcal{B}(f, p) := \int d^4x f(x) e^{ipx}$ and \tilde{G} is given by

$$\tilde{G} := \prod_{a,b} \frac{(p_a^2 - m^2)}{i} \frac{(k_b^2 - m^2)}{i} \int \prod_{a,b} d^4x_a d^4y_b e^{ip_a x_a} e^{-ik_b y_b} Z^{-\frac{n+m}{2}} \langle 0; \text{out} | T \{ \phi(x_1) \dots \phi(y_m) O \} | 0; \text{in} \rangle. \quad (2.54)$$

Formula (2.53) can be further simplified by using the on-shell spectral representation of $f(x)$ which reduces $\mathcal{B}(f, p)$ to

$$\mathcal{B}(f, p) = \int d^4x e^{ipx} \int \widetilde{d^3k} \tilde{f}(\mathbf{k}) e^{-ikx} = \frac{\pi}{p^0} \tilde{f}(\mathbf{p}) \delta(p^0 - \sqrt{\mathbf{p}^2 + m^2}). \quad (2.55)$$

Putting the result into (2.53) we arrive at the final result

$$\langle f_1, \dots, f_n; \text{out} | O | g_1, \dots, g_m; \text{in} \rangle = \int \prod_{a,b} \widetilde{d^3p_a} \widetilde{d^3k_b} \frac{\tilde{f}_a(\mathbf{p}_a)^*}{2} \frac{\tilde{g}_b(\mathbf{k}_b)}{2} \tilde{G}(p_1, \dots, k_m), \quad (2.56)$$

where \tilde{G} is now on-shell.

If the operators $O_i(x)$ are polynomials in the fields we can apply Gell-Mann and Low's formula and Wick's theorem and reduce the problem of determining matrix elements of operators to Feynman diagram calculations. In this case \tilde{G} can be interpreted as some part of the amputated, renormalized $n + m$ point Green function in momentum space.

If one of the O_i is not polynomial there is no natural access to this problem by Feynman diagram methods. Because of this we will restrict ourselves to the case of polynomial operators, in particular vertex operators occurring in the action.

2.8 Schwinger-Keldysh formalism for in-in matrix elements

As we will see below, using in-out matrix elements of pseudo-local operators will just give access to a limited class of observables. In particular the possible pseudo-local observables which are accessible by in-out matrix elements and which can be interpreted physically in terms of scattering matrix elements will strongly depend on the chosen dynamics of the system.

Another kind of observables, which are very different from in-out matrix elements, are expectation values of some operator $O(t)$ at some time t in the state of the system $|\psi\rangle$, i.e. matrix elements like $\langle \psi | O(t) | \psi \rangle$. Writing this expectation value in the interaction picture we get

$$\langle \psi | O(t) | \psi \rangle = {}_{\text{int}} \langle \psi, t | O_{\text{int}}(t) | \psi, t \rangle_{\text{int}}, \quad (2.57)$$

where $|\psi, -\infty\rangle_{\text{int}} = |\psi\rangle$ and $O_{\text{int}}(t)$ is the operator in the interaction picture.

Using the interaction picture time evolution operator, (2.57) reads

$$\langle \psi | O(t) | \psi \rangle = {}_{\text{int}} \langle \psi, -\infty | \bar{T} \{ \exp(i \int_{-\infty}^t dt' H_{\text{int}}(t')) \} O_{\text{int}}(t) T \{ \exp(-i \int_{-\infty}^t dt' H_{\text{int}}(t')) \} | \psi, -\infty \rangle_{\text{int}}, \quad (2.58)$$

where H_{int} is the interaction Hamiltonian in the interaction picture and T and \bar{T} denote time and anti-time ordering, respectively.

The basic formula (2.58) can be evaluated perturbatively by using some modified diagrammatic rules. This formalism is known as the Schwinger-Keldysh or in-in formalism, see [13] and references therein. In the following we will summarize the basic diagrammatic formalism:

- Since the expansion in the coupling constant leads to time and anti-time ordered terms, we have to distinguish between “left” and “right” vertices, where left and right means anti-time ordered and time ordered, respectively. The right vertex comes with a factor of i and the left vertex with a factor of $-i$ in Lagrangian field theory.
- A line connecting a left vertex with a left vertex or $O_{\text{int}}(t)$ is given by the anti-Feynman propagator $\langle 0|\bar{T}\{\phi(x)\phi(y)\}|0\rangle$.
- A line connecting a right vertex with a right vertex or $O_{\text{int}}(t)$ is given by the Feynman propagator $\langle 0|T\{\phi(x)\phi(y)\}|0\rangle$.
- A line connecting a left vertex with a right vertex is given by the two-point Wightman function $\langle 0|\phi(x)\phi(y)|0\rangle$, where $\phi(x)$ is associated to the left and $\phi(y)$ is associated to the right vertex.
- A line connecting an external field $a(f) = (f, \phi)_{\text{cov}}$ from the asymptotic state ${}_{\text{int}}\langle \psi, -\infty|$ with an internal field $\phi(x)$ (left vertex, right vertex or $O_{\text{int}}(t)$) is given by $[a(f), \phi(x)] = f^*(x)$, where $f(x)$ is the wave packet associated to the particle $a(f)$.
- A line connecting an external field $a^\dagger(f) = -(f^*, \phi)_{\text{cov}}$ from the asymptotic state $|\psi, -\infty\rangle_{\text{int}}$ with an internal field $\phi(x)$ (left vertex, right vertex or $O_{\text{int}}(t)$) is given by $[\phi(x), a^\dagger(f)] = f(x)$, where $f(x)$ is the wave packet associated to the particle $a^\dagger(f)$.
- All time parameters associated to the vertices have to be integrated over the range $(-\infty, t]$.
- Symmetry factors are included.

Furthermore it can be shown [13] that the vacuum to vacuum diagrams, i.e. disconnected loops, do not contribute.

Within this formalism we can, in principle, evaluate expectation values of operators at fixed time t up to the desired order in perturbation theory. In order to obtain diffeomorphism invariance we have to integrate the resulting matrix elements over all t , i.e.

$$\mathcal{O}_{\text{diff inv}} = \int_{-\infty}^{\infty} dt \langle \psi | O(t) | \psi \rangle . \quad (2.59)$$

Chapter 3

Effective theory of quantum general relativity (QGR)

In this chapter we introduce the basic framework of effective QFT applied to gravity. This approach has been applied to different problems in the existing literature, for example [14, 15]. We will also discuss the sensible definition of relational observables in gravity in the sense of [1]. One other point is the investigation of the classical gauge structure of the theory on a fixed background. Therefore we will define useful classical gauge transformations which will remain a symmetry of the system, even after a classical background is fixed. At the end of this section we will discuss the interpretation of dynamical localization on fixed backgrounds.

3.1 QGR as low-energy effective theory

Because we do not yet know the microscopic degrees of freedom (d.o.f.) of spacetime, we are forced to work within an effective description of quantum gravity in order to make predictions. Therefore and for many other reasons, effective field theory methods were developed which provide a controlled way of investigating the low-energy behavior of quantum gravity. In order to formulate an effective field theory of quantum gravity we first have to identify possible low-energy d.o.f. and their (gauge) symmetries. As low-energy d.o.f. we choose the metric field g , which classically describes spacetime very well and define the theory to be invariant under the gauge symmetry induced by classical diffeomorphisms.

With this choice we can write down the most general action for a theory respecting these conditions as

$$S = \int d^4x \sqrt{-g} \left(\Lambda + \frac{2}{\kappa^2} R + aR^2 + bR_{\mu\nu}R^{\mu\nu} + cR_{\mu\nu\alpha\beta}R^{\mu\nu\alpha\beta} + dD_\mu D_\nu R^{\mu\nu} + e\Box R + \frac{f}{M^2} R^3 + \dots \right), \quad (3.1)$$

where $\kappa = \sqrt{32\pi}/M_{\text{pl}}$, Λ is the cosmological constant, $M \leq M_{\text{pl}}$ is an energy scale larger than typical energies of the problem, and all other constants are dimensionless. Because of experimental observations we know that the cosmological constant is very small. For our purpose we can assume its renormalized value to vanish. The other constants a, b, c, \dots are assumed not to be unnaturally large in order to avoid conflicts with existing experiments.

These are only some of the operators one can write down in the action. We see that higher order operators like e.g. R^3 come with a suppression factor $\frac{1}{M^n}$, where n is some positive integer, while the operator used in the Einstein Hilbert action gets enhanced by a factor of M_{pl}^2 .

In classical GR one now argues that if the curvature R is small compared to the scale M^2 and does not vary fast, i.e. $D_\mu R^{\mu\nu} \ll M^3$ in some appropriate way, one can neglect the higher order terms and the Einstein Hilbert action is a good approximation to the problem. The higher order terms just give corrections of order R/M_{pl}^2 or $DR/(M_{\text{pl}}^2 M)$, where by DR we mean some derivatives of R .

In our work we do not describe the dynamics of the metric field itself, but only describe small fluctuations around some fixed background. We will see later that in this case we can also identify relevant and irrelevant terms of the action, where the irrelevant terms will be suppressed by powers of E/M_{pl} , where E is the graviton energy.

3.2 Pseudo-local observables in QGR from clock and rod variables

Because of the symmetries of our effective theory the low-energy observations should also be invariant under these symmetries. The problem is that diffeomorphism invariance prohibits the straightforward definition of local observables, because any local scalar observable $O(x)$ will in general change under diffeomorphisms and therefore is not a Dirac observable. One way out is to integrate local or multilo-cal observables over the whole spacetime which can be shown to be diffeomorphism invariant neglecting boundary terms [1].

The problem with these integrated observables is that we loose the concept of locality. This leads to a serious problem, since our theory should be capable to explain experiments in laboratories which are definitely local.

There have been many attempts to restore locality in an appropriate sense by defining relational observables, see [1] and references therein. The basic idea of relational observables is as follows:

Since general relativity describes the universe as a closed system, the emergence and definition of space and time has to be intrinsic. We will therefore use dynamical variables of the system, like for example metric or matter d.o.f., in order to define spatial locations and time relative to them. These variables will from now on be called clock and rod variables.

For a classical example assume a wooden rod and a mechanical clock. If these variables are in an appropriate state, e.g. the clock performs periodic oscillations, we can define time distances by counting these oscillations and space distances by using the rod. Local observations now can be performed by combining clocks and rods with a suitable subsystem on which we will perform measurements. For a classical example assume another oscillator with some time dependent frequency located at some spatial position relative to the rod. We are interested in the frequency of this oscillator averaged over some finite time interval. Using parameter time leads to a gauge variant observable and is therefore useless. But we can use our mechanical clock and rod and build some gauge invariant observable like $O := \int d^4x \sqrt{-g} O_{\text{clock}}(x) O_{\text{device}}(x)$, where $O_{\text{device}}(x)$ is a function depending on rod and observed system and $O_{\text{clock}}(x)$ is dependent on the clock variable. Now assume that $O_{\text{clock}}(x)$ is 1 if the clock is switched on and 0 else and that $O_{\text{device}}(x)$ gives delta functions on the parameter coordinates when the maximal amplitude of the observed oscillator is reached. Then O gives the number of oscillations of the investigated subsystem during the time interval defined by the number of oscillations of the clock, which is the averaged frequency, in a diffeomorphism invariant and relative way. Since the observable O defines a local quantity through a nonlocal observable by applying a suitable state, it is called a pseudo-local observable.

But now let us turn to quantum physics. In scenarios where the quantum nature of space and time plays a role we do not expect classical clocks and rods to be appropriate candidates for clock and rod variables. We expect more suitable candidates to be matter quantum fields or metric d.o.f.. The definition of pseudo-local observables by using these quantum clocks and rods works in the same way.

At this point it is useful to give an example of such a clock variable in a simple quantum system. We use the minisuperspace model of isotropic and homogeneous cosmology, in which the variable to be quantized is the scale factor operator \hat{a} of the universe. In our toy universe there has to be some matter too in order to register the evolution of the universe. We see easily that \hat{a} is not invariant under diffeomorphisms, which are reduced to time reparametrizations because of isotropy and homogeneity. But under certain circumstances we can use \hat{a} as a clock variable relative to which one can describe the flow of time.

If the state of the universe $|\psi\rangle$ is such that it can be interpreted as monotonically growing we can use \hat{a} for defining time, because our intuition would say that big values of \hat{a} correspond to late times at least classically. If we now are interested in some observable $O(t)$ at the “time” when $\langle\psi|\hat{a}|\psi\rangle$ reaches a value

τ , we can define it in a diffeomorphism invariant way by some operator like

$$O = \int dt O(t) \delta(\hat{a}(t) - \tau) . \quad (3.2)$$

By the Dirac δ -function we mean an appropriate regularization of it, maybe through a Gaussian function with small width. This δ -function acts as a projection operator onto the eigenstate of \hat{a} corresponding to the eigenvalue τ .

In a state $|\psi\rangle$ with the properties described above the expectation value of O will be

$$\langle\psi|O|\psi\rangle \simeq \langle O(\tau)\rangle , \quad (3.3)$$

where $\langle O(\tau)\rangle$ is the expectation value of the system observable in the system state encoded in $|\psi\rangle$ at the time the universe has a scale factor τ .

The important point is that the interpretation of locality depends on both, the state and the observable under consideration.

In this work we will use wave packet states of matter clock and rod fields in order to perform localization. In this approach the basic idea is to construct diffeomorphism invariant operators

$$O = \int \prod_{i=1}^N d^4x_i \sqrt{-g} O_{\text{system}}(x_1, \dots, x_N) O_{\text{clock-rod}}(x_1, \dots, x_N) , \quad (3.4)$$

such that taking matrix elements between suitable states $|\psi_1\rangle$ and $|\psi_2\rangle$ leads to

$$\langle\psi_1|O|\psi_2\rangle \sim \int_{\mathcal{V}} \prod_{i=1}^N d^4x_i \sqrt{-g} \langle O_{\text{system}}(x_1, \dots, x_N)\rangle . \quad (3.5)$$

Here \mathcal{V} denotes some region in the product manifold \mathcal{M}^N defined through the wave packets of the clock and rod fields contained in the states $|\psi_1\rangle$ and $|\psi_2\rangle$, and $\langle O_{\text{system}}\rangle$ is the expectation value of the system observable in the system state, which is also encoded in $|\psi_1\rangle$ and $|\psi_2\rangle$.

Since localization always requires energy, and since energy causes backreaction on the metric, there are restrictions on how precise localization can be performed until the quantum nature of spacetime and/or strong curvature effects set a cutoff. There are several ways to address the issue of localization from which we use the perturbative formulation of quantum gravity on a fixed background. In this framework we can give an estimation of the limits on localization by calculating the backreaction during localization. More details about the interpretation of dynamical localization on a fixed background are given in section 3.6.

As a final remark, the idea of integrating over the whole spacetime with the diffeomorphism invariant measure is equivalent to applying group averaging over the group of four-diffeomorphisms. This is how this idea of defining observables connects to a general treatment of gauge theories, where group averaging is one specific method to generate gauge invariant expressions out of gauge variant ones.

3.3 QGR with fixed background

The most intuitive access to quantum gravity from a particle physicists point of view is to describe it as the propagation of perturbative gravitons on a fixed, classical background. This approximation can of course only be done if there is a well defined distinction between a classical background and quantum fluctuations on it, which is not always the case. For example in scenarios where strong curvature effects and small distances come into play, like in the vicinity of black holes or the big bang, a separation between classical background and quantum fluctuations is not possible anymore. For these problems one requires a more fundamental theory of quantum gravity.

For the application of quantum gravity in nonsingular systems, like e.g. colliders if there are large extra dimensions, we expect that a separation of background and gravitons can be done until some threshold energy is reached where nonperturbative effects come into play. The background in these cases is assumed to be a smooth manifold, in particular a Minkowski space in our case.

In the following part of this chapter we present the method of how this separation can be done and which are the relevant terms for low-energy effective field theories. The energy scale M defined above will from now on be set to M_{pl} , because we expect the scale of new physics connected to quantum gravity to be the Planck mass.

The starting point is the expansion of the classical metric field g and its inverse g^{-1} around a classical background η , which is not necessarily flat. This expansion is given by

$$g_{\mu\nu} = \eta_{\mu\nu} + \kappa h_{\mu\nu} \quad (3.6)$$

$$g^{\mu\nu} = \eta^{\mu\nu} - \kappa h^{\mu\nu} + \kappa^2 h^\mu_\lambda h^{\lambda\nu} + \mathcal{O}(\kappa^3) , \quad (3.7)$$

where h denotes the graviton field and κ is used in this expansion in order to give h the dimension of a bosonic field. It is important to note that the indices of tensors on a fixed background are raised and lowered by the background metric. It can be seen that if we want to avoid inverse powers of the h field, which will cause problems during quantization, the expansion of the inverse metric includes terms of all orders in κ .

Since this expansion is systematic in κ we can calculate low-energy effective theories by collecting all terms up to a given order in κ from the general action (3.1) by inserting the expansion of the metric. The order in κ used for defining the effective field theory will depend on the problem and the precision one requires, because higher orders in κ are suppressed by powers of E/M_{pl} , where E is a typical energy of the problem we describe.

The required quantities for the κ expansion of the action (3.1) are the square root of the metric $\sqrt{-g}$, the Christoffel connection $\Gamma^\mu_{\alpha\beta}$ and the Riemann tensor $R^\mu_{\nu\alpha\beta}$ together with its contractions. These quantities can be calculated up to arbitrary order by inserting the expansion (3.6) into the definition of these geometric objects given in (2.6). This expansion and the expansion of the graviton action itself will be explicitly performed in section 3.5.

3.4 Gauge transformations with fixed background

When we fix a background and describe only fluctuations on it as the dynamical variables we manifestly break the usual diffeomorphism invariance. But there remains a residual gauge symmetry of the theory on a fixed background which we can identify if we reformulate the diffeomorphism transformation.

The usual symmetry transformation of the metric field g is given by the pullbacks of the infinitesimal diffeomorphisms

$$x^\mu \rightarrow \tilde{x}^\mu = x^\mu - \kappa \epsilon^\mu(x) , \quad (3.8)$$

where we used κ in order to make the vector field $\epsilon(x) = \sum \epsilon^\alpha \partial_\alpha$ dimensionless. The induced transformation on the chart representation of the metric is given by the pullbacks

$$\begin{aligned} g_{\mu\nu}(x) &\rightarrow \tilde{g}_{\mu\nu}(\tilde{x}) = \frac{\partial x^\alpha}{\partial \tilde{x}^\mu} \frac{\partial x^\beta}{\partial \tilde{x}^\nu} g_{\alpha\beta}(x) \\ &= g_{\mu\nu}(x) + \kappa (g_{\mu\alpha} \epsilon^\alpha_{,\nu} + g_{\alpha\nu} \epsilon^\alpha_{,\mu}) + \mathcal{O}(\epsilon^2) , \end{aligned} \quad (3.9)$$

and in a similar way the one of the inverse metric by the pushforwards

$$\begin{aligned} g^{\mu\nu}(x) &\rightarrow \tilde{g}^{\mu\nu}(\tilde{x}) = \frac{\partial \tilde{x}^\mu}{\partial x^\alpha} \frac{\partial \tilde{x}^\nu}{\partial x^\beta} g^{\alpha\beta}(x) \\ &= g^{\mu\nu}(x) - \kappa (g^{\mu\alpha} \epsilon^\nu_{,\alpha} + g^{\alpha\nu} \epsilon^\mu_{,\alpha}) + \mathcal{O}(\epsilon^2) . \end{aligned} \quad (3.10)$$

Fixing the background in these equations by inserting the expansion (3.6) will cause problems, because this symmetry transformation directly acts on spacetime by transforming the argument x too. A better suited transformation which can be fixed on a background is the one where we remove the spacetime dependent part by defining the $\tilde{\delta}$ gauge transformation as

$$\tilde{\delta} O := \tilde{O}(x) - O(x) = \delta O + \kappa O_{,\alpha} \epsilon^\alpha , \quad (3.11)$$

where O is some function of the variables (metric or matter fields) and δO is its transformation induced by diffeomorphisms.

With this definition we get the $\tilde{\delta}$ gauge transformations of the background η and the fluctuations h as

$$\tilde{\delta}\eta_{\mu\nu} = 0 \quad (3.12)$$

$$\tilde{\delta}\eta^{\mu\nu} = 0 \quad (3.13)$$

$$\tilde{\delta}h_{\mu\nu} = \eta_{\mu\alpha}\epsilon_{,\nu}^{\alpha} + \eta_{\alpha\nu}\epsilon_{,\mu}^{\alpha} + \eta_{\mu\nu,\alpha}\epsilon^{\alpha} + \kappa \left(h_{\mu\alpha}\epsilon_{,\nu}^{\alpha} + h_{\alpha\nu}\epsilon_{,\mu}^{\alpha} + h_{\mu\nu,\alpha}\epsilon^{\alpha} \right) \quad (3.14)$$

$$\tilde{\delta}h^{\mu\nu} = \eta^{\mu\alpha}\epsilon_{,\alpha}^{\nu} + \eta^{\alpha\nu}\epsilon_{,\alpha}^{\mu} - \eta^{\mu\nu,\alpha}\epsilon^{\alpha} + \kappa \left(h_{\beta}^{\mu}\eta^{\nu\alpha}\epsilon_{,\alpha}^{\beta} + h_{\beta}^{\nu}\eta^{\mu\alpha}\epsilon_{,\alpha}^{\beta} + \eta^{\mu\alpha}\eta^{\nu\beta}h_{\alpha\beta,\gamma}\epsilon^{\gamma} \right). \quad (3.15)$$

One easily sees from a short calculation that these transformations respect the background structure, i.e.

$$\tilde{\delta}h_{\mu\nu} = \eta_{\mu\alpha}\eta_{\nu\beta}\tilde{\delta}h^{\alpha\beta} \quad (3.16)$$

$$\tilde{\delta}h^{\mu\nu} = \eta^{\mu\alpha}\eta^{\nu\beta}\tilde{\delta}h_{\alpha\beta}, \quad (3.17)$$

and therefore are well defined.

The next step is to work out the $\tilde{\delta}$ transformation for matter field. Since we do not need fermionic matter in the following, and fermionic matter requires a reformulation of gravity in the sense of vielbein variables, we do not need to work out their gauge transformations. Hence a general matter field V , for our purpose, is a (p, q) -tensor field and transforms under the diffeomorphisms (3.8) as given by the pullbacks and pushforwards, i.e.

$$V_{\beta_1\dots\beta_q}^{\alpha_1\dots\alpha_p}(x) \rightarrow \tilde{V}_{\beta_1\dots\beta_q}^{\alpha_1\dots\alpha_p}(\tilde{x}) = \frac{\partial\tilde{x}^{\alpha_1}}{\partial x^{\mu_1}} \dots \frac{\partial\tilde{x}^{\alpha_p}}{\partial x^{\mu_p}} \frac{\partial x^{\nu_1}}{\partial\tilde{x}^{\beta_1}} \dots \frac{\partial x^{\nu_q}}{\partial\tilde{x}^{\beta_q}} V_{\nu_1\dots\nu_q}^{\mu_1\dots\mu_p}(x). \quad (3.18)$$

The definition of the $\tilde{\delta}$ transformation is according to (3.11) and given by

$$\tilde{\delta}V_{\beta_1\dots\beta_q}^{\alpha_1\dots\alpha_p}(x) := \tilde{V}_{\beta_1\dots\beta_q}^{\alpha_1\dots\alpha_p}(x) - V_{\beta_1\dots\beta_q}^{\alpha_1\dots\alpha_p}(x) = \delta V_{\beta_1\dots\beta_q}^{\alpha_1\dots\alpha_p}(x) + \kappa\epsilon^{\mu}\partial_{\mu}V_{\beta_1\dots\beta_q}^{\alpha_1\dots\alpha_p}(x), \quad (3.19)$$

where the indices are taken with respect to the background.

For completeness we give the explicit form of the $\tilde{\delta}$ gauge transformation for a scalar field ϕ and a vector field $A = \sum A^{\mu}\partial_{\mu}$. They read

$$\tilde{\delta}\phi = \kappa\epsilon^{\nu}\partial_{\nu}\phi \quad (3.20)$$

$$\tilde{\delta}A^{\mu} = -\kappa\epsilon_{,\nu}^{\mu}A^{\nu} + \kappa\epsilon^{\nu}\partial_{\nu}A^{\mu}. \quad (3.21)$$

It can be shown that the $\tilde{\delta}$ gauge transformations commute with the background covariant derivatives. This is required for representing this symmetry transformation in the Poisson algebra. It shows that the $\tilde{\delta}$ transformations are more natural for the investigation of theories on a fixed background than the usual δ transformations, since these do not have this important property.

As a final step in this section we can state the following

Proposition 1. *Let $S = \int d^4x \sqrt{-g}\hat{\mathcal{L}}$ be a diffeomorphism invariant action for the metric field g and some matter fields. Then the theory on a fixed background η is invariant under the isometrics of the background η and the $\tilde{\delta}$ gauge transformations of the fluctuations h and matter fields, if appropriate boundary (or falloff) conditions hold true. The background fixed Lagrangian is given by $\mathcal{L} = \sqrt{-g}/\sqrt{-\eta}\hat{\mathcal{L}}$.*

Proof. The proof of the isometric invariance is trivial since the theory on a fixed background inherits this structure from the former theory. The $\tilde{\delta}$ invariance of the fluctuations can be proven by a short calculation

$$\begin{aligned} 0 &= \delta S = \int \delta(d^4x) \sqrt{-g}\hat{\mathcal{L}} + \int d^4x \delta(\sqrt{-g}\hat{\mathcal{L}}) = \\ & \int d^4x \left(-\kappa\epsilon_{,\mu}^{\mu}\sqrt{-g}\hat{\mathcal{L}} + \delta(\sqrt{-g}\hat{\mathcal{L}}) \right) \stackrel{\text{P.I.}}{=} \int d^4x \left(\kappa\epsilon^{\mu}(\sqrt{-g}\hat{\mathcal{L}})_{,\mu} + \delta(\sqrt{-g}\hat{\mathcal{L}}) \right) \\ &= \int d^4x \tilde{\delta}(\sqrt{-g}\hat{\mathcal{L}}) = \int d^4x \sqrt{-\eta} \tilde{\delta}(\sqrt{-g}/\sqrt{-\eta}\hat{\mathcal{L}}) = \tilde{\delta}S, \quad (3.22) \end{aligned}$$

where P.I. denotes integration by parts and we have used $\tilde{\delta}\eta = 0$ in the last line. The technical assumption of appropriate boundary conditions was in order to avoid boundary terms while performing integration by parts. \square

With the tools developed in this section we can define theories of metric fluctuations and matter fields on a fixed background and investigate them like usual gauge theories..

3.5 Graviton expansion of geometric quantities and the Einstein-Hilbert action

This section is devoted to the κ expansion of the geometric quantities and the graviton action around a flat Minkowski background. Since the required calculations are straightforward we will only state the results without explanations.

The expansion of the geometric quantities up to the required order in κ are given by

$$\sqrt{-g} = 1 + \frac{\kappa}{2}h - \frac{1}{4}\kappa^2 h^\alpha_\beta h^\beta_\alpha + \frac{1}{8}\kappa^2 h^2 + \mathcal{O}(\kappa^3) \quad (3.23)$$

$$\Gamma^\lambda_{\alpha\beta} = \frac{\kappa}{2} \left(h^\lambda_{\beta,\alpha} + h^\lambda_{\alpha,\beta} - h^\lambda_{\alpha\beta} \right) - \frac{\kappa^2}{2} h^{\lambda\sigma} \left(h_{\beta\sigma,\alpha} + h_{\alpha\sigma,\beta} - h_{\alpha\beta,\sigma} \right) + \mathcal{O}(\kappa^3) \quad (3.24)$$

$$R := R^{(0)} + \kappa R^{(1)} + \kappa^2 R^{(2)} + \mathcal{O}(\kappa^3) \quad (3.25)$$

$$R^{(0)} = 0 \quad (3.26)$$

$$R^{(1)} = h_{,\mu}^{\cdot\mu} - h_{\mu\nu}^{\cdot\mu,\nu} \quad (3.27)$$

$$\begin{aligned} R^{(2)} = & \frac{1}{2} \left(h^{\lambda\sigma} (2h_{\mu\sigma}^{\cdot\mu} - h_{,\sigma}) \right)_{,\lambda} - \frac{1}{2} \left(h^{\lambda\sigma} h_{\lambda\sigma,\mu} \right)^{\cdot\mu} \\ & + \frac{1}{4} \left(-h_{\mu\nu,\lambda} h^{\mu\nu,\lambda} + 2h_{\mu\nu,\lambda} h^{\mu\lambda,\nu} - 2h_{,\nu} h^{\nu\mu}_{,\mu} + h_{,\mu} h^{\cdot\mu} - 2h^{\mu\nu} h_{,\mu,\nu} \right. \\ & \left. - 2h^{\mu\nu} h_{\mu\nu,\lambda} + 4h^{\mu\nu} h_{\mu\lambda,\nu} \right) . \end{aligned} \quad (3.28)$$

The graviton action can be calculated from the Einstein-Hilbert action by using (3.6), (3.23) and (3.25). In the following we require this action only up to order κ^0 . It is given by

$$S = \int d^4x \left(\frac{1}{2} h_{\mu\nu,\lambda} h^{\mu\nu,\lambda} - \frac{1}{2} h_{,\mu} h^{\cdot\mu} + h_{,\mu} h^{\mu\nu}_{,\nu} - h_{\mu\nu,\lambda} h^{\mu\lambda,\nu} \right) + \mathcal{O}(\kappa) . \quad (3.29)$$

This action agrees with the result of [16] and it can be shown to be invariant under the $\tilde{\delta}$ gauge transformations (3.12) in this particular order in κ .

The ghost and gauge fixing Lagrangian for the de Donder (or harmonic) gauge are given by

$$\mathcal{L}_{\text{ghost}} = -\bar{C}^\mu C_{\mu,\lambda}^{\cdot\lambda} \quad (3.30)$$

$$\mathcal{L}_{\text{GF}} = \left(h_{\mu\nu}^{\cdot\nu} - \frac{1}{2} h_{,\mu} \right) \left(h^{\mu\lambda}_{,\lambda} - \frac{1}{2} h^{\cdot\mu} \right) , \quad (3.31)$$

where C^μ and \bar{C}^μ are the hermitian ghosts and antithermitian antighosts, respectively. Furthermore the sum $\mathcal{L}_{\text{ghost}} + \mathcal{L}_{\text{GF}}$ is invariant under the BRST transformations

$$\delta_{\text{BRST}} C^\mu = 0 \quad (3.32)$$

$$\delta_{\text{BRST}} \bar{C}^\mu = h^{\mu\nu}_{,\nu} - \frac{1}{2} h^{\cdot\mu} \quad (3.33)$$

$$\delta_{\text{BRST}} h_{\mu\nu} = C_{(\mu,\nu)} . \quad (3.34)$$

More details on the BRST formulation and gauge fixing of linearized gravity will be given in chapter 4.

If we turn on graviton-matter interactions there will occur divergences coming from graviton induced matter tadpoles. In order to absorb these divergences we require an additional cosmological constant action given by

$$S_\Lambda = \frac{\kappa}{2}\Lambda \int d^4x h + \mathcal{O}(\kappa^2). \quad (3.35)$$

It will be used to eliminate graviton tadpoles by renormalizing the cosmological constant as shown in the appendix C.

The graviton expanded matter actions will be given in the corresponding chapters where they are required.

3.6 Dynamical localization of pseudo-local operators on semiclassical fixed backgrounds

In this thesis we work on a fixed background and describe dynamical gravity as fluctuations around the background metric in terms of gravitons. In this picture we can apply standard quantum measurement theory in terms of a semiclassical apparatus and a quantum system on which measurements are performed. This section is devoted to explain qualitatively the emergence and breakdown of this semiclassical approach to geometry and how this breakdown is related to dynamical localization.

Assume an early universe in a full quantum state of matter and geometry. In this region in spacetime the definition and interpretation of locality, in particular local measurements, is not possible in the sense of standard quantum measurement theory, since there is no separation between a sufficiently large semiclassical apparatus, the measuring device, and the subsystem on which measurements are performed. Hence our formalism can not be applied to this region.

Now assume that through some mechanism like e.g. decoherence the universe evolves into some state which contains a sufficiently large semiclassical subsystem. Assume further that this subsystem also contains the metric d.o.f. which is in agreement with the cosmological observation that the geometry of the universe became classical at a very early stage. This state now can be approximated by a classical background state and some matter and graviton quantum state on it. The classical background state can contain classical matter d.o.f. too, e.g. an apparatus producing and measuring quantum matter wave packet states.

In this work we assume for simplicity that the classical metric state is a flat Minkowski space. But in principle the classical metric state can be any smooth manifold. Furthermore we assume the quantum fields on this background to be in their vacuum state.

This classical region in spacetime can now be used in order to perform and interpret local experiments using some classical apparatus and wave packet states defining locality relative to them. Increasing the resolution is associated to increasing the energy of the wave packets, such that at some threshold energy the backreaction of the wave packet states on the geometry will destroy the semiclassicality of this spacetime region. This will be the worst at energies when the overlapping wave packets will create a black hole which is a non-classical geometry state because of the singularity. In this interpretation the limit on localization is reached when the geometry gets too fuzzy. But there is a second slightly different interpretation based on scattering theory.

Since most of today's small scale experiments are scattering experiments which are theoretically described on a fixed background we will not be able to measure the fuzziness of the geometry directly. What we will measure are gravitational effects in loop contributions to scattering processes. These contributions have their origins in quantum and classical geometry effects, but can also depend on the dynamics. Since we are restricted to the description of scattering experiments on a fixed background, the important scale setting the limits on our understanding of locality is the scale where perturbation theory on fixed backgrounds breaks down. This scale can of course be different from the scale mentioned above.

In this work we will follow the second interpretation. Additionally we try to relate the two approaches by studying geometry observables which contain information on pseudo-local geometry. With these observables we try to find out the nature of backreaction of wave packets, in particular if it is a classical or quantum effect.

Chapter 4

Canonical BRST formulation of linearized QGR on a flat background

In this chapter we study the canonical BRST formulation of linearized gravity on a flat background in order to compare it with existing results from path integral quantization [17]. We will study the constraint structure of the theory and perform the BRST extension of the phase space. The resulting classical BRST invariant system will be quantized using an auxiliary Fock space and afterwards reduced to the physical, i.e. BRST invariant, degrees of freedom. In particular we will focus on the cohomological aspects of the one- and multi-graviton Hilbert space.

Additionally we have investigated the physical states in the presence of classical matter. The result is given in appendix B, since it is not directly connected to this work. It shows connections to Newton's gravitational potential.

4.1 Hamiltonian and constraint algebra

Performing the κ expansion of the general action (3.1) to lowest order in κ on flat Minkowski background one gets

$$S = \int d^4x \left(\frac{1}{2} h_{\mu\nu,\lambda} h^{\mu\nu,\lambda} - \frac{1}{2} h_{,\mu} h^{,\mu} + h_{,\mu} h^{\mu\nu}{}_{,\nu} - h_{\mu\nu}{}^{,\nu} h^{,\mu\lambda}{}_{,\lambda} \right). \quad (4.1)$$

Since there are only quadratic terms, this action describes a free spin 2 particle propagating on a flat background neglecting the graviton selfinteraction. The action (4.1) can be shown to be invariant under the $\tilde{\delta}$ gauge transformations given by (3.12) up to order κ^0 .

In order to perform the Legendre transformation we need to calculate the conjugate momenta $\pi^{\mu\nu}$ of the variables $h_{\mu\nu}$. Therefore we use the symmetrized functional derivatives defined by

$$\frac{\delta h_{\mu\nu}(x)}{\delta h_{\alpha\beta}(y)} := \delta_{(\mu}^{\alpha} \delta_{\nu)}^{\beta} \delta(x-y) = \frac{1}{2} (\delta_{\mu}^{\alpha} \delta_{\nu}^{\beta} + \delta_{\mu}^{\beta} \delta_{\nu}^{\alpha}) \delta(x-y). \quad (4.2)$$

The momenta corresponding to $h_{\mu\nu}$ are given by

$$\pi^{00} = h_{0j,j} \quad (4.3)$$

$$\pi^{0i} = -\frac{1}{2} (h_{00,i} - h_{jj,i}) - h_{ij,j} \quad (4.4)$$

$$\pi^{ij} = h_{ij,0} + \delta_{ij} (h_{0k,k} - h_{kk,0}). \quad (4.5)$$

Solving them for the time derivatives of h we get primary constraints, because the system of equations (4.3) and (4.4) can not be solved for $h_{00,0}$ and $h_{0i,0}$. Therefore we get the solutions

$$h_{ij,0} = \pi^{ij} - \frac{1}{2} \delta_{ij} (\pi^{kk} - h_{0k,k}) \quad (4.6)$$

and the smeared primary constraints

$$\chi^{(0)}(f) = \int d^3x f(\mathbf{x}) (\pi^{00} - h_{0j,j})(\mathbf{x}) \quad (4.7)$$

$$\chi^{(i)}(f) = \int d^3x f(\mathbf{x}) (\pi^{0i} + \frac{1}{2}h_{00,i} - \frac{1}{2}h_{jj,i} + h_{ij,j})(\mathbf{x}) . \quad (4.8)$$

Performing the Legendre transformation of the Lagrangian we arrive at the following Hamiltonian

$$H = \int d^3x \left(\frac{1}{2}(\pi^{ij})^2 - \frac{1}{4}(\pi^{kk})^2 + \frac{1}{2}\pi^{jj}h_{0k,k} + \frac{1}{4}(h_{0k,k})^2 - (h_{0j,k})^2 + \frac{1}{2}(h_{ij,k})^2 \right. \\ \left. - \frac{1}{2}(h_{jj,i})^2 + h_{00,i}h_{jj,i} - h_{00,i}h_{ij,j} + h_{kk,i}h_{ij,j} - (h_{ij,j})^2 \right) . \quad (4.9)$$

Having the Hamiltonian of the system we can calculate the time evolution of the constraints in order to get possible secondary constraints χ_s . For the time evolution we omit the addition of the constraints with Lagrange multipliers to the Hamiltonian, since the primary constraints have vanishing Poisson brackets so that additional gauge transformations will not contribute to the secondary constraints. The secondary constraints are given by

$$\chi_s^{(0)}(f) := \dot{\chi}^{(0)}(f) = \{\chi^{(0)}(f), H\} = \int d^3x f(\mathbf{x}) (\Delta h_{jj} - h_{ij,i,j})(\mathbf{x}) \quad (4.10)$$

$$\chi_s^{(i)}(f) := \dot{\chi}^{(i)}(f) = \{\chi^{(i)}(f), H\} = \int d^3x f(\mathbf{x}) (\pi^{ij}_{,j} - \Delta h_{0i})(\mathbf{x}) . \quad (4.11)$$

The tertiary constraints are given by

$$\ddot{\chi}^{(0)}(f) = \int d^3x \partial_i f(\mathbf{x}) \chi_s^{(i)}(\mathbf{x}) \quad (4.12)$$

$$\ddot{\chi}^{(i)}(f) = 0 \quad (4.13)$$

and do not give rise to new constraints, since they can be expressed in terms of the other constraints. Given all 8 constraints of our system we arrive at $10 - 8 = 2$ physical d.o.f. which can be interpreted as the two helicity states of the graviton.

Calculating the Poisson brackets between the constraints one obtains that our system has an abelian constraint algebra, i.e.

$$\{\chi^a, \chi^b\} = 0 \quad \forall a, b , \quad (4.14)$$

where a, b are indices labeling the whole set of constraints, i.e. primary and secondary. This and the fact that we are dealing with a free field theory will simplify the application of the BRST formalism, in particular its quantization, in a dramatic manner.

4.2 Algebraically generated gauge transformations

Given the constraints (4.7) and (4.10) we can study the gauge transformations that they generate by their Hamilton vector fields on the subspace of configuration variables. Therefore we calculate the Poisson brackets of the smeared constraints with the graviton field h . We arrive at

$$\{h_{\mu\nu}(t_0, \mathbf{x}), \chi^{(0)}(f)\} = \delta_{\mu}^0 \delta_{\nu}^0 f(\mathbf{x}) \quad (4.15)$$

$$\{h_{\mu\nu}(t_0, \mathbf{x}), \chi^{(i)}(f_i)\} = \delta_{(\mu}^0 \delta_{\nu)}^i f_i(\mathbf{x}) \quad (4.16)$$

$$\{h_{\mu\nu}(t_0, \mathbf{x}), \chi_s^{(0)}(g)\} = 0 \quad (4.17)$$

$$\{h_{\mu\nu}(t_0, \mathbf{x}), \chi_s^{(i)}(g_i)\} = -\delta_{(\mu}^i \delta_{\nu)}^j \partial_j g_i(\mathbf{x}) . \quad (4.18)$$

Comparing the result with (3.12) we see that the constraints generate the desired gauge transformations up to order κ^0 by identifying

$$f(\mathbf{x}) = 2\epsilon_{0,0}(t_0, \mathbf{x}) \quad (4.19)$$

$$f_i(\mathbf{x}) = 2\epsilon_{0,i}(t_0, \mathbf{x}) + 2\epsilon_{i,0}(t_0, \mathbf{x}) \quad (4.20)$$

$$g_i(\mathbf{x}) = -2\epsilon_i(t_0, \mathbf{x}), \quad (4.21)$$

where t_0 is the time when we perform the gauge transformations.

So we have shown that up to leading order in κ the gauge transformations (3.12) defined from purely geometrical assumptions can be induced out of the Poisson algebra. This will be necessary for later representing the gauge transformations as operators on some Hilbert space.

4.3 BRST charge and minimal BRST invariant Hamiltonian

By knowing the constraint structure of our system we can calculate the BRST charge and the minimal BRST invariant extension of the Hamiltonian. Since we have an abelian constraint algebra the BRST charge (2.30) has an easy form given by

$$\Omega_{\text{BRST}} = \chi^a [\eta^a], \quad (4.22)$$

where a is an index running over all constraints and η^a are the corresponding ghost fields.

In order to get the minimal BRST invariant Hamiltonian one has to calculate the coefficients V^{ab} defined in (2.21). For our system the minimal BRST invariant extension of the Hamiltonian (2.31) is given by

$$H_{\text{min}} = H - \eta^{(0)} [\bar{\eta}_s^{(0)}] - \eta^{(i)} [\bar{\eta}_s^{(i)}] + \eta_s^{(0)} [\partial_i \bar{\eta}_s^{(i)}]. \quad (4.23)$$

The next step is to use the freedom of adding an exact functional to the Hamiltonian in order to manipulate the dynamics of the gauge variant parts. This addition of an exact functional does not change physics, i.e. the gauge equivalence classes, due to a theorem by Henneaux [18].

4.4 Exact functionals for extending the Hamiltonian

In this chapter we will construct the most general exact functional for extending the minimal BRST invariant Hamiltonian and therefore gauge fixing it suitably for our purposes. The conditions for possible Hamiltonian extensions \mathcal{O} are as follows:

- \mathcal{O} has dimension 1, since the Hamiltonian is the energy functional
- \mathcal{O} has to be local
- \mathcal{O} has to be real
- \mathcal{O} has to be invariant under spatial SO(3) rotations
- \mathcal{O} has to be bosonic, i.e. no odd powers of ghost fields are allowed
- \mathcal{O} has to be of ghost number 0, i.e. the power of ghost and antighost fields in each summand must agree
- \mathcal{O} has to be quadratic in the fields in order to introduce no unphysical couplings which would complicate our problem.

Now assume \mathcal{O} to be an exact functional, i.e. $\mathcal{O} := \{\Omega_{\text{BRST}}, \Psi\}$. Then the conditions posed above lead to the following expression

$$\Psi := \psi^{(0)} [\bar{\eta}^{(0)}] + \psi^{(i)} [\bar{\eta}^{(i)}] + \psi_s^{(0)} [\bar{\eta}_s^{(0)}] + \psi_s^{(i)} [\bar{\eta}_s^{(i)}], \quad (4.24)$$

where all ψ^a are real and linear in the bosonic fields. Another restriction is that the dimension of Ψ is 0 such that $\{\Omega_{BRST}, \Psi\}$ has dimension 1. This constrains the dimension of the primary ψ to $[\psi^{(a)}(\mathbf{x})] = 2$ and of the secondary ψ to $[\psi_s^{(a)}(\mathbf{x})] = 1$. Since all bosonic field variables and derivatives have dimension 1 and we have no natural energy scale in linearized pure gravity, the following expressions hold true

$$\psi^{(0)} = c_1 h_{0j,j} + c_2 \pi^{00} + c_3 \pi^{jj} \quad (4.25)$$

$$\psi^{(i)} = c_4 h_{00,i} + c_5 h_{jj,i} + c_6 h_{ij,j} + c_7 \pi^{0i} \quad (4.26)$$

$$\psi_s^{(0)} = c_8 h_{00} + c_9 h_{jj} \quad (4.27)$$

$$\psi_s^{(i)} = c_{10} h_{0i}, \quad (4.28)$$

where c_i are real dimensionless constants. This leads to the following expression for the 10 parameter family of exact functionals

$$\begin{aligned} \{\Omega_{BRST}, \Psi\} = & -\psi^a[\chi^a] + (c_4 - \frac{c_7}{2})\eta^{(0)}[\partial_i \bar{\eta}^{(i)}] - c_8 \eta^{(0)}[\bar{\eta}_s^{(0)}] + \frac{1}{2}(c_1 + c_2 - c_3)\eta^{(i)}[\partial_i \bar{\eta}^{(0)}] \\ & - \frac{c_{10}}{2}\eta^{(i)}[\bar{\eta}_s^{(i)}] + 2c_3 \eta_s^{(0)}[\Delta \bar{\eta}^{(0)}] + \frac{1}{2}(c_6 - c_7)\eta_s^{(i)}[\Delta \bar{\eta}^{(i)}] + (c_5 + \frac{c_6}{2})\eta_s^{(i)}[\partial_i \partial_j \bar{\eta}^{(j)}] - c_9 \eta_s^{(i)}[\partial_i \bar{\eta}_s^{(0)}] \end{aligned} \quad (4.29)$$

with

$$\begin{aligned} -\psi^a[\chi^a] = & \int d^3x (-c_2(\pi^{00})^2 - (c_1 - c_2)h_{0j,j}\pi^{00} - c_3\pi^{00}\pi^{jj} - c_7(\pi^{0i})^2 \\ & - (c_4 + \frac{c_7}{2})h_{00,i}\pi^{0i} - (c_5 - \frac{c_7}{2})h_{jj,i}\pi^{0i} - (c_6 + c_7)h_{ij,j}\pi^{0i} + c_3h_{0j,j}\pi^{kk} + c_{10}h_{0i,j}\pi^{ij} \\ & + c_1(h_{0k,k})^2 - c_{10}(h_{0i,j})^2 - \frac{c_4}{2}(h_{00,i})^2 - (\frac{c_5 - c_4}{2} - c_8)h_{00,i}h_{jj,i} - (c_4 + c_8 + \frac{c_6}{2})h_{00,i}h_{ij,j} \\ & + (c_9 + \frac{c_5}{2})(h_{jj,i})^2 - c_6(h_{ij,j})^2 - (c_5 + c_9 - \frac{c_6}{2})h_{jj,i}h_{ik,k}). \end{aligned} \quad (4.30)$$

From these expressions we see that the vector space of exact functionals is 10 dimensional. This is a proper subspace of the closed functionals, which can be determined to be 12 dimensional.

4.5 Equations of motion and gauge fixing conditions

In this chapter we will determine the set of parameters c_i such that we arrive at a covariant dynamics for the gravitons and the ghost fields, i.e. we want the following equations of motion (EOM) to hold

$$\square(h_{\mu\nu} - \frac{1}{2}\eta_{\mu\nu}h) = 0 \quad (4.31)$$

$$\square\eta_{s\mu} = 0 \quad (4.32)$$

$$\square\bar{\eta}_\mu = 0, \quad (4.33)$$

where we have identified the configuration variables of the ghosts and antighosts which are common in Lagrangian methods. The choice of these variables is governed by dimensionality arguments, spacelike rotational covariance and hermiticity assignments.

Using the full Hamiltonian $H_{BRST} = H_{\min} + \{\Omega_{BRST}, \Psi\}$ we can calculate the gauge fixed EOM by evaluating the required Poisson brackets. These EOM are given in appendix A.

Demanding the covariant EOM (4.31) for the gravitons and for the covariant ghost fields leads to a set of algebraic equations for the c_i . This set is underdetermined so that we can impose further restrictions.

Since we want to construct the Fock space representation of this theory and determine the tensor structure of the graviton propagator, we will get some more restrictions by demanding a manifestly covariant graviton propagator. In order to achieve this covariant tensor structure we have four possible real solutions for c_i from which we choose the one leading to the simplest Hamiltonian. This solution is given by:

c_1	c_2	c_3	c_4	c_5	c_6	c_7	c_8	c_9	c_{10}
$-\frac{1}{4}$	$-\frac{1}{4}$	$-\frac{1}{2}$	$-\frac{1}{2}$	$\frac{1}{2}$	-1	1	0	0	0

This choice even leads to the covariant graviton EOM $\square h_{\mu\nu} = 0$, which implies (4.31) and the following expressions for the time derivatives of the graviton

$$\dot{h}_{00} = \frac{1}{2}\pi^{00} + \frac{1}{2}\pi^{jj} \quad (4.34)$$

$$\dot{h}_{0i} = -\pi^{0i} \quad (4.35)$$

$$\dot{h}_{ij} = \pi^{ij} + \frac{1}{2}(\pi^{00} - \pi^{kk})\delta_{ij} . \quad (4.36)$$

and the following time derivatives of the ghosts and antighosts

$$\dot{\eta}_s^{(0)} = -\eta^{(0)} \quad , \quad \dot{\eta}_s^{(i)} = -\eta^{(i)} - \partial_i \eta_s^{(0)} \quad (4.37)$$

$$\dot{\bar{\eta}}^{(0)} = \bar{\eta}_s^{(0)} + \partial_i \bar{\eta}^{(i)} \quad , \quad \dot{\bar{\eta}}^{(i)} = \bar{\eta}_s^{(i)} . \quad (4.38)$$

These equations give relations among the time derivatives of the variables and the variables themselves, i.e. they can be used to express some variables through their solved dynamics. This will be fundamental in defining the BRST charge in a suitable form and performing the Fock quantization of the theory.

The only small drawback of this formulation, so far, is that some of the time derivatives of the ghost fields (4.37) come with an additional term which would not be present using standard Lagrangian methods and de Donder gauge fixing. But this problem can be solved by applying a suitable canonical transformation on the ghost sector as shown in the next section.

4.6 Canonical transformation to suitable ghost variables

In this chapter we briefly give the canonical transformation on the ghost sector which cancels the undesired terms in (4.37). Consider the following transformation of the ghost fields and their momenta

$$\eta^{(i)} \rightarrow \Upsilon^{(i)} = \eta^{(i)} + \partial_i \eta_s^{(0)} \quad (4.39)$$

$$\bar{\eta}_s^{(0)} \rightarrow \bar{\Upsilon}_s^{(0)} = \bar{\eta}_s^{(0)} + \partial_i \bar{\eta}^{(i)} , \quad (4.40)$$

where the rest of the variables remain untransformed. It can be shown by a short calculation that this transformation conserves the Poisson bracket and therefore is a canonical transformation.

Using the new variables, the time derivatives of the energy dimension 1 ghost fields are given by

$$\dot{\eta}_s^{(0)} = -\eta^{(0)} \quad , \quad \dot{\eta}_s^{(i)} = -\Upsilon^{(i)} \quad (4.41)$$

$$\dot{\bar{\eta}}^{(0)} = \bar{\Upsilon}_s^{(0)} \quad , \quad \dot{\bar{\eta}}^{(i)} = \bar{\eta}_s^{(i)} , \quad (4.42)$$

which is nicer than (4.37) since it is in accordance to the full covariant ghosts from Lagrangian methods. The new dimension 1 ghost fields also acquire a free covariant EOM by acting a second time derivative on them.

In the following we will always use the new ghost variables Υ and therefore will rename them back to η again. But we have to be careful since we must always keep in mind that in the formulas derived in the sections above the “old” ghost variables appear such that they have to be expressed in terms of the new variables before proceeding.

To be specific and in order to avoid confusion we insert the derived constants c_i into the Hamiltonian $H_{\text{BRST}} = H_{\text{min}} + \{\Omega_{\text{BRST}}, \Psi\}$ and simplify it using the relations between old and new ghosts. This leads to

$$H_{\text{BRST}} = H_{\text{grav}} + H_{\text{ghost}} \quad (4.43)$$

with

$$H_{\text{grav}} = \int d^3x \left(\frac{1}{2}(\pi^{ij})^2 - \frac{1}{4}(\pi^{jj})^2 + \frac{1}{4}(\pi^{00})^2 - (\pi^{0i})^2 + \frac{1}{2}\pi^{00}\pi^{jj} \right. \\ \left. + \frac{1}{4}(h_{00,i})^2 + \frac{1}{2}h_{00,i}h_{jj,i} - \frac{1}{4}(h_{jj,i})^2 + \frac{1}{2}(h_{ij,k})^2 - (h_{0i,j})^2 \right) \quad (4.44)$$

and

$$H_{\text{ghost}} = \int d^3x \left(-\eta^{(0)}\bar{\eta}_s^{(0)} - \eta^{(i)}\bar{\eta}_s^{(i)} - \eta_s^{(0)}\Delta\bar{\eta}^{(0)} - \eta_s^{(i)}\Delta\bar{\eta}^{(i)} \right). \quad (4.45)$$

It can be seen that the ghost fields decouple from the gravitons, as expected, since we investigate the free theory of the graviton. Furthermore it can be checked explicitly that the Poisson bracket between the BRST charge and the Hamiltonian is 0, i.e. the Hamiltonian is strongly BRST invariant. The result for the graviton Hamiltonian and (after the canonical transformation) also the result for the ghost part is in accordance with the result one gets by first applying the harmonic gauge fixing $\mathcal{L}_{\text{GF}} = (h_{\mu\nu} - \frac{1}{2}h_{,\mu})^2$ at Lagrangian level and then performing the Legendre transformation.

4.7 Covariant expression of the BRST charge

The BRST charge of our system reads after the insertion of the new ghost variables

$$\Omega_{\text{BRST}} = \chi^{(0)}[\eta^{(0)}] + \chi^{(i)}[\eta^{(i)}] + (\chi_s^{(0)} + \partial_i\chi^{(i)})[\eta_s^{(0)}] + \chi_s^{(i)}[\eta_s^{(i)}]. \quad (4.46)$$

It can be simplified by using the gauge fixed dynamics to the form

$$\Omega_{\text{BRST}} = i(\chi^{(0)}, \eta_s^{(0)})_{\text{cov}} + i(\chi^{(j)}, \eta_s^{(j)})_{\text{cov}}. \quad (4.47)$$

Here we have used that the gauge fixed time evolution of the theory leads to the following time derivatives of the primary constraints

$$\dot{\chi}^{(0)} = \{\chi^{(0)}, H_{\text{BRST}}\} = \chi_s^{(0)} + \partial_i\chi^{(i)} \quad (4.48)$$

$$\dot{\chi}^{(i)} = \{\chi^{(i)}, H_{\text{BRST}}\} = \chi_s^{(i)}, \quad (4.49)$$

while the time derivatives in the ghost sector are given by (4.41) in term of the new ghost variables.

In order to achieve a full covariant form of the BRST charge, i.e. express the constraints and ghosts in terms of 4-(co)vectors, we define $\eta_{s\mu} := (\eta_s^{(0)}, \eta_s^{(i)})$ to be a 4-covector. This is in accordance to the symmetries in Lagrangian methods, what can be seen by an inverse Legendre transformation of the Hamiltonian. Note that this only holds after the canonical transformation on the ghost sector.

Furthermore it can be checked explicitly that $\chi_\mu := (\chi^{(0)}, -\chi^{(i)})$ is a 4-covector too, by either representing the Noether charge of Lorentz transformations in the Poisson algebra and showing that it leads to a covariant transformation property of the constraint vector or using the EOM to express the constraint vector in an explicit covariant form.

For the first method we have constructed the Noether charge of the Lorentz transformations by Noether's theorem. It is given by the antisymmetric tensorial functional on phase space $Q_{\mu\nu}(h, \pi)$ with the components

$$Q_{0i} = \int d^3x \left(4\pi_{[0\beta}h_{i]}^\beta - x_0\pi^{\alpha\beta}h_{\alpha\beta,i} + \frac{x_i}{2}(\pi^{\alpha\beta}\pi_{\alpha\beta} + h_{\alpha\beta,i}h^{\alpha\beta,i} - \frac{1}{2}\pi^2 - \frac{1}{2}h_{,j}h^{,j}) \right) \quad (4.50)$$

$$Q_{ij} = \int d^3x \left(4\pi_{[i\beta}h_{j]}^\beta - 2x_{[i}\pi^{\alpha\beta}h_{\alpha\beta,j]} \right), \quad (4.51)$$

where $[\dots]$ denotes antisymmetrization. With this charge it can be shown that χ_μ transforms as a 4-covector.

The second method is somewhat easier since the constraint vector can be expressed as

$$\chi_\mu = h_{\mu\nu}{}^{,\nu} - \frac{1}{2}h_{,\mu} \quad (4.52)$$

by using the EOM and therefore is obviously a Lorentz covector. Note that the constraint vector χ_μ is exactly the harmonic gauge fixing condition from the Lagrangian approach. This will be used later in order to compare the BRST approach with the Gupta-Bleuler approach and show their equivalence.

Hence we have the following expression for the BRST charge

$$\Omega_{\text{BRST}} = i(\chi_\mu, \eta_s^\mu)_{\text{cov}} , \quad (4.53)$$

which is a scalar under Lorentz transformations.

This completely covariant form has two advantages. First we can simultaneously diagonalize the BRST charge and the Lorentz group generators such that we can assign a BRST quantum number to representations of the Lorentz group. This will be necessary if we want to investigate the representations of the BRST charge on one particle states. Second, when we quantize this charge it will obviously annihilate the Fock vacuum since the covariant scalar product projects onto the combination of positive-negative frequency solutions and therefore picks out one annihilation operator in each summand.

4.8 Auxiliary Fock space representation

In this section we construct the kinematical Fock space together with a representation of the (auxiliary) observable algebra in terms of the generated associative \star -algebra of linear variables.

Since we have used the freedom of adding BRST invariant terms $\{\Omega_{\text{BRST}}, \Psi\}$ to the Hamiltonian in order to achieve a free and covariant dynamics given by the Hamiltonian (4.43) we can perform the isomorphism from the canonical phase space to the covariant one by the following equations

$$h_{\mu\nu}(t, \mathbf{x}) = \int \widetilde{d^3k} (a_{\mu\nu}(\mathbf{k})e^{-ikx} + a_{\mu\nu}^\dagger(\mathbf{k})e^{ikx}) \quad (4.54)$$

$$\eta_{s\mu}(t, \mathbf{x}) = \int \widetilde{d^3k} (c_\mu(\mathbf{k})e^{-ikx} + c_\mu^\dagger(\mathbf{k})e^{ikx}) \quad (4.55)$$

$$\bar{\eta}_\mu(t, \mathbf{x}) = \int \widetilde{d^3k} (\bar{c}_\mu(\mathbf{k})e^{-ikx} - \bar{c}_\mu^\dagger(\mathbf{k})e^{ikx}) , \quad (4.56)$$

where the operators $a_{\mu\nu}$, c_μ and \bar{c}_μ together with their adjoints represent the annihilation and creation operators. The minus sign in the definition of $\bar{\eta}_\mu$ is due to its antihermiticity.

There are similar expressions for the field momenta in terms of the creation and annihilation operators which can be calculated by inverting the time derivatives of the fields (4.34). We do not specify them here since we only require their existence.

The Fock vacuum $|0\rangle$ is defined by

$$a_{\mu\nu}(f)|0\rangle = c_\mu(f)|0\rangle = \bar{c}_\mu(f)|0\rangle = 0 \quad \forall \text{wave packets } f \in \mathcal{L}^2(\mathcal{M}^4) \quad (4.57)$$

and the wave packet creation and annihilation operators can be expressed as

$$a_{\mu\nu}(f) = (f, h_{\mu\nu})_{\text{cov}} \quad , \quad a_{\mu\nu}^\dagger(f) = -(f^*, h_{\mu\nu})_{\text{cov}} \quad (4.58)$$

$$c_\mu(f) = (f, \eta_{s\mu})_{\text{cov}} \quad , \quad c_\mu^\dagger(f) = -(f^*, \eta_{s\mu})_{\text{cov}} \quad (4.59)$$

$$\bar{c}_\mu(f) = (f, \bar{\eta}_\mu)_{\text{cov}} \quad , \quad \bar{c}_\mu^\dagger(f) = (f^*, \bar{\eta}_\mu)_{\text{cov}} \quad (4.60)$$

where f is a wave packet, i.e. it has a positive frequency spectrum.

Using (4.58) we can determine the (anti-) commutators between the creation and annihilation operators using the canonical (anti-) commutators between the fields and their momenta. They are given by

$$[a_{\mu\nu}(f), a_{\alpha\beta}^\dagger(g)] = (f, g)_{\text{cov}} \frac{1}{2} (\eta_{\mu\alpha}\eta_{\nu\beta} + \eta_{\mu\beta}\eta_{\nu\alpha} - \eta_{\mu\nu}\eta_{\alpha\beta}) \quad (4.61)$$

$$\{c_\mu(f), \bar{c}_\nu^\dagger(g)\} = (f, g)_{\text{cov}} \eta_{\mu\nu} \quad (4.62)$$

$$\{\bar{c}_\mu(f), c_\nu^\dagger(g)\} = -(f, g)_{\text{cov}} \eta_{\mu\nu} \quad (4.63)$$

and 0 for other (anti-) commutators. Here we have used the fact that $(f, g^*)_{\text{cov}} = (f^*, g)_{\text{cov}} = 0$ for two wave packets f and g , because the complex conjugation changes the positive frequency into negative frequency and therefore the scalar product vanishes because of orthogonality. Since these relations are Lorentz covariant, they will lead to a Lorentz covariant tensor structure of the propagators. The propagators will be constructed later in this chapter, but before we have to construct the Hilbert space and the algebra of observables.

Using the graviton and ghost wave packet creators (4.58), we can construct the one particle (pre) Hilbert space for the gravitons and the one for the ghosts and hence the Fock space by tensor producting them with symmetrization for the graviton multiparticle Hilbert spaces and antisymmetrization for the ghosts. The scalar product on Fock space induced from the covariant scalar product on the one particle states does not induce a positive definite norm. Therefore we must investigate the action of the BRST operator on the auxiliary Hilbert space and identify the physical subspace in order to construct a Hilbert space of positive norm states.

The Heisenberg algebra can be constructed since we have representations of the field and conjugate momentum variables through the annihilation and creation operators. The algebra of BRST closed operators of ghost number 0 can be found by demanding invariance under BRST transformations. This algebra also contains exact operators. In classical physics the algebra of Dirac observables is isomorphic to the cohomology of the ghost number 0 observables [18]. In quantum theory there is no rigorous proof for this isomorphism to exist, but it is guaranteed that for each Dirac observable there exists a BRST invariant extension which is in our case given by (2.31), such that the cohomology of ghost number 0 operators at least contains the Dirac observables. Using this fact we can map every Dirac observable to a strongly BRST invariant operator, like we have done it for example with the Hamiltonian.

Next we have to discuss the operator ordering. In our case we have linear constraints so that we do not have to specify an operator ordering for the constraints. The same holds true for the BRST operator since the ghost and graviton variables commute. The quantum Hamiltonian is defined through normal ordering in terms of creation and annihilation operators. This fixes the operator ordering for the operators required in the following.

4.9 Graviton propagator in harmonic gauge

The graviton propagator in position space is defined as

$$G(x, y)_{\mu\nu\alpha\beta} := \langle 0 | T \{ h_{\mu\nu}(x) h_{\alpha\beta}(y) \} | 0 \rangle. \quad (4.64)$$

Using the mode expansion (4.54) and the commutators (4.61) we get

$$\begin{aligned} G(x, y)_{\mu\nu\alpha\beta} &= \frac{1}{2} (\eta_{\mu\alpha} \eta_{\nu\beta} + \eta_{\mu\beta} \eta_{\nu\alpha} - \eta_{\mu\nu} \eta_{\alpha\beta}) \int \widetilde{d^3 k} \left(\Theta(x^0 - y^0) e^{-ik(x-y)} + \Theta(y^0 - x^0) e^{ik(x-y)} \right) \\ &= \frac{1}{2} (\eta_{\mu\alpha} \eta_{\nu\beta} + \eta_{\mu\beta} \eta_{\nu\alpha} - \eta_{\mu\nu} \eta_{\alpha\beta}) \int \frac{d^4 k}{(2\pi)^4} \frac{i}{k^2 + i\epsilon} e^{-ik(x-y)}. \end{aligned} \quad (4.65)$$

This expression for the propagator is in accordance with existing results [15, 17, 16].

4.10 Cohomology of the one graviton subspace

In this chapter we want to study the action of the BRST operator on the auxiliary Fock space constructed in the last section. In particular we are interested in its action on one particle states with 0 ghosts and antighosts, since we suppose that physical free graviton states will lie in this sector in the Fock space. Since we can decompose the Fock space as $\mathcal{H}_{\text{Fock}} := \mathcal{H}_{\text{graviton}} \otimes \mathcal{H}_{\text{ghost}} \otimes \mathcal{H}_{\text{antighost}}$, where the factors are the Fock spaces for gravitons, ghosts and antighosts, we are interested in the closed and exact states in $\mathcal{H}_{\text{graviton}}^1 \otimes \mathcal{H}_{\text{ghost}}^0 \otimes \mathcal{H}_{\text{antighost}}^0$. Here the upper indices refer to the particle number of the different particle species.

By taking the full covariant form of the BRST charge (4.53) and the mode expansion (4.54) we arrive at the following BRST operator represented in terms of annihilation and creation operators

$$\Omega_{\text{BRST}} = - \int \widetilde{d^3k} \left((k_\nu a^{\mu\nu\dagger}(\mathbf{k}) - \frac{1}{2} k^\mu a^\dagger(\mathbf{k})) c_\mu(\mathbf{k}) + (k_\nu a^{\mu\nu}(\mathbf{k}) - \frac{1}{2} k^\mu a(\mathbf{k})) c_\mu^\dagger(\mathbf{k}) \right), \quad (4.66)$$

where $a := \eta^{\mu\nu} a_{\mu\nu}$.

When restricting the BRST operator to definite particle number states we see that it is given by a sum of operators $\Omega_{\text{BRST}} = \Omega_1 + \Omega_2$ with the following domains and co-domains

$$\Omega_1 : \mathcal{H}_{\text{graviton}}^n \otimes \mathcal{H}_{\text{ghost}}^m \otimes \mathcal{H}_{\text{antighost}}^l \rightarrow \mathcal{H}_{\text{graviton}}^{n+1} \otimes \mathcal{H}_{\text{ghost}}^m \otimes \mathcal{H}_{\text{antighost}}^{l-1} \quad (4.67)$$

$$\Omega_2 : \mathcal{H}_{\text{graviton}}^n \otimes \mathcal{H}_{\text{ghost}}^m \otimes \mathcal{H}_{\text{antighost}}^l \rightarrow \mathcal{H}_{\text{graviton}}^{n-1} \otimes \mathcal{H}_{\text{ghost}}^{m+1} \otimes \mathcal{H}_{\text{antighost}}^l. \quad (4.68)$$

By knowing the (co-) domains of the restricted BRST operator we can simply show the following proposition for the exact states.

Proposition 2. *All exact states in $\mathcal{H}_{\text{graviton}}^1 \otimes \mathcal{H}_{\text{ghost}}^0 \otimes \mathcal{H}_{\text{antighost}}^0$ have their preimage under Ω_{BRST} in the sub-vector space $\mathcal{H}_{\text{graviton}}^0 \otimes \mathcal{H}_{\text{ghost}}^0 \otimes \mathcal{H}_{\text{antighost}}^1$. Every exact state can be written as $\Omega_{\text{BRST}} \bar{c}_\mu^\dagger(f^\mu)|0\rangle = -\frac{1}{2} \int \widetilde{d^3k} (k^\mu \tilde{f}^\nu(\mathbf{k}) + k^\nu \tilde{f}^\mu(\mathbf{k}) - k \tilde{f}(\mathbf{k}) \eta^{\mu\nu}) a_{\mu\nu}^\dagger|0\rangle$, where \tilde{f}^μ is the spectrum of an antighost wave packet.*

Proof. Use the specification of the restricted (co-) domains above with $(n, m, l) = (0, 0, 1)$ for Ω_1 . Ω_2 does not contribute to the desired states, since it requires $(n, l, m) = (2, -1, 0)$ which does not exist. The expression of the image of an antighost wave packet can be determined by a short calculation as above. \square

The next step is to investigate the subspace of closed one graviton states. The following proposition holds.

Proposition 3. *The subspace of closed states in $\mathcal{H}_{\text{graviton}}^1 \otimes \mathcal{H}_{\text{ghost}}^0 \otimes \mathcal{H}_{\text{antighost}}^0$ is given by the states $a_{\mu\nu}^\dagger(f^{\mu\nu})|0\rangle$ with a spectrum satisfying $k_\mu \tilde{f}^{\mu\nu}(\mathbf{k}) = 0 \forall \mathbf{k} \in \mathbb{R}^3$.*

Proof. Demanding the restriction $0 = \Omega_{\text{BRST}} a_{\mu\nu}^\dagger(f^{\mu\nu})|0\rangle$ leads directly to $\int \widetilde{d^3k} k_\mu \tilde{f}^{\mu\nu}(\mathbf{k}) c_\nu^\dagger(\mathbf{k})|0\rangle = 0$ by using the commutators (4.61). This identity holds true if and only if $k_\mu \tilde{f}^{\mu\nu}(\mathbf{k}) = 0 \forall \mathbf{k} \in \mathbb{R}^3$, since the 0 state has a unique spectrum given by 0. This is because there is an isomorphism between position space and momentum space representations of the wave packets. \square

It can be checked explicitly that the exact states are closed since we have $\frac{1}{2} k_\mu (k^\mu \tilde{f}^\nu(\mathbf{k}) + k^\nu \tilde{f}^\mu(\mathbf{k}) - k \tilde{f}(\mathbf{k}) \eta^{\mu\nu}) = \frac{1}{2} k^2 f^\nu(\mathbf{k}) = 0$ by using the graviton on-shell condition $k^2 = 0$.

In the following we investigate explicitly the case of plane wave states with $k = (k, 0, 0, k)$, i.e. we will use spectra of the form $f^{\mu\nu}(\mathbf{p}) = (2\pi)^3 2p^0 \delta(\mathbf{p} - \mathbf{k}) A^{\mu\nu}$. This helps us to determine explicitly the polarization tensors $A^{\mu\nu}$ of the physical, i.e. closed but non-exact states. For the case of a general momentum we have to perform a Lorentz transformation by using for example (4.50).

For a closed state the polarization tensor must be of the following form

$$A^{\mu\nu} = \begin{pmatrix} A^{00} & A^{01} & A^{02} & A^{00} \\ A^{01} & C & B & A^{01} \\ A^{02} & B & D & A^{02} \\ A^{00} & A^{01} & A^{02} & A^{00} \end{pmatrix}, \quad (4.69)$$

where the 6 constants are arbitrary and lead to 6 linearly independent states.

Among these 6 states we find 4 exact states given by

$$\begin{aligned}
A_{\text{ex } 1}^{\mu\nu} &\sim \begin{pmatrix} 1 & 0 & 0 & 1 \\ 0 & 1 & 0 & 0 \\ 0 & 0 & 1 & 0 \\ 1 & 0 & 0 & 1 \end{pmatrix}, & A_{\text{ex } 2}^{\mu\nu} &\sim \begin{pmatrix} 0 & 1 & 0 & 0 \\ 1 & 0 & 0 & 1 \\ 0 & 0 & 0 & 0 \\ 0 & 1 & 0 & 0 \end{pmatrix} \\
A_{\text{ex } 3}^{\mu\nu} &\sim \begin{pmatrix} 0 & 0 & 1 & 0 \\ 0 & 0 & 0 & 0 \\ 1 & 0 & 0 & 1 \\ 0 & 0 & 1 & 0 \end{pmatrix}, & A_{\text{ex } 4}^{\mu\nu} &\sim \begin{pmatrix} 1 & 0 & 0 & 1 \\ 0 & -1 & 0 & 0 \\ 0 & 0 & -1 & 0 \\ 1 & 0 & 0 & 1 \end{pmatrix}.
\end{aligned} \tag{4.70}$$

The remaining 2 linearly independent states are closed and non-exact and therefore physical. Their polarizations are given by

$$A_{\text{phys } 1}^{\mu\nu} \sim \begin{pmatrix} 0 & 0 & 0 & 0 \\ 0 & 1 & 0 & 0 \\ 0 & 0 & -1 & 0 \\ 0 & 0 & 0 & 0 \end{pmatrix}, \quad A_{\text{phys } 2}^{\mu\nu} \sim \begin{pmatrix} 0 & 0 & 0 & 0 \\ 0 & 0 & 1 & 0 \\ 0 & 1 & 0 & 0 \\ 0 & 0 & 0 & 0 \end{pmatrix}, \tag{4.71}$$

which is in agreement with Veltman and van Dam's results [19].

The norm of the physical states is given by

$$\langle A_{\text{phys } 1}, k | A_{\text{phys } 1}, k \rangle = 2 (2\pi)^3 2k^0 \delta(0) \tag{4.72}$$

$$\langle A_{\text{phys } 2}, k | A_{\text{phys } 2}, k \rangle = 2 (2\pi)^3 2k^0 \delta(0), \tag{4.73}$$

and such they are distributional states of positive norm, which can be “normalized” canonically by a factor of $\frac{1}{\sqrt{2}}$ in the polarization tensor.

4.11 Structure of the physical multi-graviton space

In this section we will investigate the general structure of multiparticle subspaces in free gauge theories with decoupling ghosts. This will give the structure of the entire physical Fock space. In particular we are interested if in this (very) restrictive case the physical n particle Hilbert space is isomorphic to the n -th product of the physical 1 particle space.

Because we deal with a free QFT we can decompose the BRST operator into

$$\Omega_{\text{BRST}} = \Omega_1 + \Omega_2, \tag{4.74}$$

where Ω_1 increases the number of particles by 1 and decreases the antighosts by 1, and Ω_2 decreases the number of particles by 1 and increases the ghosts by 1.

The action of the BRST operator on the n particle space is given by the part Ω_2 , since Ω_1 annihilates this state. The most general n particle state can be written as

$$|\psi; n\rangle := a^\dagger(f_1) a^\dagger(f_2) \dots a^\dagger(f_n) |0\rangle, \tag{4.75}$$

where a^\dagger is the creation operator of the particles and f_j are wave packets.

The condition for closed states is given by the action of Ω_2 on $|\psi; n\rangle$

$$0 = \sum_j a^\dagger(f_1) \dots [\Omega_2, a^\dagger(f_j)] \dots a^\dagger(f_n) |0\rangle. \tag{4.76}$$

The problem with exact n particle states is that Ω_{BRST} can not be simply restricted to the domain $\mathcal{H}_{\text{particle}}^{n-1} \otimes \mathcal{H}_{\text{ghost}}^0 \otimes \mathcal{H}_{\text{antighost}}^1$ in order to produce exact n particle states, because the image of Ω_2 would be a subset of $\mathcal{H}_{\text{particle}}^{n-2} \otimes \mathcal{H}_{\text{ghost}}^1 \otimes \mathcal{H}_{\text{antighost}}^1$ and hence no n particle state. Therefore exact states in the n particle Hilbert space have their preimage in $\mathcal{H}_{\text{particle}}^{n-1}|_{\text{closed}} \otimes \mathcal{H}_{\text{ghost}}^0 \otimes \mathcal{H}_{\text{antighost}}^1$, since now the action of Ω_2 leads to the zero vector.

In order to solve the main problem we require the following lemmas.

Lemma 1. *A state in the n particle Hilbert space is closed if and only if it is a product of closed 1 particle states.*

Proof. The reverse direction is trivial since if every 1 particle state is closed then every commutator vanishes and equation (4.76) is satisfied.

The other direction is proved by contraposition. Let $\{a^\dagger(f_j)|0\rangle : j \in J\}$ be a set of non-closed 1 particle states. Then their commutator with Ω_2 leads to ghost creation operators with some wave packet determined by f_j . Equation (4.76) then is given by

$$0 = \sum_{j \in J} a^\dagger(f_1) \dots c^\dagger(g_j) \dots a^\dagger(f_n)|0\rangle, \quad (4.77)$$

where c^\dagger is the ghost creator and g_j the wave packet determined by f_j .

If the f_j are linearly independent the equation can not hold true. Even if some f_j are linearly dependent these contributions come with the same sign and therefore can not cancel. This completes the proof. \square

The next lemma is devoted to the exact n particle states.

Lemma 2. *A state in the n particle Hilbert space is exact if and only if its preimage under Ω_{BRST} lies in $\mathcal{H}_{\text{particle}}^{n-1}|_{\text{closed}} \otimes \mathcal{H}_{\text{ghost}}^0 \otimes \mathcal{H}_{\text{antighost}}^1$.*

Proof. The reverse direction is trivial since for any state in $|\phi\rangle \in \mathcal{H}_{\text{particle}}^{n-1}|_{\text{closed}} \otimes \mathcal{H}_{\text{ghost}}^0 \otimes \mathcal{H}_{\text{antighost}}^1$ we have

$$\Omega_{\text{BRST}}|\phi\rangle = \Omega_1|\phi\rangle \in \mathcal{H}_{\text{particle}}^n \otimes \mathcal{H}_{\text{ghost}}^0 \otimes \mathcal{H}_{\text{antighost}}^0.$$

Let now $|\psi\rangle = \Omega_{\text{BRST}}|\phi\rangle$ be a n particle state and $|\phi\rangle \notin \mathcal{H}_{\text{particle}}^{n-1}|_{\text{closed}} \otimes \mathcal{H}_{\text{ghost}}^0 \otimes \mathcal{H}_{\text{antighost}}^1$. Because of the restricted domains and co-domains of the BRST operator it holds true that $|\phi\rangle \in \mathcal{H}_{\text{particle}}^{n-1} \otimes \mathcal{H}_{\text{ghost}}^0 \otimes \mathcal{H}_{\text{antighost}}^1$. In order for $\Omega_{\text{BRST}}|\phi\rangle$ to be a n particle state the sum

$$\sum_{j=1}^{n-1} a^\dagger(f_1) a^\dagger(f_2) \dots [\Omega_2, a^\dagger(f_j)] \dots a^\dagger(f_{n-1}) \bar{c}^\dagger(f_n)|0\rangle$$

must vanish, where we have written $|\phi\rangle$ in terms of creation operators. This is only possible if all commutators are 0, because of the same linear independence and/or same sign arguments as in the lemma above. \square

The main statement of this section is the following

Proposition 4. *Assume a free QFT in which the BRST operator takes the form $\Omega_{\text{BRST}} = \chi^a[\eta^a] = \Omega_1 + \Omega_2$, where χ^a are first class constraints, η^a are the ghost variables and Ω_i as above. Then the physical n particle Hilbert space for the ordinary variables is isomorphic to the n -th symmetrized product of the physical 1 particle space, i.e.*

$$\mathcal{H}_{\text{phys}}^n \simeq \bigotimes_s^n \mathcal{H}_{\text{phys}}^1.$$

If the physical 1 particle Hilbert space consists of positive norm states, all physical multiparticle states will have positive norm, too.

Proof. Using lemma 1 and 2 and the definition of the physical n particle space we see that

$$\mathcal{H}_{\text{phys}}^n := \text{Ker}(\Omega_{\text{BRST}})|_n / \text{Im}(\Omega_{\text{BRST}})|_n \simeq \bigotimes_s^n \text{Ker}(\Omega_{\text{BRST}})|_1 / \text{Im}(\Omega_{\text{BRST}})|_1 = \bigotimes_s^n \mathcal{H}_{\text{phys}}^1,$$

where $|_n$ denotes the restricted action of the BRST operator on n particle states.

The positivity of the norm gets inherited by the canonical definition of the scalar product on the multi-particle Hilbert spaces in terms of the annihilation and creation operators. \square

4.12 Equivalence to Gupta-Bleuler method

Gupta and Bleuler's method of quantizing abelian gauge theories can be roughly described as follows.

First of all we need to perform a gauge fixing of the Lagrangian by some gauge condition $G = 0$. This gauge conditions enters the Lagrangian in the following way:

$$\mathcal{L} \xrightarrow{\text{gauge fixing}} \mathcal{L} + G^2 \quad (4.78)$$

The gauge fixed theory can now be quantized canonically without the appearance of constraints, since the gauge freedom is fixed. By investigating the resulting (pre) Hilbert space one obtains in general that there are also unphysical d.o.f., so that we have to use some subsidiary condition in order to eliminate them. As subsidiary condition we use the gauge fixing, more precisely the annihilating part, and define physical states according to

$$G^{(+)}|\text{phys}\rangle = 0, \quad (4.79)$$

where the superscript $+$ denotes the positive frequency part.

The (pre) Hilbert space of physical states $\mathcal{V}_{\text{phys}}$ has in general a positive semidefinite norm, because additional norm zero states solve the subsidiary condition. That is why factoring out the norm zero states $\mathcal{V}_0 \subset \mathcal{V}_{\text{phys}}$ is required.

We arrive at the physical Gupta - Bleuler Hilbert space

$$\mathcal{H}_{\text{GB}} := \overline{\mathcal{V}_{\text{phys}} / \mathcal{V}_0}. \quad (4.80)$$

To compare this method with our BRST approach we just have to note that the gauge fixing G defined above is nothing else but the constraint covector χ_μ and the subsidiary condition is equivalent to the action of the BRST operator on zero ghost and antighost states. Furthermore the BRST exact states are exactly the norm zero states so that we have

$$\mathcal{H}_{\text{BRST}} \simeq \mathcal{H}_{\text{GB}}. \quad (4.81)$$

The advantage of the BRST approach compared to Gupta - Bleuler's formalism in free and abelian theories is that we get a constructive method for finding norm zero states in the graviton Fock space by applying the BRST operator on states containing one antighost. This leads to exact graviton states which are (in well behaved cases) the only norm zero states in $\mathcal{V}_{\text{phys}}$.

Chapter 5

Pseudo-local matter observables with matter clocks and rods

In this chapter we will investigate a model proposed by Hartle, Giddings and Marolf [1] in the framework of perturbative effective quantum gravity on a fixed flat background. In the original version of this so-called $\psi^2\phi$ model one uses one scalar field ψ as clock and rod variable for localizing observables of another scalar field ϕ . For reasons explained later we will use four clock and rod fields ψ_i , $i = 1, 2, 3, 4$. In this model gravity just acts as a perturbation on the localization through radiative corrections. The main goal of this chapter is to define this model and give constraints on the localization of the two point correlation function of the ϕ field.

5.1 Definition of the theory and observables

It is instructive to first define the desired observables and then the dynamical part of the theory, since by choosing this order we can argue which terms of the effective action will contribute to our problem.

As mentioned above the theory to be defined should contain the five scalar fields ψ_i and ϕ interacting through some three point vertex of the form $V^{ij}\psi_i\psi_j\phi$, where V^{ij} is some symmetric 4×4 matrix to be defined later. Now we define the integrated interaction operator $O_{\psi^2\phi} := \int d^4x \sqrt{-g} V^{ij} \psi_i \psi_j \phi$ which is obviously diffeomorphism invariant and identify it with a part of the action. This operator, and in particular powers of it, will be used as Dirac observables in this chapter.

Given such an operator we can in analogy to [1] investigate matrix elements of products of these operators in specially prepared states and identify them as pseudo-local observables. In the following we are only interested in the square of the operator and we will restrict ourselves to this case.

The pseudo-local structure of a product of $O_{\psi^2\phi}$ operators can be seen in the following way. Assume that we have prepared some states $|f_1, f_2\rangle$ and $|f_3, f_4\rangle$, where f_i is a wave packet state for the particle ψ_i such that there is no overlap among these wave packets, except for f_1 and f_2 overlapping around some spacetime point x and f_3 and f_4 are overlapping around y . We can understand by using (2.56) that the matrix element of the time ordered operator squared at tree-level is given by

$$\langle f_3, f_4; \text{out} | T \{ O_{\psi^2\phi} O_{\psi^2\phi} \} | f_1, f_2; \text{in} \rangle \sim V^{12} V^{34} \langle 0 | T \phi(x) \phi(y) | 0 \rangle, \quad (5.1)$$

which is local relative to the wave packets.

We assume the index of the ψ_i fields to be a quantum number of a conserved current transmitted through the ϕ particles such that gravity only couples to singlets. This allows us to avoid tree-level diagrams including gravitons in the scattering matrix $\langle f_3, f_4; \text{out} | f_1, f_2; \text{in} \rangle$. In this case the the matrix elements of our pseudo-local operator (5.1) can be measured directly through the scattering of the four different clock and rod particles without further effort of extracting the information about our observable from the scattering process. The scattering experiment of wave packet states requires some nonstandard experimental setup which is not practically available today. We will discuss this topic in appendix E.2. It has to be stated

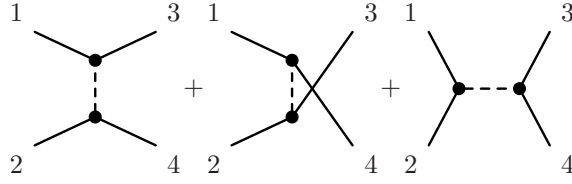


Figure 5.1: Tree-level localization graphs. They coincide with the S -matrix element for $\psi_1 \psi_2 \rightarrow \psi_3 \psi_4$ scattering, if the ψ fields carry quantum numbers of some conserved current.

again that the main purpose of this work is to perform a Gedankenexperiment and not a detailed technical description of a realistic experimental setup.

In the following part of this section we will collect the required terms from the effective action in order to study this matrix element up to order $\lambda^2 \kappa^2$, where $\lambda := \lambda m_\psi$ is a dimensionful coupling defining the overall strength of the three point scalar couplings and $\tilde{\lambda}$ is dimensionless. We assume the right energy scale for the constant λ to be the particle mass m_ψ , since this interaction is assumed to be independent of gravity and should only be defined from the particle properties. But in the presence of gravity the form of the interaction will receive correction terms, where the natural scale is the Planck scale.

Focussing the problem we have to think about to which order in κ we need the action of the gravitons and the scalars. Since the observable we want to calculate is based on the Feynman diagrams shown in fig. 5.1 plus the associated graviton loop contributions, effective vertices and the real emission of one soft graviton, we see that even at tree-level we already are at order λ^2 so that virtual scalars can be neglected since they come with a factor of λ . We also see that the effective three point scalar vertex is limited by κ^2 . The four point scalar interaction naturally comes with a factor $\lambda^2 \kappa^2$, if we assume this operator to be induced from the three point interactions and gravity. Hence it has to be included into the next to leading order corrections in the following too. Furthermore there are effective scalar two point operators which are of order κ^2 .

Since we calculate the matrix element of the squared operator in ψ_i particle states the gravitons only contribute as virtual particles in loop diagrams or as soft real emission. In the case of the virtual corrections every emitted graviton must connect somewhere to the graph again. This sets the limit for a scalar-scalar-graviton and scalar-scalar-scalar-graviton vertex to order κ^1 . The same holds true for soft real graviton emission. Double graviton emission is forbidden in our desired order, since every graviton comes with at least a factor of κ and has to connect to some other leg of the graph with another factor of κ . The only exceptions are graviton tadpole loop diagrams, but these diagrams vanish in dimensional regularization, because gravitons are massless.

Next we write down the most general diffeomorphism invariant action for the scalars respecting the conditions posed above on the order of κ and respecting the quantum number conservation of the ψ_i fields. It is given by

$$\begin{aligned}
S_m = \int d^4x \sqrt{-g} & \left(\frac{1}{2} (g^{\mu\nu} \partial_\mu \phi \partial_\nu \phi - m_\phi^2 \phi^2 + aR\phi^2) + \frac{\Xi_\phi}{2} \kappa^2 \square \phi \square \phi \right. \\
& + \frac{1}{2} (g^{\mu\nu} \partial_\mu \psi_i \partial_\nu \psi_i - m_\psi^2 \psi_i \psi_i + bR\psi_i \psi_i) + \frac{\Xi_\psi}{2} \kappa^2 \square \psi_i \square \psi_i \\
& \left. + \frac{\lambda}{2} (V^{ij} \psi_i \psi_j \phi + c^{ij} \kappa^2 g^{\mu\nu} \partial_\mu \psi_i \partial_\nu \psi_j \phi + d^{ij} \kappa^2 \psi_i \phi \square \psi_j + e^{ij} \kappa^2 \psi_i \psi_j \square \phi) \right) \\
& - \lambda_4 \lambda^2 \kappa^2 M^{ijkl} \psi_i \psi_j \psi_k \psi_l, \quad (5.2)
\end{aligned}$$

where a, b, c, d and e are dimensionless constants and the matrix structure of c, d and e has to be chosen such that the action is a ψ quantum number singlet. Furthermore Ξ_ψ and Ξ_ϕ are dimensionless constants parameterizing the effective scalar two point interactions. The four point scalar interaction comes with some tensor structure M and is parameterized by the dimensionless constant λ_4 . In this action we have omitted redundant operators like e.g. $\square(\psi_i \psi_j) \phi$, since they can be expressed through the other ones by using integration by parts and do not contribute to the Feynman rules.

Expanding this action using (3.6), (3.23) and (3.25) we get the following action on a flat background

$$S_m = \int d^4x \left(\mathcal{L}_m^{(0)} + \kappa \mathcal{L}_m^{(1)} + \kappa^2 \mathcal{L}_m^{(2)} \right) + \mathcal{O}(\kappa^3) \quad (5.3)$$

$$\mathcal{L}_m^{(0)} = \frac{1}{2} \left(\partial_\mu \phi \partial^\mu \phi - m_\phi^2 \phi^2 + \partial_\mu \psi_i \partial^\mu \psi_i - m_\psi^2 \psi_i \psi_i + \lambda V^{ij} \psi_i \psi_j \phi \right) \quad (5.4)$$

$$\begin{aligned} \mathcal{L}_m^{(1)} = & -\frac{1}{4} h^{\mu\nu} \left(2\partial_\mu \phi \partial_\nu \phi - \eta_{\mu\nu} \left(\partial_\lambda \phi \partial^\lambda \phi - m_\phi^2 \phi^2 \right) + 2\partial_\mu \psi_i \partial_\nu \psi_i - \eta_{\mu\nu} \left(\partial_\lambda \psi_i \partial^\lambda \psi_i - m_\psi^2 \psi_i \psi_i \right) \right) \\ & + \frac{1}{2} \left(h_{,\mu}^{\cdot\mu} - h_{\mu\nu}^{\cdot\mu,\nu} \right) (a\phi^2 + b\psi_i \psi_i) + \frac{\lambda}{4} h V^{ij} \psi_i \psi_j \phi \end{aligned} \quad (5.5)$$

$$\begin{aligned} \mathcal{L}_m^{(2)} = & \frac{\Xi_\phi}{2} \square \phi \square \phi + \frac{\Xi_\psi}{2} \square \psi_i \square \psi_i - \lambda_4 \lambda^2 M^{ijkl} \psi_i \psi_j \psi_k \psi_l + \frac{1}{2} h^\mu_\lambda h^{\lambda\nu} \left(\partial_\mu \phi \partial_\nu \phi + \partial_\mu \psi_i \partial_\nu \psi_i \right) \\ & + \frac{1}{2} R^{(2)} (a\phi^2 + b\psi_i \psi_i) + \frac{\lambda}{2} \left(c^{ij} \partial_\mu \psi_i \partial^\mu \psi_j \phi + d^{ij} \psi_i \phi \square \psi_j + e^{ij} \psi_i \psi_j \square \phi \right) \\ & + \frac{\hbar}{4} \left(-h^{\mu\nu} \left(\partial_\mu \phi \partial_\nu \phi + \partial_\mu \psi_i \partial_\nu \psi_i \right) + R^{(1)} (a\phi^2 + b\psi_i \psi_i) \right) + \frac{1}{4} \left(\frac{1}{2} h^2 - h^\alpha_\beta h^\beta_\alpha \right) \mathcal{L}_m^{(0)}, \end{aligned} \quad (5.6)$$

which can be shown to be invariant under the $\tilde{\delta}$ gauge transformations given by (3.12) and (3.20) up to order κ^2 . Although the quadratic graviton terms of this action will not directly contribute to our problem we will keep them in order to have a manifestly gauge invariant Lagrangian.

Given the action (5.2) we can identify the most general diffeomorphism invariant three point scalar operator as

$$O_{\psi^2\phi} := \int d^4x \sqrt{-g} \frac{\lambda}{2} \left(V^{ij} \psi_i \psi_j \phi + c^{ij} \kappa^2 g^{\mu\nu} \partial_\mu \psi_i \partial_\nu \psi_j \phi + d^{ij} \kappa^2 \psi_i \phi \square \psi_j + e^{ij} \kappa^2 \psi_i \psi_j \square \phi \right). \quad (5.7)$$

The expansion of this operator around a fixed flat background in order κ^2 is given by

$$\begin{aligned} O_{\psi^2\phi} = & \int d^4x \frac{\lambda}{2} \left(V^{ij} \psi_i \psi_j \phi + \frac{\kappa}{2} h V^{ij} \psi_i \psi_j \phi - \frac{\kappa^2}{4} \left(h^\alpha_\beta h^\beta_\alpha - \frac{1}{2} h^2 \right) V^{ij} \psi_i \psi_j \phi \right. \\ & \left. + c^{ij} \kappa^2 \eta^{\mu\nu} \partial_\mu \psi_i \partial_\nu \psi_j \phi + d^{ij} \kappa^2 \psi_i \phi \square \psi_j + e^{ij} \kappa^2 \psi_i \psi_j \square \phi \right) + \mathcal{O}(\kappa^3). \end{aligned} \quad (5.8)$$

This expression can be shown to be invariant under the $\tilde{\delta}$ gauge transformations up to order κ^2 .

The expansion of the graviton action in the required order has already been performed in section 3.5 and is given by (3.29).

The goal of the following part of this chapter is to find limitations on the localization of the two point correlator of the ϕ fields in the presence of gravity. Therefore we will first calculate the localization process to order $\kappa^0 \lambda^4$ in order to get some insights into the dynamics of this process. Then the radiative corrections up to order $\kappa^2 \lambda^4$ are calculated, which give bounds on localization.

5.2 Feynman rules

In this section the relevant Feynman rules are derived from the Lagrangian using standard methods. We can summarize the general method in the following steps:

- every field in the interaction Lagrangian gets replaced by the corresponding external leg
- the prefactors are multiplied by i
- every derivative ∂_μ gets replaced by $-ip_\mu$, where p is the incoming momentum of the corresponding field
- permutation symmetry factors are included

Performing these steps for the Lagrangians (5.3) and (3.29) we arrive at the Feynman rules given in fig. 5.2, omitting the parts we do not require for our problem, like for example the two graviton emission from scalars. The graviton propagator was derived in the section 4.9 above and is given by (4.65).

$$\begin{aligned}
\text{---} &= \frac{i}{p^2 - m_\psi^2} \delta_{ij} \\
\text{---} &= \frac{i}{p^2 - m_\phi^2} \\
\text{~~~~~} &= \frac{i}{2} \frac{\eta_{\mu\alpha} \eta_{\nu\beta} + \eta_{\mu\beta} \eta_{\nu\alpha} - \eta_{\mu\nu} \eta_{\alpha\beta}}{p^2} \\
\begin{array}{c} q \\ \diagup \\ \text{---} \bullet \\ \diagdown \\ p \\ \diagup \\ q \end{array} &= i\lambda \left(V^{ij} - \frac{\kappa^2}{2} (2c^{ij} pq + d^{ij} (p^2 + q^2) + 2e^{ij} k^2) \right) \\
\begin{array}{c} q \\ \diagup \\ \text{~~~~~} \bullet \\ \diagdown \\ p \\ \diagup \\ q \end{array} &= \frac{i\kappa}{2} \delta_{ij} (p_\mu q_\nu + p_\nu q_\mu - \eta_{\mu\nu} (pq + m_\psi^2) + 2bk_\mu k_\nu - 2b\eta_{\mu\nu} k^2) \\
\begin{array}{c} q \\ \diagup \\ \text{~~~~~} \bullet \\ \diagdown \\ p \\ \diagup \\ q \end{array} &= \frac{i\kappa}{2} (p_\mu q_\nu + p_\nu q_\mu - \eta_{\mu\nu} (pq + m_\phi^2) + 2ak_\mu k_\nu - 2a\eta_{\mu\nu} k^2) \\
\begin{array}{c} \diagup \\ \bullet \\ \diagdown \end{array} &= \frac{i\lambda\kappa}{2} V^{ij} \eta_{\mu\nu} \\
\text{---} \square \text{---} &= i \Xi_\psi \kappa^2 p^4 \delta_{ij} \\
\text{---} \square \text{---} &= i \Xi_\phi \kappa^2 p^4 \\
\begin{array}{c} \diagup \\ \square \\ \diagdown \end{array} &= -i\lambda_4 \lambda^2 \kappa^2 4! M^{(ijkl)}
\end{aligned}$$

Figure 5.2: Required Feynman rules for the $\psi^2\phi$ model. All momenta are flowing into the vertex. We did not have to include the indices of the graphs, since they are understood.

5.3 Tree-level localization

In this section we will calculate the pseudo-local observable defined above in order $\lambda^2 \kappa^0$ through the corresponding tree-level Feynman diagrams, see fig. 5.1. Therefore we will use the LSZ reduction formula (2.56) in order to relate the matrix element to the Green functions. The matrix element will be squared, since this is the quantity which is measured.

Using the Feynman rules we obtain for the Green function

$$\mathcal{M}_{\text{tree}} = -i\lambda^2 \left(\frac{V^{13}V^{24}}{T - m_\phi^2} + \frac{V^{14}V^{23}}{U - m_\phi^2} + \frac{V^{12}V^{34}}{S - m_\phi^2} \right), \quad (5.9)$$

where $S = (k_1 + k_2)^2$, $T = (k_1 - k_3)^2$ and $U = (k_1 - k_4)^2$ are the standard Mandelstam variables dependent on the momenta k_i of the particles ψ_i .

According to the LSZ formula (2.56) we have to perform the following integral in order to get the matrix element

$$\begin{aligned} \langle f_3, f_4; \text{out} | T \{ O_{\psi^2\phi} O_{\psi^2\phi} \} | f_1, f_2; \text{in} \rangle &= -i\lambda^2 \int \prod_{i=1}^4 \widetilde{d^3 k_i} \tilde{f}_1(\mathbf{k}_1) \tilde{f}_2(\mathbf{k}_2) \tilde{f}_3^*(\mathbf{k}_3) \tilde{f}_4^*(\mathbf{k}_4) \\ &\quad \pi^4 \delta(k_1 + k_2 - k_3 - k_4) \left(\frac{V^{13}V^{24}}{T - m_\phi^2} + \frac{V^{14}V^{23}}{U - m_\phi^2} + \frac{V^{12}V^{34}}{S - m_\phi^2} \right), \end{aligned} \quad (5.10)$$

where \tilde{f}_i are the spectra of the wave packets f_i . As a remark we do not have to take into account the nonconnected terms of the LSZ formula, since the initial and final state particles are distinct.

Now we want to interpret the individual contributions to (5.10). Using the relation

$$\frac{i}{p^2 - m_\phi^2 + i\epsilon} = \int d^4 x e^{ipx} \langle 0 | T \{ \phi(x+y) \phi(y) \} | 0 \rangle \quad (5.11)$$

we can find for each individual term

$$\begin{aligned} &\int \prod_{i=1}^4 \widetilde{d^3 k_i} \tilde{f}_1(\mathbf{k}_1) \tilde{f}_2(\mathbf{k}_2) \tilde{f}_3^*(\mathbf{k}_3) \tilde{f}_4^*(\mathbf{k}_4) \pi^4 \delta(k_1 + k_2 - k_3 - k_4) \frac{1}{S - m_\phi^2} \\ &= -\frac{i}{2^4} \int d^4 x d^4 y f_1(x) f_2(x) f_3^*(y) f_4^*(y) \langle 0 | T \{ \phi(x) \phi(y) \} | 0 \rangle \end{aligned} \quad (5.12)$$

$$\begin{aligned} &\int \prod_{i=1}^4 \widetilde{d^3 k_i} \tilde{f}_1(\mathbf{k}_1) \tilde{f}_2(\mathbf{k}_2) \tilde{f}_3^*(\mathbf{k}_3) \tilde{f}_4^*(\mathbf{k}_4) \pi^4 \delta(k_1 + k_2 - k_3 - k_4) \frac{1}{T - m_\phi^2} \\ &= -\frac{i}{2^4} \int d^4 x d^4 y f_1(x) f_2(y) f_3^*(x) f_4^*(y) \langle 0 | T \{ \phi(x) \phi(y) \} | 0 \rangle \end{aligned} \quad (5.13)$$

$$\begin{aligned} &\int \prod_{i=1}^4 \widetilde{d^3 k_i} \tilde{f}_1(\mathbf{k}_1) \tilde{f}_2(\mathbf{k}_2) \tilde{f}_3^*(\mathbf{k}_3) \tilde{f}_4^*(\mathbf{k}_4) \pi^4 \delta(k_1 + k_2 - k_3 - k_4) \frac{1}{U - m_\phi^2} \\ &= -\frac{i}{2^4} \int d^4 x d^4 y f_1(x) f_2(y) f_3^*(y) f_4^*(x) \langle 0 | T \{ \phi(x) \phi(y) \} | 0 \rangle, \end{aligned} \quad (5.14)$$

where we have used translation invariance for the ϕ two point function.

We now see that we can choose the relevant scattering channel by choosing the overlaps among the wave packets, since the integrals above will only contribute if there is some pairwise spacetime overlap among the wave packets. We call the localization S -type if there is overlap between wave packets 1,2 and 3,4, T -type if there is overlap between 1,3 and 2,4 and finally U -type, if 1,4 and 2,3 overlaps.

In the following we will investigate the different types of localization. We will restrict ourselves to the S - and T -type localizations, since T and U are related by interchanging the center of mass system scattering angle θ with $\pi - \theta$ and therefore are not independent. When we investigate e.g. S -type localization we will switch off all couplings V^{ij} except for V^{12} and V^{34} , since they will not contribute.

In S -type localization we use products of the first order approximated Gaussian wave packets given in appendix E.1 such that f_1 is moving in z -direction, f_2 in $-z$ -direction, f_3 in y -direction and f_4 in $-y$ -direction. The overlap of f_1 and f_2 should be w.l.o.g. around $x_0 = (t_{x_0}, \mathbf{x}_0)$ and the overlap of f_3 and f_4 around 0. Note that due to translation invariance only the distance between these points is relevant. This leads to the following result

$$\begin{aligned} \langle f_3, f_4; \text{out} | T \{ O_{\psi^2\phi} O_{\psi^2\phi} \} | f_1, f_2; \text{in} \rangle &= -\mathcal{N}_s \lambda^2 \int d^4x d^4y \exp \left(-\frac{q^4}{4} ((\mathbf{x} - \mathbf{x}_0)^2 + (t_x - t_{x_0})^2) \right) \\ &\times \exp \left(-\frac{q^4}{4} (\mathbf{y}^2 + t_y^2) \right) \langle 0 | T \{ \phi(x) \phi(y) \} | 0 \rangle, \quad (5.15) \end{aligned}$$

where \mathcal{N}_s is some complex prefactor coming from the normalization of the wave packets. This shows that we can increase the resolution by increasing the momentum $q = \|\mathbf{q}\|$. Since we have not included higher order corrections we have no upper bound for q , so that at this stage the resolution can be arbitrarily high. This of course does not hold true in the presence of gravity, as we will show it in the following sections. Finally we can square the amplitude (5.15) in order to relate it to a cross section.

In T -type localization we can use the same Gaussian wave packets, but with different overlap properties. Since this requires the multiplication of non-anti-parallel moving wave packets, some corrections are present in their product, see (E.10). But these slightly deformed Gaussian functions describing the overlap can also be adjusted to an arbitrary small width by increasing the momentum q . Hence T -type localization behaves in the same way as S -type localization, at least at leading order.

5.4 One loop corrections and counterterms

In this section we will discuss the one loop corrections in κ to the matrix element. They are part of the next to leading order (NLO) corrections to the process. For their evaluation we have used the *Mathematica* packages *FeynArts*, *FormCalc* and *LoopTools*, see e.g. [3] and references therein. These tools can be used for diagram generation, analytical simplifications and numerical evaluation of loop integrals. But in order to apply FeynArts and FormCalc we had to modify the packages to include spin 2 particles. This modification is described in appendix F.

The regularization of the UV divergent integrals is automatically performed by dimensional regularization in LoopTools, where we use the convention $d = 4 - \epsilon$. As renormalization scheme we choose the $\overline{\text{MS}}$ scheme in which the counterterms are calculated by modified minimal subtraction, i.e. the counterterms are given by $\frac{2}{\epsilon} + \log 4\pi - \gamma_E$ times some diagram dependent prefactors and tensor structure, where γ_E is the Euler gamma. The divergences for the individual diagrams occurring in our problem are given later.

Since gravitons are massless, we have to take care of the occurring IR divergences. This is done by introducing a small graviton mass as IR cutoff which is later removed by taking into account Bremsstrahlung corrections. This IR regularization is performed automatically for the loop amplitudes by FormCalc and LoopTools, but the soft real emission diagrams had to be regularized by hand. This will be explained in more detail in the next section.

Now we will discuss the loop contributions to our process and give the required counterterms. Therefore we will divide the loop diagrams according to FeynArts into the diagram types *boxes*, *self energies*, *triangles*, *tadpoles* and *wavefunction corrections*. We will only investigate S -type graphs, since they are isomorphic to the T -type graphs by crossing.

In our model all order κ^2 tadpole graphs vanish, since there are no scalar tadpoles and the graviton induced tadpoles are renormalized to 0 by a renormalized cosmological constant, see appendix C.

The wavefunction renormalization graphs are given by the tree diagram with renormalized external legs.

They will enter the amplitude through the following relation coming from LSZ formula

$$\left(Z_{\psi}^{\frac{1}{2}}\right)^4 \mathcal{M}_{\text{tree}} = (1 + 2\delta Z_{\psi})\mathcal{M}_{\text{tree}} + \mathcal{O}(\kappa^3) =: \mathcal{M}_{\text{tree}} + \mathcal{M}_{\text{WF}} + \mathcal{O}(\kappa^3), \quad (5.16)$$

where $Z_{\psi} = 1 + \delta Z_{\psi}$ is the renormalized wavefunction renormalization, i.e. the residuum of the one loop ψ propagator in $\overline{\text{MS}}$ scheme. The calculation of Z_{ψ} can be performed automatically in FormCalc, but we will also give the required off-shell one loop divergence, i.e. the counterterm, for the scalar propagator explicitly

$$\text{---} \text{---} \text{---} \text{---} = i \frac{\kappa^2}{8\pi^2\epsilon} \left(\frac{b}{2} k^4 - k^2 m_{\psi}^2 \left(1 + \frac{3}{2}b - \frac{3}{2}b^2\right) + m_{\psi}^4 \left(1 + 3b + \frac{3}{2}b^2\right) \right) + \text{finite}. \quad (5.17)$$

In the category of self energy corrections there is only one diagram given by

$$\begin{array}{c} 1 \\ | \\ \text{---} \text{---} \text{---} \text{---} \\ | \\ 2 \end{array} \text{---} \text{---} \text{---} \text{---} \begin{array}{c} 3 \\ | \\ \text{---} \text{---} \text{---} \text{---} \\ | \\ 4 \end{array} \quad (5.18)$$

The counterterm for the divergent subdiagram is given by (5.17) with m_{ψ} replaced by m_{ϕ} and b replaced by a . Hence this diagram is renormalized by the propagator counterterm.

The triangle diagrams are given by all possible permutations of the following basic diagram types

$$\begin{array}{c} 1 \\ | \\ \text{---} \text{---} \text{---} \text{---} \\ | \\ 2 \end{array} \text{---} \text{---} \text{---} \text{---} \begin{array}{c} 3 \\ | \\ \text{---} \text{---} \text{---} \text{---} \\ | \\ 4 \end{array} + \begin{array}{c} 1 \\ | \\ \text{---} \text{---} \text{---} \text{---} \\ | \\ 2 \end{array} \text{---} \text{---} \text{---} \text{---} \begin{array}{c} 3 \\ | \\ \text{---} \text{---} \text{---} \text{---} \\ | \\ 4 \end{array} + \begin{array}{c} 1 \\ | \\ \text{---} \text{---} \text{---} \text{---} \\ | \\ 2 \end{array} \text{---} \text{---} \text{---} \text{---} \begin{array}{c} 3 \\ | \\ \text{---} \text{---} \text{---} \text{---} \\ | \\ 4 \end{array} + \begin{array}{c} 1 \\ | \\ \text{---} \text{---} \text{---} \text{---} \\ | \\ 2 \end{array} \text{---} \text{---} \text{---} \text{---} \begin{array}{c} 3 \\ | \\ \text{---} \text{---} \text{---} \text{---} \\ | \\ 4 \end{array} \quad (5.19)$$

These diagrams have subdivergences which have to be renormalized by the three point scalar interaction counterterm. The off-shell divergence of the sum of all scalar three point diagrams is given by

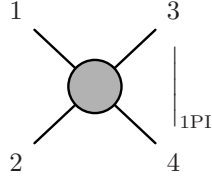
$$\begin{array}{c} k_2 \\ | \\ \text{---} \text{---} \text{---} \text{---} \\ | \\ k_3 \end{array} \Bigg|_{1\text{PI}} = -i\lambda V^{ij} \frac{\kappa^2}{4\pi^2\epsilon} \left(m_{\psi}^2 \left(1 + \frac{3}{2}a + \frac{3}{2}ab + 3b + \frac{3}{2}b^2\right) + \frac{m_{\phi}^2}{2} \left(1 + \frac{3}{2}a + 3ab + 3b\right) - \frac{k_1^2}{4} \left(1 - 3ab + 3b + \frac{3}{2}b^2\right) - \frac{k_2^2 + k_3^2}{4} \left(1 + \frac{3a + 3b}{2} - \frac{3b^2}{2}\right) \right) + \text{finite}. \quad (5.20)$$

We obtain that the divergences have the same coupling matrix V^{ij} like in the original definition of the theory. This is because gravitons do not change the quantum numbers, so that graviton loop corrections are the same for all combinations of ij , of course weighted by V^{ij} .

The last type of contributions are the boxes given by all possible permutations of the following diagrams

$$\begin{array}{c} 1 \\ | \\ \text{---} \text{---} \text{---} \text{---} \\ | \\ 2 \end{array} \text{---} \text{---} \text{---} \text{---} \begin{array}{c} 3 \\ | \\ \text{---} \text{---} \text{---} \text{---} \\ | \\ 4 \end{array} + \begin{array}{c} 1 \\ | \\ \text{---} \text{---} \text{---} \text{---} \\ | \\ 2 \end{array} \text{---} \text{---} \text{---} \text{---} \begin{array}{c} 3 \\ | \\ \text{---} \text{---} \text{---} \text{---} \\ | \\ 4 \end{array} + \begin{array}{c} 1 \\ | \\ \text{---} \text{---} \text{---} \text{---} \\ | \\ 2 \end{array} \text{---} \text{---} \text{---} \text{---} \begin{array}{c} 3 \\ | \\ \text{---} \text{---} \text{---} \text{---} \\ | \\ 4 \end{array} \quad (5.21)$$

The divergence of the sum of all box diagrams is given by



$$= iV^{12}V^{34} \frac{\lambda^2 \kappa^2}{8\pi^2 \epsilon} (1 + 6b + 6b^2) + \text{finite}, \quad (5.22)$$

where we have restricted ourselves to S -type localization as mentioned above, i.e. only V^{12} and V^{34} are nonzero. We see that the prefactor of the divergence is in general nonzero, so that we will have an induced effective four point interaction.

This completes the list of all occurring one loop divergences for S -type localization and by crossing also for T -type localization. The next step was to square the renormalized matrix elements, i.e. multiplying the loop matrix element with the tree level matrix element. Since we integrate the matrix elements themselves over the external wave packets, the following formula holds true

$$\begin{aligned} \left| \langle f_3, f_4; \text{out} | T \{ O_{\psi^2 \phi} O_{\psi^2 \phi} \} | f_1, f_2; \text{in} \rangle \right|^2 &= \int dk dp \mathcal{F}(k) \mathcal{F}^*(p) \mathcal{M}(k) \mathcal{M}^*(p) \\ &= \int dk dp \mathcal{F}(k) \mathcal{F}^*(p) (\mathcal{M}_{\text{tree}}(k) \mathcal{M}_{\text{tree}}^*(p) + \mathcal{M}_{\text{tree}}(k) \mathcal{M}_{\text{loop}}^*(p) + \mathcal{M}_{\text{loop}}(k) \mathcal{M}_{\text{tree}}^*(p)) \\ &\quad + \text{higher orders}, \end{aligned} \quad (5.23)$$

where k and p label collectively all four 4-momenta of the $2 \rightarrow 2$ process, and \mathcal{F} is defined as follows:

$$\mathcal{F}(k) = \pi^4 \tilde{f}_1(\mathbf{k}_1) \tilde{f}_2(\mathbf{k}_2) \tilde{f}_3^*(\mathbf{k}_3) \tilde{f}_4^*(\mathbf{k}_4) \delta(k_1 + k_2 - k_3 - k_4). \quad (5.24)$$

Next we can express the NLO corrections to the wave packet process in terms of the corrections to the momentum eigenstate scattering process given by $2\text{Re}(\mathcal{M}_{\text{tree}}(k) \mathcal{M}_{\text{loop}}^*(k))$. For this we have to use the phase information about $\mathcal{F}(k)$ and $\mathcal{M}_{\text{tree}}(k)$.

As we have seen in section 5.3 above, the tree-level matrix element has a trivial phase which is independent of the momenta. The collective wave packet $\mathcal{F}(k)$ has a nontrivial, k dependent phase due to the phases of the wave packet spectra. For Gaussian wave packets we have found in appendix E.1 that the phase of the spectrum is given by e^{ikx_0} , where x_0 is the spacetime position of the narrowest spatial wave packet. This specific phase is quite natural for more general localized states.

To see this we use the spectral representation of the wave packet $f(x) = \int \widetilde{d^3k} e^{-ikx} \tilde{f}(\mathbf{k})$. Since the localized wave packet contains some preferred position x_0 around which it is localized with the smallest width, this position must be encoded in the spectrum. Assume some translation $x \rightarrow x + \delta$. This translation transforms the wave packet localized around x_0 to the same wave packet localized around $x_0 + \delta$. Since the translation acts as a multiplication in momentum space we have the following relation

$$\tilde{f}_{x_0+\delta}(\mathbf{k}) = e^{ik\delta} \tilde{f}_{x_0}(\mathbf{k}). \quad (5.25)$$

Therefore the only information about the point x_0 is contained in the phase factor e^{ikx_0} .

There can be additional phases depending only on the momenta k . But these phases are quite unnatural if we use the following natural construction for localized states:

We take a real spectrum for assigning the relevant momenta. This real spectrum gets multiplied by the minimal phase, which contains the information about the preferred spacetime point x_0 , i.e. the real spectrum gets multiplied by e^{ikx_0} .

With this natural restriction on the spectra we can show that the corrections to our process can in general be calculated from the momentum eigenstate process corrections.

In our specific case we have the preferred positions x_0 and 0, such that the phase factor is given by $\mathcal{F}(k) = |\mathcal{F}(k)| e^{i(k_1+k_2)x_0}$. Furthermore we use the following identity for the time-ordered two point function

$$\langle 0 | T \{ \phi(x) \phi(0) \} | 0 \rangle = \langle 0 | T \{ \phi(0) \phi(x) \} | 0 \rangle = \langle 0 | T \{ \phi(-x) \phi(0) \} | 0 \rangle, \quad (5.26)$$

where we have used translation invariance. Applying these two relations we can average (5.23) using x_0 and (5.23) using $-x_0$ (they are the same) and obtain

$$\begin{aligned} \left| \langle f_3, f_4; \text{out} | T \{ O_{\psi^2\phi} O_{\psi^2\phi} \} | f_1, f_2; \text{in} \rangle \right|^2 &= \int dk dp \mathcal{F}(k) \mathcal{F}^*(p) \mathcal{M}_{\text{tree}}(k) \mathcal{M}_{\text{tree}}^*(p) \\ &\times \left(1 + \frac{\mathcal{R}(k)}{2} + \frac{\mathcal{R}(p)}{2} \right) + \text{higher orders}. \end{aligned} \quad (5.27)$$

In this expression we have identified the relative corrections to the momentum eigenstate scattering process defined by

$$\mathcal{R}(k) := \frac{\mathcal{M}_{\text{tree}}(k) \mathcal{M}_{\text{loop}}^*(k) + \mathcal{M}_{\text{loop}}(k) \mathcal{M}_{\text{tree}}^*(k)}{|\mathcal{M}_{\text{tree}}(k)|^2}. \quad (5.28)$$

The condition for the perturbative theory to be valid is

$$|\mathcal{R}(k)| \ll 1 \quad (5.29)$$

for all k which contribute to the wave packet process, i.e. for all k for which the wave packet does not vanish (or at least is very small).

Because of this insight we can study the phenomenology of the simpler case of a momentum eigenstate scattering process in the following sections and therewith derive the phenomenology of the localization process.

5.5 Bremsstrahlung corrections

In this section we give a short introduction into how one can compute Bremsstrahlung corrections in general and in our specific case. We will restrict ourselves to the momentum eigenstate scattering process, since we only require the Bremsstrahlung corrections in order to render the loop corrections IR finite and therefore well defined.

The physical idea behind considering the emission of an on-shell Bremsstrahlung particle is as follows. Since the Bremsstrahlung particles under consideration are massless, they can in principle be generated without being detected in the detector if they carry very little energy. So we can not distinguish between a n to m process and the corresponding process with an additional soft Bremsstrahlung particle in the final state, if it is soft enough. Thus we have to calculate the transition probability for a n to m process by using the formula

$$|\mathcal{M}_{\text{tot}}|^2 = |\mathcal{M}_{n \rightarrow m}|^2 + \sum_{i=1}^{\infty} \int_{\text{soft}} d\Phi_i |\mathcal{M}_{n \rightarrow m+i}|^2, \quad (5.30)$$

where the sum goes over the emission of i massless particles and Φ_i denotes the phase space of them. The integration range denoted by “soft” will be specified later.

In a perturbative framework it is sufficient to include n particle emission if we restrict ourselves to n loop diagrams, since they are of the same order in the perturbation series.

Including the Bremsstrahlung corrections is very important, since they will cancel the IR divergences coming from the massless particles in loop diagrams [20, 21]. To check the cancellation the divergences are in general regularized by introducing small masses m_g for the massless particles. The result $|\mathcal{M}_{\text{tot}}|^2$ must be verified to be cutoff independent and therefore well defined in the limit of vanishing cutoff in order to be physically sensible.

The last task of this section is to define the integration range for the Bremsstrahlung corrections. Since we are interested in soft emission we approximately neglect the recoil of the emitted quanta and do not include the soft particle in the energy-momentum conservation for the remaining particles. This will simplify the phase space integration in a dramatic way. Moreover we have to put a cutoff to the energy of the emitted quanta in order to stay “soft”. The choice of this cutoff energy is specific to the detector in use,

but we assume it to be $\sqrt{S}/10$, which is a typical value suitable for purely theoretical investigations, like in this work. The precise knowledge of this cutoff energy is not necessary at all, since the result will only depend logarithmically on it so that $\mathcal{O}(1)$ prefactors do not matter.

The natural volume element for one particle emission together with the integration range is given by

$$\int_{\text{soft}} d\Phi := \int_{|\mathbf{k}| < \sqrt{S}/10} \widetilde{d^3k}, \quad (5.31)$$

where k is the four momentum of the emitted quanta and is on-shell, of course.

Our phase space integration is performed by using the Monte Carlo integration package *CUBA* [22]. To arrive at more stable results it is convenient to use spherical coordinates together with some importance sampling for the radial integration dk . The integration before the importance sampling is given by

$$\int_0^{\sqrt{S}/10} \int_{\Omega} d\Omega dk \frac{k^2}{(2\pi)^3 2k^0} |\mathcal{M}_{n \rightarrow m+1}|^2 \quad (5.32)$$

where $k = \|\mathbf{k}\|$ and Ω is the solid angle. Since the k dependence of the squared amplitude can be roughly estimated as

$$|\mathcal{M}_{n \rightarrow m+1}|^2 \sim \frac{1}{k^2} \quad \text{for } k \gg m_g \quad \Leftrightarrow \quad \int \widetilde{d^3k} |\mathcal{M}_{n \rightarrow m+1}|^2 \sim \int \frac{dk}{k} \quad \text{for } k \gg m_g \quad (5.33)$$

it is natural to perform importance sampling by a coordinate transformation $k \rightarrow x = \log(k/M_{\text{pl}})$, where we use M_{pl} as a natural dimension. The integration element in the new variables is given by

$$\int_{-\infty}^{\log(\sqrt{S}/(10M_{\text{pl}}))} \int_{\Omega} d\Omega dx M_{\text{pl}}^3 \frac{e^{3x}}{(2\pi)^3 2k^0(x)} |\mathcal{M}_{n \rightarrow m+1}|_{k \rightarrow k(x)}^2. \quad (5.34)$$

At first sight this reparametrization does not help since we receive a noncompact integration range for x . But it can be shown that for $x \rightarrow -\infty$ the integrand vanishes as $\exp 2x$ since the estimation (5.33) only holds true for $k \gg 0$ and for small k we have an approximately constant squared amplitude. Hence we can insert a lower bound to the integral range without affecting the results too much. We have found a suitable bound to be $2 \log(m_g/M_{\text{pl}})$, where m_g is the mass of the emitted particle, i.e. the IR regulator. This bound is motivated by the fact that the squared amplitude has a local maximum at $x \approx \log(m_g/M_{\text{pl}})$ because of collinear effects and decreases sufficiently fast for smaller x to a constant value. The x dependence of the integrand in the small x region is determined by $\exp 2x$. Figure 5.3 shows this rapid falloff in the example of our problem for some set of parameters. This falloff property is universal, i.e. it does not depend on the parameters we use.

To calculate the one particle emission we have to sum over its polarizations. The polarization sum can for example be performed by using the formula [19]

$$\sum_{i=1}^2 \epsilon_{\mu\nu}^{(i)} \epsilon_{\alpha\beta}^{(i)*} = \frac{1}{2} (\bar{\eta}_{\mu\alpha} \bar{\eta}_{\nu\beta} + \bar{\eta}_{\mu\beta} \bar{\eta}_{\nu\alpha} - \bar{\eta}_{\mu\nu} \bar{\eta}_{\alpha\beta}), \quad (5.35)$$

where $\bar{\eta}_{\mu\nu} := \eta_{\mu\nu} - (\bar{k}_\mu \bar{k}_\nu + k_\mu k_\nu) / \bar{k} k$ and \bar{k} is the space reflected graviton four momentum.

Evaluating this expression leads to

$$\sum_{i=1}^2 \epsilon_{\mu\nu}^{(i)} \epsilon_{\alpha\beta}^{(i)*} = \frac{1}{2} (\eta_{\mu\alpha} \eta_{\nu\beta} + \eta_{\mu\beta} \eta_{\nu\alpha} - \eta_{\mu\nu} \eta_{\alpha\beta}) + \text{terms prop. to } k \quad (5.36)$$

so that we can neglect the additional terms proportional to k if we can show that the QED-like on-shell Ward identity $k^\mu \mathcal{M}_{\mu\nu} = 0$ holds true for our amplitude $\mathcal{M}_{\mu\nu}$.

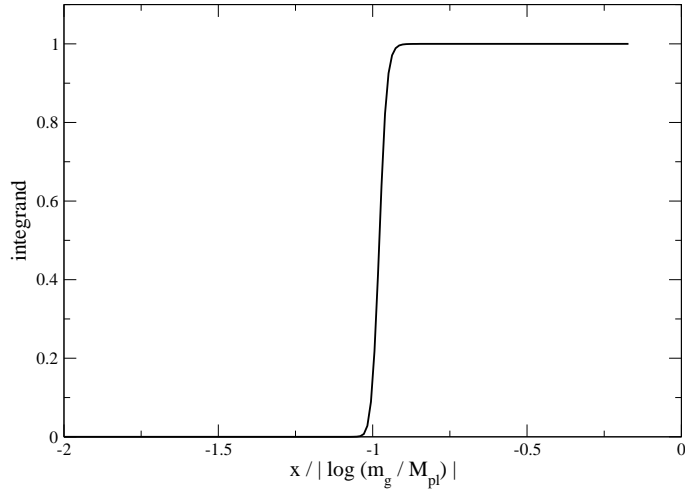


Figure 5.3: The Bremsstrahlung integrand expressed in the new variable $x = \log(k/M_{\text{pl}})$ for some set of parameters. The plateau has been normalized to 1. The vanishing for $x < \log(m_g/M_{\text{pl}}) < 0$ is universal, but the larger x part, where the integral is evaluated, of course depends on the parameters we use.

Another way of performing the polarization sum is to multiply the matrix elements directly with the two physical polarization tensors from (4.71) after suitable rotations and summing them up. This second method has three advantages. First, it can be applied even if the QED-like Ward identity $k_\mu \mathcal{M}^{\mu\nu} = 0$ does not hold true. As we will see in section 5.7 this can in principle be the case in perturbative gravity, because of some additional terms in the Ward identity. Second, the direct method leads to a faster numerical integration of the Bremsstrahlung phase space due to a more compact expression of the squared amplitude. And third, since we work in soft approximation, the amplitude is not in a physical configuration, i.e. the QED-like Ward identity will not exactly hold and there are additional small contributions from the unphysical d.o.f. in the polarization sum (5.36). But we have seen that for our processes both methods lead to approximately the same results, in particular both methods lead to the cancellation of the IR divergences. In the following we will restrict ourselves to the numerical faster one, i.e. using only physical polarizations, and do not use (5.36) anymore.

5.6 Effective vertices

The general matter action (5.3) contains several effective interactions of order κ^2 which have to be included in the framework of effective quantum field theory.

A second approach to effective theories is writing down the most simple action we require for our problem and calculating the required process to the desired order in the perturbation series. This action should of course be compatible with the symmetries of our system. If the divergences of the fundamental interaction operators can not be renormalized by counterterms having the same structure as the interactions itself, we include additional operators having this structure to the Lagrangian. These operators are called induced interactions and carry some prefactor including inverse powers of the new physics scale, i.e. M_{pl} in our case, and a dimensionless constant which has to be fixed by experiment. In order to avoid inconsistencies one assumes that all dimensionless constants are of order one or smaller [23].

In our example one would start with a minimal theory with an interaction term $\lambda V^{ij} \psi_i \psi_j \phi$. The graviton loop corrections in order κ^2 to this operator can not be renormalized by using a counterterm with the same structure. As we have seen in section 5.4, the one loop corrections will induce the operators $\kappa^2 V^{ij} \square \psi_i \psi_j \phi$ and $\kappa^2 V^{ij} \psi_i \psi_j \square \phi$. These operators are of course part of the general action (5.3), but they are motivated additionally by being induced dynamically.

Next we give the relative NLO corrections to the S -type process due to the effective three point operators.

Therefore we assume that the matrix structure of the constant matrices is the same as V^{ij} , i.e. $c^{ij} = c V^{ij}$, $d^{ij} = d V^{ij}$ and $e^{ij} = e V^{ij}$, since this is motivated by the one loop counterterms. The relative NLO corrections are given by

$$\frac{\mathcal{M}_{3\text{point}}\mathcal{M}_{\text{tree}}^* + \mathcal{M}_{3\text{point}}^*\mathcal{M}_{\text{tree}}}{|\mathcal{M}_{\text{tree}}|^2} = -2\kappa^2 (S(c + 2e) + 2m_\psi^2(d - c)) . \quad (5.37)$$

We see that there are two types of contributions, the ones proportional to m_ψ^2 which are irrelevant for the high energy limit, and the ones proportional to S which are relevant. Taking only the induced operators into account also leads to relevant and irrelevant contributions. Furthermore we see that we can adjust the sign and magnitude of the relevant NLO contributions of the effective vertices by the parameter $c + 2e$.

The relative contribution of the effective four point interaction to the squared amplitude is given by

$$\frac{\mathcal{M}_{4\text{point}}\mathcal{M}_{\text{tree}}^* + \mathcal{M}_{4\text{point}}^*\mathcal{M}_{\text{tree}}}{|\mathcal{M}_{\text{tree}}|^2} = 2\lambda_4\kappa^2(S - m_\phi^2) . \quad (5.38)$$

We see that it also has relevant contributions to the high energy limit through the linear S dependence.

Finally we discuss the contributions due to effective scalar two point operators. These operators can either appear in the wavefunction renormalization or as correction to the internal ϕ propagator. The contributions to the wavefunction renormalization will be irrelevant in the high energy limit, so that we can neglect them. The contributions to the internal ϕ propagator will contain relevant terms, so that we have to include them. They are given by

$$\frac{\mathcal{M}_{2\text{point}}\mathcal{M}_{\text{tree}}^* + \mathcal{M}_{2\text{point}}^*\mathcal{M}_{\text{tree}}}{|\mathcal{M}_{\text{tree}}|^2} = -2\Xi_\phi\kappa^2\frac{S^2}{S - m_\phi^2} , \quad (5.39)$$

which is proportional to S in the high energy limit $S \gg m_\phi^2$.

When we sum up all NLO contributions from the scalar effective vertices we arrive at a total contribution which we can be parameterized as

$$\frac{\mathcal{M}_{\text{totaleff}}\mathcal{M}_{\text{tree}}^* + \mathcal{M}_{\text{totaleff}}^*\mathcal{M}_{\text{tree}}}{|\mathcal{M}_{\text{tree}}|^2} \approx A\kappa^2 S + B\kappa^2 m_\phi^2 + C\kappa^2 m_\phi^2 \quad \text{for } S \gg m_\phi^2, \quad (5.40)$$

where A , B and C are dimensionless constants which can be expressed through the fundamental parameters of the effective interactions. Note that this formula only applies to the high energy limit, since we had to use the approximation $\frac{S^2}{S - m_\phi^2} \approx S + m_\phi^2$, for $S \gg m_\phi^2$, in order to expand the contributions from the two point operators. We will neglect B and C , since they do not contribute in the high energy limit, and we will only discuss the dependence of the results on the effective parameter A in the following without resolving the individual contributions (5.37), (5.38) and (5.39) anymore.

The phenomenology of the effective scalar-scalar-graviton couplings parameterized by a and b is harder to investigate, since this interaction occurs in loop diagrams. We will discuss it later numerically.

5.7 On-shell Ward identity

Since the Bremsstrahlung diagrams come with an external graviton, we are in the position to check the validity of the on-shell Ward identity. The Ward identity expresses gauge invariance on amplitude level and therefore is a good check to find possible calculational errors. The problem with the gravitational Ward identity is that at a first sight only

$$\frac{\partial}{\partial x_\mu} \langle 0 | h_{\mu\nu}(x) \Phi_1 \Phi_2 \dots \Phi_n | 0 \rangle = \frac{1}{2} \frac{\partial}{\partial x^\nu} \langle 0 | h(x) \Phi_1 \Phi_2 \dots \Phi_n | 0 \rangle \quad (5.41)$$

holds true, because the BRST transformation of the antighost is given by $\delta_{\text{BRST}} \bar{C}_\mu = h_{\mu\nu}{}^\nu - \frac{1}{2} h_{,\mu}$. Here Φ_i denotes some other fields and the amplitudes are assumed to be on-shell and amputated.

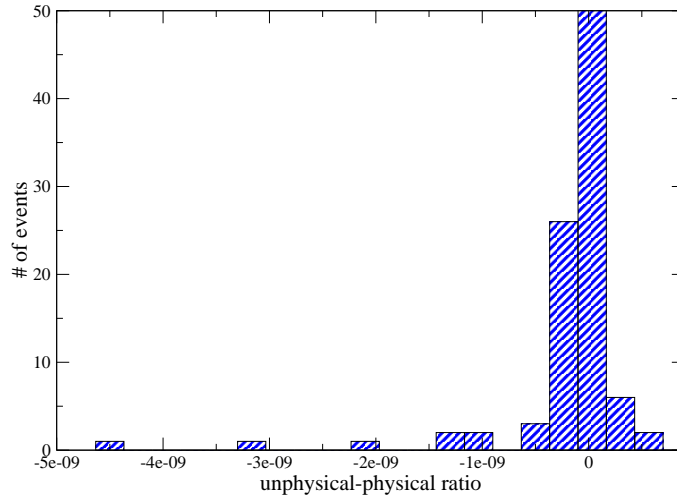


Figure 5.4: Numerically determined values of the Ward identity. The peak at 0 has a height of around 40000.

But we have found out that for our processes both sides vanish independently, i.e. the QED-like Ward identity

$$\frac{\partial}{\partial x_\mu} \langle 0 | h_{\mu\nu}(x) \Phi_1 \Phi_2 \dots \Phi_n | 0 \rangle = 0 \quad (5.42)$$

holds true. Since we can not prove this statement, we have to check (5.42) in every process under consideration in order to have the possibility to apply simplified polarization sums.

We have automatized the calculations which are required for checking the existence of Ward identities by using FeynArts, FormCalc and some additional small programs and Mathematica notebooks we have written by ourselves. This routine generates all graph topologies and field insertions by using FeynArts. The amplitude is calculated by using FormCalc and the graviton polarization tensors occurring in the analytical expressions of the amplitudes are replaced by the corresponding graviton momenta. The next part is to generate physical configurations, i.e. generating a physical combination of the external particles momenta. Since we have a $2 \rightarrow 3$ process, we have generated the configurations by a numerical procedure using the *MAMBO* algorithm [24], since it is easier than an analytical study of the three (massive) particle final state phase space.

The numerical procedure works as follows:

- generate a random set of physical momenta for the external particles
- calculate the value of $k^\mu \mathcal{M}_{\mu\nu}$ for the desired amplitude $\mathcal{M}_{\mu\nu}$
- calculate the value of the amplitude $\mathcal{M}_{\mu\nu} \epsilon^{\mu\nu}$, where ϵ are physical polarization tensors
- verify that $|k^\mu \mathcal{M}_{\mu\nu} / \mathcal{M}_{\alpha\beta} \epsilon^{\alpha\beta}| \approx 0 \quad \forall \nu$

It has to be mentioned here that the Ward identity was checked for massless gravitons, since for massive ones it does not hold. Since the only artifact of the mass regulator in the Ward identity is the on-shell condition $k^2 = m_g^2$, we have a smooth limit for $m_g \rightarrow 0$ and it is justified to restrict ourselves to the massless graviton case.

The histogram 5.4 shows the distribution of the ratios $|k^\mu \mathcal{M}_{\mu\nu} / \mathcal{M}_{\alpha\beta} \epsilon^{\alpha\beta}|$ for 10000 physical combinations of momenta and all ν . For this calculation we have used the *S*-type localization graphs. The results for *T*-type graphs are similar. It can be seen that within the numerical precision the Ward identity holds true. The maximal deviation from 0 was only 1 out of 40000 events with a ratio of about $-4.5 \cdot 10^{-9}$.

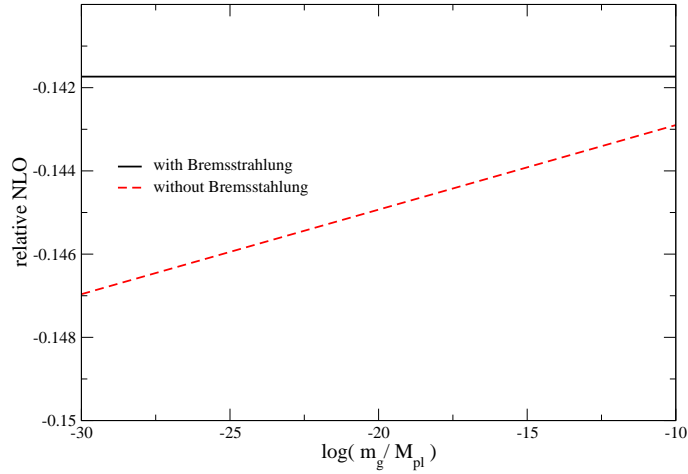


Figure 5.5: IR cutoff (in)dependence of the result. The reference value for the particle masses is $m_\psi = m_\phi = 10^{-15} M_{\text{pl}}$, i.e. in the TeV range. The cutoff independence is not dependent on the choice of parameters and kinematic quantities.

5.8 Results and interpretation

5.8.1 IR cutoff independence of the results

Since we had to introduce a small graviton mass m_g as an IR regulator, we have to study the (in)dependence of the results under variations of this mass in order to perform the limit of vanishing m_g . Figure 5.5 shows the m_g (in)dependence of the relative NLO corrections with and without adding the Bremsstrahlung contributions. We see that the corrections without Bremsstrahlung show a logarithmic dependence on m_g , while the inclusive NLO correction are rather independent over a wide range of the regulator. This result is universal, i.e. it is not dependent on the parameters we choose, such as masses, couplings and kinematical quantities.

In the following we will set $m_g = 10^{-20} M_{\text{pl}}$ which is also far below the assumed particle mass and study the individual parts of the relative NLO contributions for this particular value of the cutoff.

5.8.2 Relative NLO contributions for S -type localization

In this section we will discuss the parameter dependence of the NLO corrections for S -type localization. In particular we are interested in the dependence on the center of mass energy \sqrt{S} , the scattering angle θ and the particle masses. For these basic investigations we will set the effective coupling constants a and b to zero and assume natural values for V , i.e. $V^{12} = V^{21} = 1$, $V^{34} = V^{43} = 1$ and $V^{ij} = 0$ else. The effective interactions will be included through the relevant effective coupling constant A , for which we choose the natural value $A = 1$. Variations of this parameter, in particular changing the sign, will be discussed later.

Furthermore we will use the graviton mass $m_g = 10^{-20} M_{\text{pl}}$ and our particular gauge fixing for comparing the individual NLO contributions. Of course only the total NLO contributions including Bremsstrahlung are IR cutoff independent and gauge invariant, and therefore physical, but it is also useful to understand which individual diagrams have large contributions and find out if there are any cancellations between different contributions.

The relative NLO contributions will not depend on the coupling λ since both, the NLO and the squared tree amplitude, are of order λ^4 , such that this dependency cancels in the ratio.

Figure 5.6 shows the angular dependence of the NLO corrections at a center of mass energy $\sqrt{S} = 0.01 M_{\text{pl}}$ using particle masses $m_\psi = m_\phi = 10^{-16} M_{\text{pl}}$, i.e. TeV particles. One sees that there is very little angular dependence and the largest NLO corrections are for $\theta = \pi/2$ scattering. This very

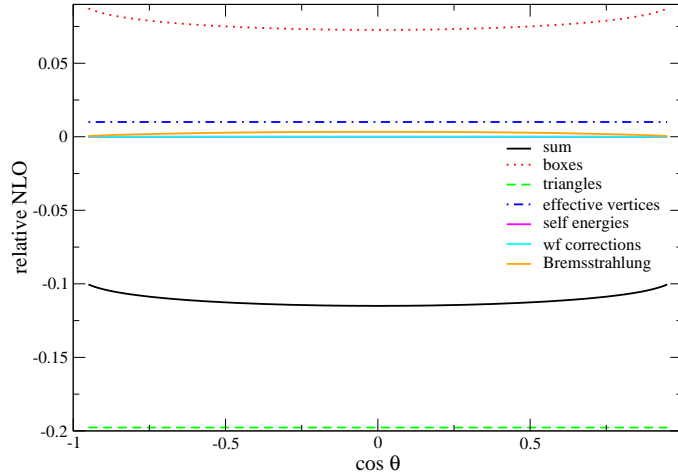


Figure 5.6: Angular dependence of the relative NLO corrections for S -type localization. The center of mass energy was chosen as $\sqrt{S} = 0.01 M_{\text{Pl}}$. We have chosen the particle masses $m_\psi = m_\phi = 10^{-16} M_{\text{Pl}}$.

little angular dependence is natural for models with three point scalar couplings in S -channel scattering, since the scalar vertices are independent from the angles. The only contributions showing some angular dependencies are the boxes and the Bremsstrahlung. This can be understood since the boxes are the only diagrams connecting in and out lines with some angular dependent vertex, the graviton emission, and thus depend on the scattering angle. The Bremsstrahlung angular dependence is due to the interference between initial and final state Bremsstrahlung diagrams.

Furthermore one obtains that the main contributions are coming from triangles, boxes and effective vertices. The self energies, Bremsstrahlung and especially wavefunction corrections are only marginal contributions, at least for this particular choice of the IR cutoff. But it has to be mentioned that the self energy diagrams are IR independent and therefore have only small contributions compared to the total NLO for every IR regulator.

Moreover we see that the boxes and effective vertices come with a different sign than the triangles and therefore lower the absolute value of the NLO contributions. But the contribution from the effective vertices can have also a negative sign by assigning the effective constant A a negative value.

Figure 5.7 shows the energy dependence for $\theta = \pi/2$ scattering and particle masses $m_\psi = m_\phi = 10^{-16} M_{\text{Pl}}$. We obtain again that triangles, boxes and effective vertices give the main contributions. Furthermore one sees that the NLO corrections exceed 10% at energies of about $M_{\text{Pl}}/100$ and grow to nearly 50% at $\sqrt{S} = M_{\text{Pl}}/50$. This shows that we can not use the effective theory for higher energies than around $M_{\text{Pl}}/100$, since the result will then also depend on the higher loop corrections and the higher order operators. This specific scale will also set a limit on localization, as we will discuss below. Note that the particular choice of the critical value of the relative NLO is a very subjective task. We choose 10% as a sensible value throughout this work. Different choices like e.g. 50% will only give order one prefactors which do matter in our discussion.

Next we will investigate the particle mass dependence of the NLO corrections. Therefore we will not resolve the NLO corrections into their individual terms anymore, but we will only consider the total NLO. We will vary the ψ particle mass from $10^{-16} M_{\text{Pl}}$ to $10^{-8} M_{\text{Pl}}$ and the ϕ particle mass from 0 to $10^{-8} M_{\text{Pl}}$. The reason why we can not choose $m_\psi = 0$ is the emergence of collinear divergences in this limit.

Figure 5.8 shows the mass dependence of the inclusive NLO corrections. As expected they decrease by increasing the particle masses. The pictorial reason for this is that loops are suppressed if they contain heavy particles, because of the denominators $1/(k^2 - m^2)$ of the massive propagators. This means that we can enhance the validity of our theory by using heavier particles. Furthermore the dependence on the internal field mass m_ϕ is stronger than on the clock and rod field mass m_ψ . As a note, we noticed that the relevance of the Bremsstrahlung contributions increases by increasing the particle masses.

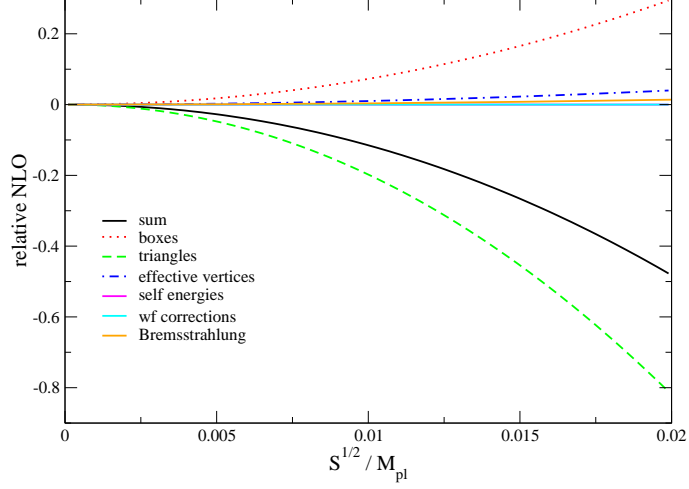


Figure 5.7: Center of mass energy dependence of the relative NLO corrections for S -type localization. The scattering angle was chosen as $\Theta = \frac{\pi}{2}$. We have chosen the particle masses $m_\psi = m_\phi = 10^{-16} M_{\text{pl}}$.

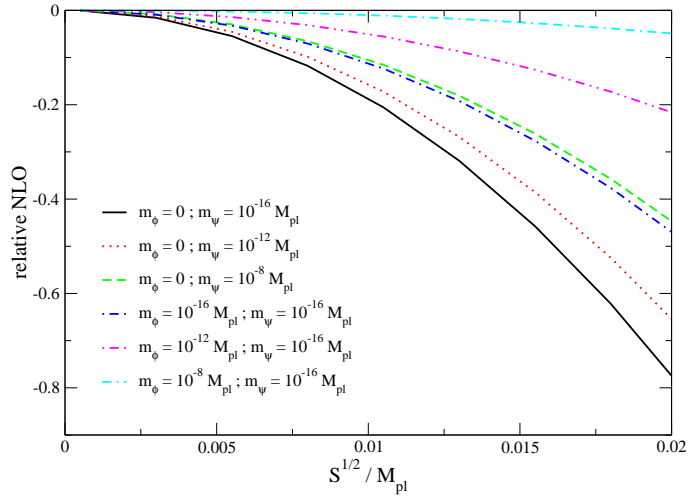


Figure 5.8: Center of mass energy dependence of the relative NLO corrections for S -type localization with different particle masses. The scattering angle was chosen as $\Theta = \frac{\pi}{2}$.

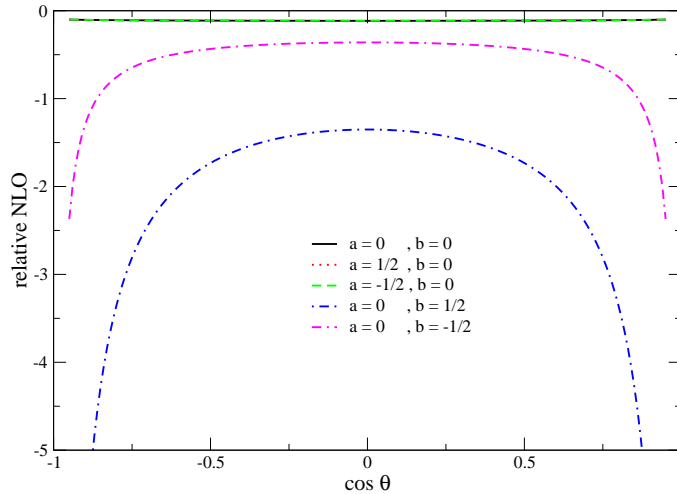


Figure 5.9: Angular dependence of the relative NLO corrections for S -type localization with different effective couplings a and b . The center of mass energy was chosen as $\sqrt{S} = 0.01 M_{\text{Pl}}$. We have chosen the particle masses $m_\psi = m_\phi = 10^{-16} M_{\text{Pl}}$.

Since the angular dependence with different particle masses behaves as expected, i.e. it decreases like shown in figure 5.8 without changing its form, we do not have to show the graphs.

Next we investigate the dependence of the results on the effective coupling parameters a and b which give additional terms to the graviton-scalar-scalar vertex. Figure 5.9 shows the angular dependence of the total NLO corrections for different a and b . One obtains that in particular for small or large angle scattering the effective interactions have large effects if b does not vanish. These large effects come from the box diagrams, where the new kinematical structure of the graviton-scalar-scalar vertex leads to an enhanced forward and backward scattering. Furthermore we see that the scale where the effective theory breaks down will depend strongly on the choice of a and especially b . Moreover if we assume the effective interaction to be of the natural order of the standard interaction, i.e. $a = b = 1/2$, we have 20% NLO corrections at $\sqrt{S} = 0.004 M_{\text{Pl}}$ for $\theta = \pi/2$ scattering of $m_\psi = m_\phi = 10^{-16} M_{\text{Pl}}$ particles. This becomes even worse for smaller and larger angles. We will further discuss this feature in the following sections.

Finally we discuss the dependence of the results on the effective scalar vertices. We have chosen the effective parameter describing the total effective vertex contributions as $A = 1$ and we have obtained that this particular choice helps to lower the NLO contributions a little bit, see fig. 5.7. By interchanging the sign of A we would have slightly larger NLO corrections. But if the effective constant A has a magnitude smaller than around 1 its contributions are only marginal compared to the boxes and triangles, at least for TeV particles. Heavier particles will be more affected by the effective vertex contributions, since these contributions do not decrease by increasing the masses, like e.g. the loops. But in most scenarios the breakdown of the effective theory is not strongly affected by the effective scalar vertices.

5.8.3 Relative NLO contributions for T -type localization

In this section we perform the same analysis as above for the phenomenology of T -type localization. For this purpose we will choose $V^{13} = V^{31} = V^{24} = V^{42} = 1$ and $V^{ij} = 0$ else. Again we will choose $m_g = 10^{-20} M_{\text{Pl}}$ for the IR cutoff and $A = 1$ for the effective scalar vertices. We will start our investigations with $a = b = 0$ for the general discussion and will study the a and b dependence separately later.

Figure 5.10 shows the angular dependence of the relative NLO corrections. The relevance of the individual contributions is the same as in S -type localization, i.e. the triangles, boxes and effective vertices give the main contributions and self energies, wavefunction corrections and Bremsstrahlung are marginal.

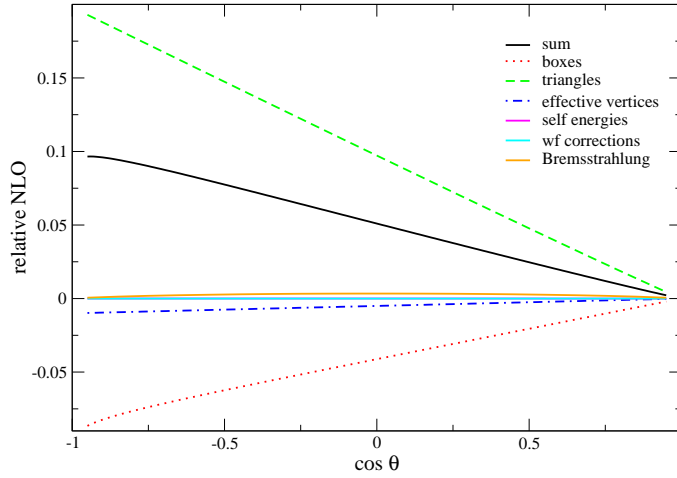


Figure 5.10: Angular dependence of the relative NLO corrections for T -type localization. The center of mass energy was chosen as $\sqrt{S} = 0.01 M_{\text{pl}}$. We have chosen the particle masses $m_\psi = m_\phi = 10^{-16} M_{\text{pl}}$.

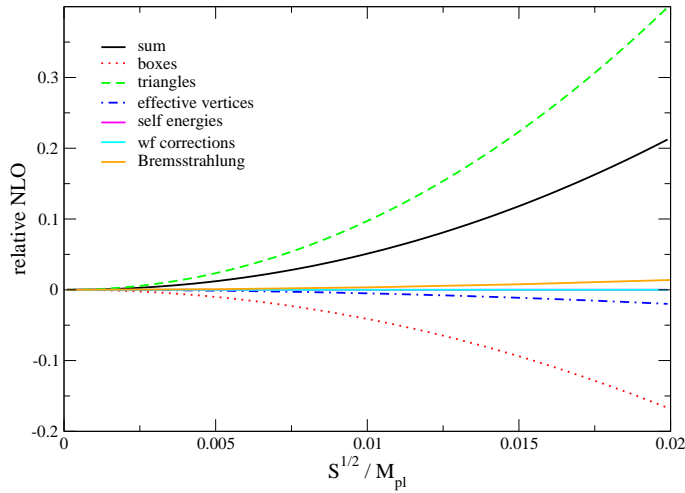


Figure 5.11: Center of mass energy dependence of the relative NLO corrections for T -type localization. The scattering angle was chosen as $\Theta = \frac{\pi}{2}$. We have chosen the particle masses $m_\psi = m_\phi = 10^{-16} M_{\text{pl}}$.

One sees that the NLO corrections increase by increasing the scattering angle. This is natural since the squared tree amplitude decreases roughly as $1/T^2$ such that for large angles it becomes small. Therefore also small absolute corrections at large angles will be large relative corrections.

Figure 5.11 shows the energy dependence of $\theta = \pi/2$ scattering for $m_\psi = m_\phi = 10^{-16} M_{\text{pl}}$ particles. The 10% NLO corrections are reached at $\sqrt{S} = 0.015 M_{\text{pl}}$ which is similar to S -type localization.

The mass dependence of the NLO corrections is the same as in the case of S -type localization, i.e. increasing the masses leads to decreasing NLO contributions. The dependence of the internal mass m_ϕ is stronger than the dependence on the clock and rod field mass m_ψ . We omit a figure showing this dependence since the behavior is very similar to S -type localization.

The dependence of the results on the effective scalar vertices can again be described by an effective parameter, like in the case of S -type localization. Variations of this parameter in the range $[-1, 1]$ do only lead to small changes in the total NLO contributions. Hence the value of A does not affect strongly the breakdown of the effective theory. This is exactly like in the case of S -type localization.

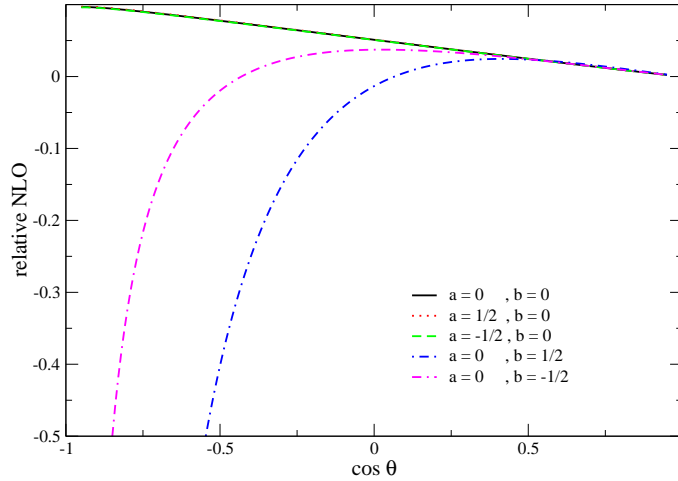


Figure 5.12: Angular dependence of the relative NLO corrections for T -type localization with different effective couplings a and b . The center of mass energy was chosen as $\sqrt{S} = 0.01 M_{\text{pl}}$. We have chosen the particle masses $m_\psi = m_\phi = 10^{-16} M_{\text{pl}}$.

Finally we investigate the dependence on the effective graviton couplings a and b . Again the box diagram contributions will lead to large effects by a change in especially b . This is shown in figure 5.12. The large effects on variations of b is predominantly for large angle scattering and confirms our suspicion that through the modified coupling structure there is a strongly enhanced scattering in tree-level suppressed regions in phase space through the box diagrams. The same effect occurs also for S -type scattering, where we have enhancements in both, the small and large angle region of phase space due to the forward-backward symmetry.

To conclude we have found out that there are no striking differences in using either S - or T -type localization. Both models suffer from a strong dependence on the effective graviton-scalar-scalar coupling parameterized by b .

5.8.4 Physical implications to the problem of dynamical localization

As we have seen in section 5.4, the corrections to the localization process are related to the corrections of the momentum eigenstate scattering process, see (5.27). In this section we will use the results obtained above about the NLO corrections to the momentum eigenstate scattering processes in order to estimate a maximal spacetime resolutions by this kind of model. For this estimation we will use the Gaussian wave packets discussed in appendix E.1.

Focussing on (5.27) and (5.29) we see that for the NLO corrections to the localization process we have to integrate the corrections to the momentum eigenstate process over the momentum range defined by the momentum space wave packets. Therefore we have to assure that the effective theory is well defined over this range. Assume that all four wave packets have a central 3-momentum of magnitude q . Then, as explained in appendix E.1, we can use the maximal width $\sigma = q/2$ for each of the wave packets. Since the spectra drop off quickly outside the range defined by the width, the main contributions come from the inside. We can estimate the highest energy which contributes to the intergal by $E_{\text{max}} \approx \sqrt{(\frac{3}{2}q)^2 + m_\psi^2}$. This maximal energy is the same for all four particles, since we assume all central momenta to be of the same magnitude. With the maximal particle energy we can estimate the maximal center of mass energy as $\sqrt{S}_{\text{max}} = 2E_{\text{max}} \approx 3q$ for the high energy limit, where $m_\psi \ll q$.

Next we have to find out which angular range contributes to the process of localization. The central momenta are chosen such that they correspond to $\pi/2$ scattering. Using again the width of the wave packets we identify the relevant angular range to be $\theta \in [\pi/2 - 2\arctan(1/2), \pi/2 + 2\arctan(1/2)]$. Using the $\cos \theta$ variable this becomes $\cos \theta \in [-0.8, 0.8]$.

If we now assume that the effective theory breaks down at about 10% NLO corrections, we see that in S -type localization with TeV mass particles and zero effective coupling a and b the maximal center of mass energy is given by $\sqrt{S_{\max}} = 0.01 M_{\text{pl}}$ for the whole angular range, see fig. 5.6 and 5.7. Hence we can estimate an maximal resolution of $\sqrt{2}/q = 3\sqrt{2}/\sqrt{S_{\max}} = 300\sqrt{2}/M_{\text{pl}}$ by using the resolution properties of overlapping Gaussian functions discussed in appendix E.1.

This resolution can be enhanced by increasing the particle masses, see fig. 5.8, but it could also be decreased if there are effective couplings a and especially b , see fig. 5.9.

This result is rather independent on the scattering channel we use for the localization process. Figure 5.10 shows that despite of the fact that the NLO corrections for T -type localization are a little bit smaller than for S -type localization at $\pi/2$ -scattering (see also fig. 5.11), the growing NLO corrections for large angles will lead to a maximal center of mass energy of about $\sqrt{S_{\max}} = 0.01 M_{\text{pl}}$ too, since the theory has to be defined for the whole angular range $\cos\theta \in [-0.8, 0.8]$. By increasing the mass we can increase the resolution like in S -type localization. Switching on a and especially b will degrade the validity and the resolution of the theory, see fig. 5.12.

Alltogether we see that the results for S - and T -type localization are very similar, and in particular that the maximal resolution of both processes can be spoiled in the presence of effective graviton interactions a and b .

Chapter 6

Pseudo-local Yang-Mills observables with matter clocks and rods

In this chapter we will discuss an explicit realization of the type of model discussed in the last chapter through a $SU(N)$ Yang-Mills theory coupled to scalar fields serving as clocks and rods. The advantage of this theory is that it is a non-super-renormalizable matter model which has stronger connections to nature than the pure scalar model investigated in the last chapter. Furthermore the additional $SU(N)$ gauge invariance will constrain the structure of effective interactions.

6.1 Definition of the theory and observables

In our new model we use two distinct complex scalar fields, ψ_1 and ψ_2 , which live in the fundamental representation of the $SU(N)$ gauge group, i.e. they transform as

$$\psi_1 \rightarrow e^{i\alpha} \psi_1 \quad , \quad \psi_2 \rightarrow e^{i\alpha} \psi_2 \quad , \quad (6.1)$$

where $\alpha = \alpha^a T^a$ are the generators of the $SU(N)$ gauge transformations in the fundamental representation and α^a are the corresponding scalar parameters fields.

The gauge algebra is given by

$$[T^a, T^b] = i f^{abc} T^c \quad , \quad \text{tr}(T^a T^b) = \frac{1}{2} \delta^{ab} \quad , \quad (6.2)$$

where f^{abc} are the $SU(N)$ structure constants. Note that all gauge indices will appear as upper indices.

The action of the gauge covariant derivatives on the scalars is defined by

$$D_\mu \psi_i = \partial_\mu \psi_i - i g_s A_\mu \psi_i \quad , \quad \text{for } i = 1, 2 \quad , \quad (6.3)$$

where g_s is the Yang-Mills coupling and $A_\mu = A_\mu^a T^a$ is the gauge connection one-form transforming under gauge transformations as

$$A_\mu \rightarrow e^{i\alpha} (A_\mu + \frac{i}{g_s} \partial_\mu) e^{-i\alpha} \quad . \quad (6.4)$$

The $SU(N)$ gauge transformation property of the covariant derivative is given by

$$D_\mu \psi_i \rightarrow e^{i\alpha} D_\mu \psi_i \quad . \quad (6.5)$$

The gauge curvature, or field strength, corresponding to the gauge connection is defined as

$$F_{\mu\nu} := \partial_\mu A_\nu - \partial_\nu A_\mu - i g_s [A_\mu, A_\nu] \quad (6.6)$$

and it transforms under the $SU(N)$ gauge transformations as

$$F_{\mu\nu} \rightarrow e^{i\alpha} F_{\mu\nu} e^{-i\alpha} . \quad (6.7)$$

With these ingredients we can construct the familiar $SU(N)$ Yang-Mills action for scalar matter fields coupled to the gauge field A , which is given in the presence of an arbitrary smooth metric g as

$$S_{\text{YM}} := \int d^4x \sqrt{-g} \left(-\frac{1}{2} g^{\mu\alpha} g^{\nu\beta} \text{tr} F_{\mu\nu} F_{\alpha\beta} + \sum_{i=1}^2 g^{\mu\nu} (D_\mu \psi_i)^\dagger D_\nu \psi_i - \sum_{i=1}^2 m^2 \psi_i^\dagger \psi_i + \sum_{i=1}^2 a R \psi_i^\dagger \psi_i - \tilde{\lambda}_4 M^{ijkl} \psi_i^\dagger \psi_j \psi_k^\dagger \psi_l \right) . \quad (6.8)$$

This action is also invariant under diffeomorphisms. Note that the derivatives in the field strength (6.6) are ordinary partial derivatives, because F is constructed as the exterior derivative of the one-form A and hence is independent of the metric connection. Furthermore the covariant derivatives on the scalar fields include only gauge connections and no metric connections. This means that in the action (6.8) the metric, i.e. gravity, just enters through $\sqrt{-g}$ and $g^{\mu\nu}$ and not through Christoffel connections.

The action above is incomplete since the one-form gauge field is a constrained dynamical system which has to be gauge fixed. We can think about different realizations of gauge fixing, e.g. we can use the minimal diffeomorphism invariant extension of the Feynman gauge fixing action given by

$$S_{\text{YM-GF}}^{\text{cov}} := -\text{tr} \int d^4x \sqrt{-g} g^{\mu\nu} D_\mu A_\nu g^{\alpha\beta} D_\alpha A_\beta , \quad (6.9)$$

where now the metric covariant derivatives enter and the trace is over the gauge group. Another possibility is to choose the non-covariantized version of this gauge fixing given by

$$S_{\text{YM-GF}} := -\text{tr} \int d^4x \eta^{\mu\nu} \partial_\mu A_\nu \eta^{\alpha\beta} \partial_\alpha A_\beta , \quad (6.10)$$

where only the flat background enters. If we include the corresponding ghost action too, the choice of the gauge fixing is irrelevant in physical observables like cross sections, since both combinations, the covariantized gauge fixing together with the covariantized ghosts or the non-covariantized combination, will only be an additional Yang-Mills BRST exact term in the action and therefore does not effect physical quantities. We will choose the non-covariantized version of the gauge fixing in the following, since with this choice the off-shell Ward identity of the gluon propagator will hold true after including the graviton corrections at one loop level. The covariantized version of the gauge fixing will have a different off-shell behavior, because of the additional nonlinear terms. We do not need to compute the explicit form of the ghost action since it does not contribute to our process in the desired order.

In this model there are also effective operators which contribute to our process. They will be discussed later in the corresponding section on effective vertices below.

Now we can expand the metric around the flat Minkowski spacetime and describe only gravitons dynamically. Inserting the metric expansion into the action (6.8) and (6.10) will lead to interaction terms among scalars, vectors and gravitons. We will not give the expanded action here for reasons of compactness. We will only give the collection of the required Feynman rules in the next section. The graviton action has been derived in section 3.5 above and is given by (3.29).

We now proceed with the definition of a possible pseudo-local observable in this model. Assume the following operator

$$O_{\text{YM}} := i g_s \sum_{i=1}^2 \int d^4x \sqrt{-g} (\psi_i^\dagger A_\mu \partial^\mu \psi_i - \partial^\mu \psi_i^\dagger A_\mu \psi_i) , \quad (6.11)$$

which is obviously diffeomorphism invariant but not Yang-Mills gauge invariant. Now assume two scalar two-particle states $|f_1^{\text{red}}, \bar{f}_1^{\text{blue}}\rangle$ and $|f_2^{\text{red}}, \bar{f}_2^{\text{blue}}\rangle$, where f_i^{color} is a wave packet state of the particle species

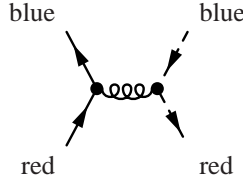


Figure 6.1: Tree-level localization graph for S -type localization in Yang-Mills theory. It coincides with the S -matrix element for $\psi_1^{\text{red}}\bar{\psi}_1^{\text{blue}} \rightarrow \psi_2^{\text{red}}\bar{\psi}_2^{\text{blue}}$ scattering, if $\tilde{\lambda}_4 = 0$.

i with generalized color, i.e. $SU(N)$ quantum number, and $\bar{\cdot}$ denotes the antiparticle. The wave packets should have similar overlapping properties as in the chapter above for S -type localization, i.e. the two in-state wave packets should overlap around some spacetime point x_0 and the two out-state wave packets w.l.o.g. around 0. Note that the states are not $SU(N)$ gauge invariant either.

If we now take the in-out matrix element of the time ordered square of this operator between the two states at tree-level, see fig. 6.1, we obtain

$$\langle f_2^{\text{red}}, \bar{f}_2^{\text{blue}}; \text{out} | T \{ O_{\text{YM}} O_{\text{YM}} \} | f_1^{\text{red}}, \bar{f}_1^{\text{blue}}; \text{in} \rangle = \frac{g_s^2}{16} \int d^4x d^4y (\bar{f}_1^{\text{blue}} \overleftrightarrow{\partial}^\mu f_1^{\text{red}})(x) (\bar{f}_2^{\text{blue}} \overleftrightarrow{\partial}^\nu f_2^{\text{red}})^*(y) \sum_{a \in \mathcal{A}} \langle 0 | T A_{(\mu}^a(x) A_{\nu)}^a(y) | 0 \rangle. \quad (6.12)$$

This is the correlation function of the gauge fields summed over all gauge fields which contribute to the particular transition denoted by $\mathcal{A} \subseteq \{1, 2, \dots, N^2 - 1\}$. The Lorentz indices of the correlation function are projected on the left-right derivatives on the wave packets. For first order Gaussian wave packets these projectors are given by

$$(f_i \overleftrightarrow{\partial}^\mu f_j)(x) = (-i(q_j^\mu - q_i^\mu) - \sigma^2(\vec{\xi}_j \partial^\mu \vec{\xi}_j - \vec{\xi}_i \partial^\mu \vec{\xi}_i)) f_i(x) f_j(x), \quad (6.13)$$

where q_i are the central four-momenta of f_i and $\xi_i := \mathbf{x} - \mathbf{v} - \frac{\mathbf{q}_i}{E_{q_i}}(t - v^0)$, with $(v^0, \mathbf{v}) = x_0$ for the incoming states and $(v^0, \mathbf{v}) = 0$ for the outgoing ones. Therefore the left-right derivatives of the Gaussian wave packets have similar locality properties as the wave packets themselves.

In order to interpret the matrix element of the pseudo-local operators directly as a scattering matrix element the four point interaction given in the action (6.8) has to vanish, or at least to be very small so that we can neglect it. This is the same problem as in the pure scalar model, where we have circumvented it by the assumption that the four point interaction operator is induced from the three point interactions and gravity. Here we have to use some other arguments, since we have no second dimensionful coupling in this model.

Assume that the interaction $\tilde{\lambda}_4$ is 0 at one particular scale. Then the gluon corrections to this coupling constant are at least of order g_s^4 and gravitons will not induce this operator through radiative corrections at all, if the scalars are massless (or at least very light compared to M_{pl}). This is because internal graviton exchanges lead only to contributions to non-renormalizable operators by using power counting. Therefore the four point contact interaction is of order g_s^4 and negligible compared to the g_s^2 diagrams if we choose g_s to be very small.

Another motivation for dropping this kind of interaction is that we want to model matter clocks and rods, which are in general fermions. The only reason why we use scalars is that in this case we can describe gravity through metric variables which simplifies the calculations. Fermionic fields can not have renormalizable four point interactions, so that for them this kind of problem does not occur. Thus we can also motivate the vanishing of $\tilde{\lambda}_4$ by arguing that we do not want to introduce interactions to the action which differ fundamentally from fermion interactions.

It has to be mentioned that the vanishing of the four point coupling $\tilde{\lambda}$ is not fundamental for our model. We could also extract the desired observable from the scattering process with four point interactions included. But we will nevertheless demand it to vanish, because in this case the desired observable is directly given by the scattering process without performing further calculations.

Since the tree-level observable is given by the S -matrix element for vanishing $\tilde{\lambda}_4$, it is invariant under the $SU(N)$ gauge transformations. Even if the four point coupling is nonvanishing the results are gauge invariant. This is because the scalar contact terms are gauge invariant in their own right.

This shows that this model offers us a pseudo-local observable which is accessible by scattering of differently colored particles. By using different states given by $|f_1^{\text{red}}, f_2^{\text{blue}}\rangle$ and $|f_1^{\text{blue}}, f_2^{\text{red}}\rangle$ we can also perform T -type localization as in the model above.

We could now perform a similar analysis as in section 5.3 in order to investigate tree-level localization in both S and T channel. The result would be again that at tree-level we could have an arbitrary high spacetime resolutions by using very small width wave packets. Since this analysis is the same as in section 5.3 we do not have to repeat it here.

The next step is to include the NLO contributions due to gravity and discuss the phenomenology of localization in the Yang-Mills model and compare it to the pure scalar model. In the following, in particular for the phenomenology, we will constrain ourselves to the case of $SU(3)$ Yang-Mills theory since this gauge group is already included in FeynArts and FormCalc so that we do not have to perform any other modifications in these codes. We will from now on call the one-form gauge field gluon.

The problem of the non-existence of asymptotic colored states in conventional QCD, because of confinement, can be avoided by including sufficiently many massless (or at least very light) colored scalar and fermionic particles to our model, which do not couple to our process in the desired order, but do change the sign of the QCD β -function, such that there is no more asymptotic freedom. We assume the reader to be familiar with renormalization group, anomalous dimensions and β -functions such that we only give the result for the $SU(3)$ Yang-Mills β -function, if there are N_s scalars and N_f fermions in the fundamental representation, without explaining the required calculations. It is given by

$$\beta_{\text{QCD}} = -\frac{g_s^3}{96\pi^2} (66 - 4N_f - N_s) . \quad (6.14)$$

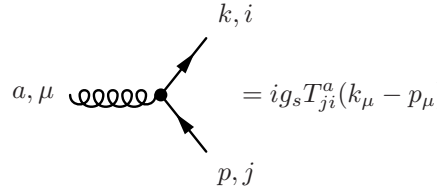
It has to be mentioned that this calculation has been performed using FormCalc in order to determine the required UV divergences and therewith the anomalous dimensions.

6.2 Feynman rules

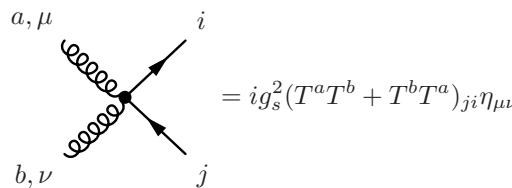
We give the required Feynman rules for the Yang-Mills model including scalar matter and linearized gravity. We will use the convention that all momenta flow into the vertex. The scalar and graviton propagator are the same as given in fig. 5.2, as well as the scalar-scalar-tensor interaction. The gluon propagator in Feynman gauge is given by

$$\text{gluon propagator} = -\frac{i}{p^2} \eta_{\mu\nu} \delta^{ab} . \quad (6.15)$$

The gluon-scalar interactions are given by the following three and four point interactions for both species of matter

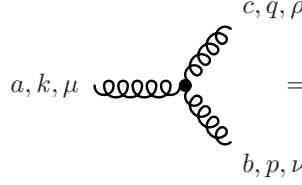


$$= ig_s T_{ji}^a (k_\mu - p_\mu) \quad (6.16)$$



$$= ig_s^2 (T^a T^b + T^b T^a)_{ji} \eta_{\mu\nu} \quad (6.17)$$

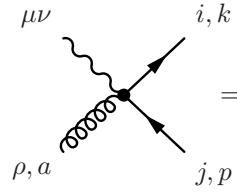
The three point gluon self interaction is also required for our process and is given by



$$= -g_s f^{abc} ((k - q)_\nu \eta_{\mu\rho} + (p - k)_\rho \eta_{\mu\nu} + (q - p)_\mu \eta_{\rho\nu}) . \quad (6.18)$$

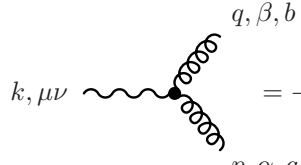
We do not require the gluon four point interaction in our process.

The scalar-scalar-gluon-graviton interaction is given by



$$= i \frac{g_s \kappa}{2} ((k - p)_\rho \eta_{\mu\nu} - (k - p)_\nu \eta_{\mu\rho} - (k - p)_\mu \eta_{\nu\rho}) T_{ji}^a \quad (6.19)$$

The last required interaction is the gluon-gluon-graviton vertex. It is given by



$$= -i \delta^{ab} \frac{\kappa}{2} ((\eta_{\mu\alpha} \eta_{\nu\beta} + \eta_{\mu\beta} \eta_{\nu\alpha} - \eta_{\mu\nu} \eta_{\alpha\beta}) p q + p_\beta q_\alpha \eta_{\mu\nu} + 2 p_{(\mu} q_{\nu)} \eta_{\alpha\beta} - 2 q_{(\mu} \eta_{\nu)\alpha} p_\beta - 2 p_{(\mu} \eta_{\nu)\beta} q_\alpha) + i \lambda_{\text{gf}} \delta^{ab} \frac{\kappa}{2} (\eta_{\mu\nu} (p_\alpha k_\beta + p_\alpha q_\beta + k_\alpha q_\beta) + 2 p_{(\mu} \eta_{\nu)\beta} p_\alpha + 2 q_{(\mu} \eta_{\nu)\alpha} q_\beta) , \quad (6.20)$$

where $\lambda_{\text{gf}} = 1$ for the covariantized and $\lambda_{\text{gf}} = 0$ for the non-covariantized gauge fixing, i.e. $\lambda_{\text{gf}} = 0$ in the following.


This completes the set of required Feynman rules for investigating the matrix elements in order $g_s^2 \kappa^2$ and also the soft real graviton and gluon emission.

6.3 One loop corrections and counterterms

In this section we perform a similar discussion of the one loop divergences and the required counterterms to cure them like in section 5.4. Again we use the $\overline{\text{MS}}$ renormalization scheme to determine the counterterms. Thus we only require the divergences of the one loop diagrams occurring in our process at order $g_s^2 \kappa^2$. We will divide the diagrams into the diagram classes *tadpoles*, *wavefunction corrections*, *self energies*, *triangles* and *boxes*.

In our particular order there are no nonvanishing tadpole diagrams, since the graviton induced tadpoles are renormalized to 0 by an effective cosmological constant and the gluon tadpoles vanish because of Lorentz invariance.

The wavefunction corrections can be determined by the renormalized wavefunction renormalization, i.e. the residuum of the one loop propagator, by using the relation $\mathcal{M}_{\text{WF}} = 2\delta Z_\psi \mathcal{M}_{\text{tree}}$. The one loop divergence of the scalar propagator is given by



$$= i \delta_{ij} \frac{\kappa^2}{8\pi^2 \epsilon} \left(\frac{a}{2} k^4 - k^2 m^2 \left(1 + \frac{3}{2} a - \frac{3}{2} a^2 \right) + m^4 \left(1 + 3a + \frac{3}{2} a^2 \right) \right) + \text{finite} . \quad (6.21)$$

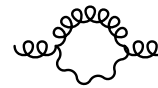
This is of course exactly the same result as in the pure scalar model. There is no difference between ψ_1 and ψ_2 and different colors. Because of this we can call the renormalized wavefunction renormalization Z_{ψ} for both particle species and all colors.

There is one self energy correction diagram given by



$$(6.22)$$

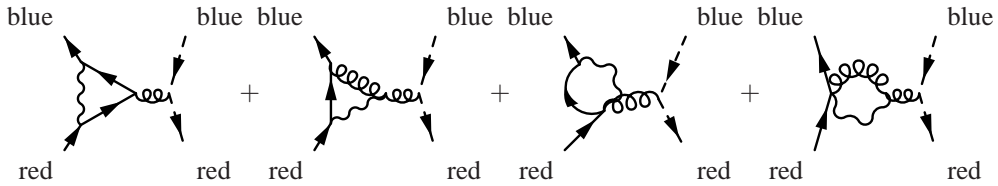
which is renormalized through the gluon propagator counterterm. The required divergence is given by



$$= i\delta^{ab} \frac{k^2}{48\pi^2\epsilon} k^2 (k^2 \eta^{\mu\nu} - k^\mu k^\nu) + \text{finite} . \quad (6.23)$$

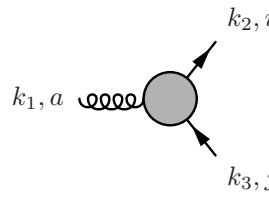
Note that the Lorentz tensor structure of the propagator corrections is exactly the one demanded by the off-shell Ward identity. This is only the case if we use the non-covariantized gauge fixing (6.10).

The triangle diagrams are given by all possible permutations of the following basic diagrams



$$(6.24)$$

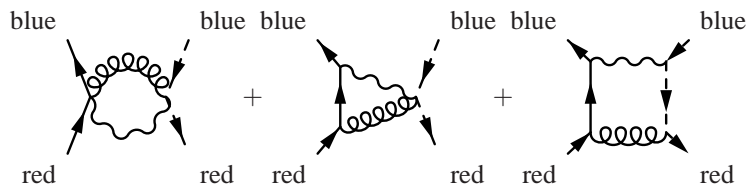
They are renormalized by the counterterm to the scalar-scalar-gluon coupling, which is identical for ψ_1 and ψ_2 and can be calculated from the following divergence



$$\left. \begin{array}{l} k_1, a \\ k_2, i \\ k_3, j \end{array} \right|_{1\text{PI}} = -iT_{ji}^a \frac{g_s k^2}{4\pi^2\epsilon} \left(\frac{1}{2}(k_2 - k_3)_\mu m^2 + a(k_2 - k_3)_\mu \left(\frac{3}{4}m^2 - \frac{1}{3}k_1^2 \right) \right. \\ \left. + ak_{3\mu} \left(\frac{7}{12}k_2^2 - \frac{1}{12}k_3^2 \right) - ak_{2\mu} \left(\frac{7}{12}k_3^2 - \frac{1}{12}k_2^2 \right) \right. \\ \left. - \frac{a^2}{4}(k_2 - k_3)_\mu (3m^2 - \frac{k_1^2}{2}) + \frac{a^2}{8}k_{3\mu}(k_3^2 - k_2^2) - \frac{a^2}{8}k_{2\mu}(k_2^2 - k_3^2) \right) + \text{finite} . \quad (6.25)$$

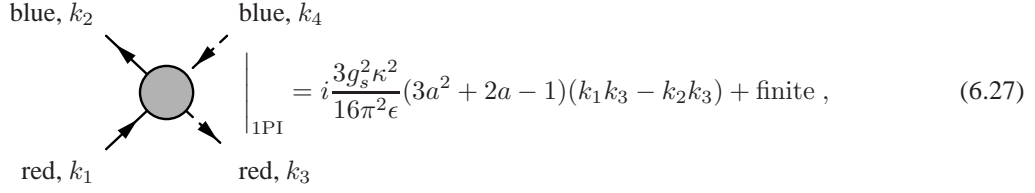
This divergence leads to induced effective interactions to be discussed later.

And finally the box diagrams are given by all permutations of the following basic diagrams



$$(6.26)$$

The on-shell divergence of the sum of all box diagrams is given by



$$= i \frac{3g_s^2 \kappa^2}{16\pi^2 \epsilon} (3a^2 + 2a - 1)(k_1 k_3 - k_2 k_3) + \text{finite} , \quad (6.27)$$

where all momenta are flowing into the vertex. This shows that there is in general an induced effective four point scalar interaction due to this counterterm.

Note that this model has the same diagrammatic structure as the scalar model in chapter 5 before. The diagrams of this model can be constructed by interchanging the ϕ scalars by the gluons. Of course the Feynman rules, and therewith the results of the process, are changed due to the difference in the interaction terms.

6.4 Graviton and Yang-Mills Bremsstrahlung

Since there are IR divergences coming from the gravitons and gluons in loop diagrams we have to include the Bremsstrahlung for both, gravitons and gluons, in our calculation in order to achieve IR finiteness. The soft graviton emissions are taken into account by the same method as in section 5.5, but the gluon emissions require some more effort. The problem with massless particles carrying quantum numbers, like the gluons, is that we have to treat the color quantum number inclusively. For curing soft divergences an inclusive treatment of the final state is sufficient, since only collinear divergences require a summation over degenerate initial states.

As discussed in the appendix D, the Kinoshita-Lee-Nauenberg theorem is compatible with our color flip process in S channel, since the non-inclusive squared amplitude for the colored process $\psi_1^{\text{red}} \bar{\psi}_1^{\text{blue}} \rightarrow \psi_2^{\text{red}} \bar{\psi}_2^{\text{blue}}$ is the same as the non-inclusive squared amplitude of the final state color summed process $\psi_1^{\text{red}} \bar{\psi}_1^{\text{blue}} \rightarrow \psi_2^{\text{col1}} \bar{\psi}_2^{\text{col2}}$.

If we now take the soft gluon emissions into account, i.e. we consider the final state summed process $\psi_1^{\text{red}} \bar{\psi}_1^{\text{blue}} \rightarrow \psi_2^{\text{col1}} \bar{\psi}_2^{\text{col2}} A^a$, where A^a is the gluon with quantum number a , the order $\kappa^2 g_s^4$ terms of the squared amplitude will cancel the gluon IR divergence.

As a note, the same approach works also by using the color summed initial state instead of the final state and taking into account only the initial state gluon Bremsstrahlung while holding the final states at some fixed color. This is due to the crossing relations among amplitudes.

For completeness we mention that in the gluon emission process only the color combinations $(\text{col1}, \text{col2}) \in \{(\text{red}, \text{red}), (\text{blue}, \text{blue}), (\text{green}, \text{green})\}$ contribute to our desired order in the coupling constants.

In the case of T -type localization the final state color summed process does not agree with the colored process $\psi_1^{\text{red}} \bar{\psi}_2^{\text{blue}} \rightarrow \psi_1^{\text{blue}} \bar{\psi}_2^{\text{red}}$ at tree-level. But since all diagrams for this process can be constructed by crossing of S -type diagrams, we can get an IR finite result by summing the color quantum number of only particle species (1 or 2) and keeping the other particle's color quantum numbers fixed. We can use for example the process $\psi_1^{\text{red}} \bar{\psi}_2^{\text{col1}} \rightarrow \psi_1^{\text{blue}} \bar{\psi}_2^{\text{col2}}$, which is the crossed process to the final state color summed S -type process.

This will give us IR finite inclusive cross sections in both S - and T -type localization.

6.5 Effective vertices

In this section we will discuss the effective interaction operators, which contribute to our process in order $g_s^4 \kappa^2$. The possible effective operators occurring in our problem can be divided into the following classes

- (i) higher derivative scalar two point operators
- (ii) higher derivative gluon two point operators

(iii) higher derivative scalar-scalar-gluon operators

(iv) higher derivative four point scalar operators coupling particle species 1 and 2

Note that the operator classes are not gauge invariant in their own right, but we will of course construct them from $SU(N)$ gauge invariant operators working on a flat background. This will lead to relations among the coupling constants, as we will see below. These relations will assure that gauge invariance is manifest in the process in our desired order in the coupling constants. The effective scale will be set by κ .

The contributions for (i) can be constructed from all possible contractions of the following Lorentz tensor operator with the Minkowski metric

$$\mathcal{O}_{\mu\nu\alpha\beta}^1 := \sum_{j=1}^2 \int d^4x \psi_j^\dagger D_\mu D_\nu D_\alpha D_\beta \psi_j . \quad (6.28)$$

We have used the identity $\overleftarrow{D}_\mu^\dagger = D_\mu$, which holds true under the integral because one can integrate by parts. Performing all contractions will lead to redundant operators, because we can use the relation $[D_\mu, D_\nu] = ig_s F_{\mu\nu}$ in order to perform simplifications. By using this commutator relation it can be shown that the tensor operator $\mathcal{O}_{\mu\nu\alpha\beta}^{(1)}$ gives only one independent contribution to the required Feynman rules. This interaction is given by the contraction

$$\mathcal{O}^1 := \eta^{\mu\nu} \eta^{\alpha\beta} \mathcal{O}_{\mu\nu\alpha\beta}^1 = c_1 \kappa^2 \sum_{j=1}^2 \int d^4x (D^2 \psi_j)^\dagger D^2 \psi_j , \quad (6.29)$$

where c_1 is a dimensionless effective coupling constant parameterizing this operator. For the operator class (i) it is sufficient to include the partial derivative parts of the covariant derivatives, i.e. the most general effective operator in this class is given by

$$\mathcal{O}^{(i)} := c_1 \kappa^2 \sum_{j=1}^2 \int d^4x \square \psi_j^\dagger \square \psi_j . \quad (6.30)$$

Note that this reduced operator is not gauge invariant anymore, but it will lead to gauge invariant contributions to the process in our desired order. This is because the terms missing for formal gauge invariance, i.e. the connection parts of the derivatives, will either contribute through the scalar-scalar-gluon vertex (iii) or will be of higher order in the process.

To operator class (ii) contractions of the following kind of tensor operator will contribute

$$\mathcal{O}_{\mu\nu\rho\alpha\beta\gamma}^2 := \text{tr} \int d^4x F_{\mu\nu} D_\rho D_\alpha F_{\beta\gamma} , \quad (6.31)$$

where we also have to allow permutations in the sequence of the individual terms. But since we only require the partial derivative part of the covariant derivatives for the Feynman rules, only two of the permutations will contribute. Therewith the most general non-redundant contracted operator of class (ii) is given by

$$\mathcal{O}^{(ii)} := \kappa^2 \text{tr} \int d^4x (c_2 \partial_\mu F_{\alpha\beta} \partial^\mu F_{\alpha\beta} + c_3 \partial_\mu F^{\mu\nu} \partial_\alpha F^\alpha{}_\nu) , \quad (6.32)$$

where we have inserted dimensionless constants for the purpose of parameterization and used only partial derivatives.

For the operator class (iii) we have contributions from (6.29). Additional operators which could have contributions are contractions of e.g. the following operator

$$\mathcal{O}_{\mu\nu\alpha\beta}^3 := \sum_{j=1}^2 \int d^4x \psi_j^\dagger D_\mu D_\nu F_{\alpha\beta} \psi_j , \quad (6.33)$$

or similar operators with exchanged positions of the covariant derivatives. But those contributions vanish since we only require the partial derivative parts from the covariant derivatives such that we have commuting derivatives and thus only one nontrivial metric contractions remains. The remaining operator is anti-hermitian and therefore does not contribute to the action. This shows that all operators of class (iii) are included in (6.29). The terms which are relevant for operator class (iii) are given by

$$\mathcal{O}^{(iii)} := -ic_1 g_s \kappa^2 \sum_{j=1}^2 \int d^4x \square \psi_j^\dagger (\partial^\mu A_\mu + 2A_\mu \partial^\mu) \psi_j + \text{h.c.} \quad (6.34)$$

Note that in order to assure gauge invariance the coupling constant of the (i) and (iii) operators have to be the same.

The class (iv) operators can be constructed from the renormalizable four point scalar operator by making all possible insertions of two Lorentz contracted covariant derivatives and assuring hermiticity of the operator by adding the hermitian conjugate. Since we require only the partial derivatives for our problem, we will neglect the additional gluon terms in order to arrive at a shorter expression. There are 10 possible insertions of the two partial derivatives from which 4 are redundant by integration by parts and 3 of the remaining 6 are constrained by the hermiticity of the operator. One possible parameterization of this operator is given by

$$\mathcal{O}^{(iv)} := \kappa^2 g_s^2 \int d^4x (c_4 \partial_\mu \psi_1^\dagger \partial^\mu \psi_2 \psi_2^\dagger \psi_1 + c_5 \partial_\mu \psi_1^\dagger \psi_2 \partial^\mu \psi_2^\dagger \psi_1 + c_6 \partial_\mu \psi_1^\dagger \psi_2 \psi_2^\dagger \partial^\mu \psi_1 + \text{h.c.}) . \quad (6.35)$$

In the remaining part of this section we will present the Feynman rules corresponding to these operators and their contributions to the process.

The expression for the effective scalar two point vertex is for both particle species given by

$$\longrightarrow \square \longrightarrow = i c_1 \kappa^2 p^4 \delta_{ij} . \quad (6.36)$$

The effective gluon two point interaction yields

$$\text{oooo} \square \text{oooo} = i (2c_2 + c_3) \kappa^2 p^2 (\eta_{\mu\nu} p^2 - p_\mu p_\nu) \delta^{ab} . \quad (6.37)$$

It obeys the off-shell Ward identity. Moreover we see that c_2 or c_3 is redundant on the level of Feynman amplitudes. A distinction between the c_2 and c_3 operator may get important at higher orders, when the gluon emitting terms of these operators become important. For our case we can set w.l.o.g. $c_2 = 0$.

The effective scalar-scalar-gluon interaction is given by

$$\begin{array}{c} \begin{array}{c} \text{---} \text{oooo} \text{---} \square \begin{array}{c} \nearrow \text{---} \\ \searrow \text{---} \end{array} \\ \begin{array}{c} a, \mu \\ k, i \\ p, j \end{array} \end{array} \\ \end{array} = i c_1 g_s \kappa^2 T_{ji}^a (k^2 + p^2) (k - p)_\mu \quad (6.38)$$

and the effective four point vertex by the following Feynman rule

$$\begin{array}{c} \begin{array}{c} \begin{array}{c} \nearrow \text{---} \\ \searrow \text{---} \end{array} \square \begin{array}{c} \nearrow \text{---} \\ \searrow \text{---} \end{array} \\ \begin{array}{c} k_1, i_1 \\ k_2, i_2 \\ k_3, i_3 \\ k_4, i_4 \end{array} \end{array} \\ \end{array} = -i \kappa^2 g_s^2 \delta_{i_1 i_3} \delta_{i_2 i_4} \left(c_4 (k_1 k_2 + k_3 k_4) + c_5 (k_1 k_3 + k_2 k_4) + c_6 (k_1 k_4 + k_2 k_3) \right) . \quad (6.39)$$

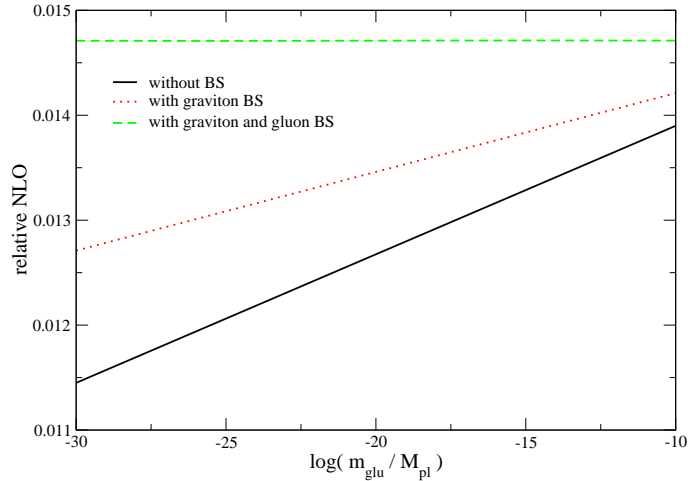


Figure 6.2: IR cutoff (in)dependence of the result. Both cutoffs, the gluon and graviton mass, are chosen to be the same. The reference value for the particle mass is $m = 10^{-15} M_{\text{pl}}$, i.e. in the TeV range. The cutoff independence is not dependent on the choice of parameters and kinematical quantities.

When we compare the operators with the structure of the counterterms (see section 6.3) we see that the counterterms can be expressed through gauge invariant operators, at least when we take the on-shell limit. We see that the three point scalar-scalar-gluon interaction has additional terms which cancel only in the on-shell limit. In this limit the relations from gauge invariance, i.e. the equality of the prefactor labeled above by c_1 of the scalar self energies and the scalar-gluon interaction holds true for the counterterms as well. This shows that we can renormalize the on-shell amplitudes in a gauge invariant way. As a note, the off-shell amplitudes are not physical and can be gauge dependent. This is exactly what we obtain, since the off-shell self energy of the gluon and the scalar-scalar-gluon counterterms depend on which gauge we choose, e.g. the covariantized or non-covariantized one. Only in the on-shell limit this dependence cancels.

With the Feynman rules for the effective vertices above we can calculate the NLO contributions from the effective vertices. They are given by

$$\frac{\mathcal{M}_{\text{eff}}\mathcal{M}_{\text{tree}}^* + \mathcal{M}_{\text{tree}}\mathcal{M}_{\text{eff}}^*}{\mathcal{M}_{\text{tree}}\mathcal{M}_{\text{tree}}^*} = 8c_1\kappa^2 m^2 + 2c_3\kappa^2 S - 2\kappa^2 \frac{-(c_4 - c_5 - c_6)S + (c_4 + c_5 - c_6)T + (c_4 - c_5 + c_6)U}{T - U}. \quad (6.40)$$

In the following we assume that the form of the four point interaction is the same as estimated from the induced interactions, i.e. the numerator in (6.40) should cancel the denominator $T - U$ and lead to an angular independent relative correction proportional to S . This is achieved by choosing $c_4 = 0$ and $c_5 = -c_6$. We can parameterize the relevant high energy contributions of the effective interactions by one parameter for which we can use e.g. c_3 .

The dependence on the effective graviton coupling parameter a will later be discussed numerically, since these couplings are included in the one loop calculations and lead to rather long expressions.

6.6 Results and comparison to the pure scalar model

6.6.1 IR cutoff independence of the results

As we have mentioned above the inclusion of graviton and gluon Bremsstrahlung will render our inclusive squared amplitude IR finite. This is shown in fig. 6.2, where we have displayed the individual contributions coming from graviton and gluon Bremsstrahlung. We have used only one IR regulator for regularizing

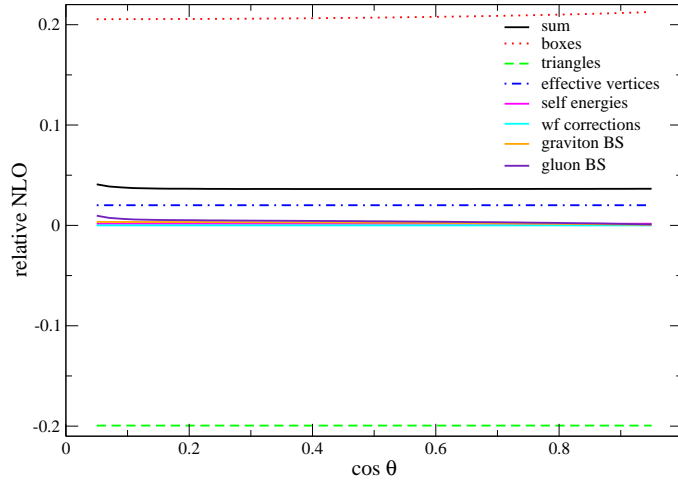


Figure 6.3: Angular dependence of the relative NLO corrections for S -type localization. We show only the $\cos \theta > 0$ part, since the result is symmetric. We leave out $\cos \theta = 0$, since at this angle the tree-level cross section (i.e. the denominator) is 0 and the numerical errors blow up. The center of mass energy was chosen as $\sqrt{S} = 0.01 M_{\text{pl}}$ and the particle mass $m = 10^{-16} M_{\text{pl}}$.

both, the gluon and graviton IR divergences. We have chosen particle masses of $m = 10^{-15} M_{\text{pl}}$, i.e. TeV particles. The IR independence holds irrespective on the scattering angle, the center of mass energy and the particle masses.

In the following we will set the IR regulator, i.e. the gluon and graviton mass, to $m_{\text{glu}} = m_{\text{grav}} = 10^{-20} M_{\text{pl}}$ in order to resolve the individual contributions as in the analysis above. This is far below the assumed particle masses.

6.6.2 Relative NLO contributions for S -type localization

In this section we perform a similar analysis as in section 5.8.2. We will investigate the center of mass energy dependence, the angular dependence and the mass dependence of the relative NLO corrections in S -channel. The T -type process will be discussed in the next section. At the end we will discuss the dependence of the results on variations of the effective graviton coupling parameter a . The particle mass was chosen as $m = 10^{-16} M_{\text{pl}}$, i.e. TeV particles. The values for the effective scalar and scalar-gluon interactions are chosen as $c_3 = 1$ and $c_1 = c_2 = c_4 = c_5 = c_6 = 0$. The high energy behavior of the effective interactions is therefore parameterized by one parameter c_3 . We will later discuss the behavior of the results under variations of this parameter. As mentioned above the gluon and graviton mass will be chosen as $m_{\text{glu}} = m_{\text{grav}} = 10^{-20} M_{\text{pl}}$ in order to display the individual contributions. But again only the inclusive NLO corrections are IR independent and therefore physical.

Figure 6.3 shows the angular dependence of the NLO corrections at $\sqrt{S} = 0.01 M_{\text{pl}}$. We have plotted only the range $\cos \theta > 0$, since the result is symmetric in this variable. We have left out $\cos \theta = 0$, where the denominator, i.e. the tree-level squared amplitude goes to 0 and numerical errors blow up. As in the pure scalar model there is only a very small dependence on the angle. We see that the boxes, triangles and effective vertices give the main contributions, and the self energies, Bremsstrahlung and especially the wavefunction corrections are only marginal contributions. Furthermore we see that the combined NLO contributions are below 5% over the whole angular range at this energy. This is roughly half of the NLO corrections in the pure scalar model at this particular center of mass energy, see fig. 5.6.

Figure 6.4 shows the center of mass energy dependence of the NLO corrections at $\theta = \pi/4$. The reason why we do not choose $\theta = \pi/2$ as in the scalar model is that the tree-level process has a zero at this scattering angle. We see that boxes, triangles and effective vertices are the relevant contributions and the others are irrelevant. This agrees with the pure scalar model. We furthermore see that the 10% NLO

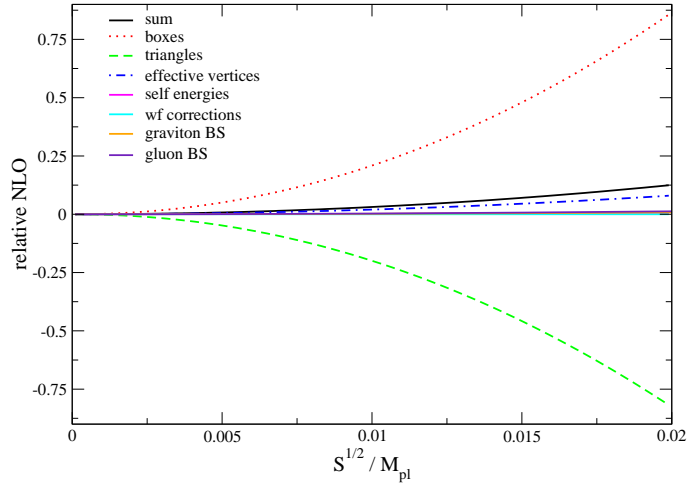


Figure 6.4: Center of mass energy dependence of the relative NLO corrections for S -type localization. The scattering angle was chosen as $\Theta = \frac{\pi}{4}$. We have chosen the particle mass $m = 10^{-16} M_{\text{pl}}$.

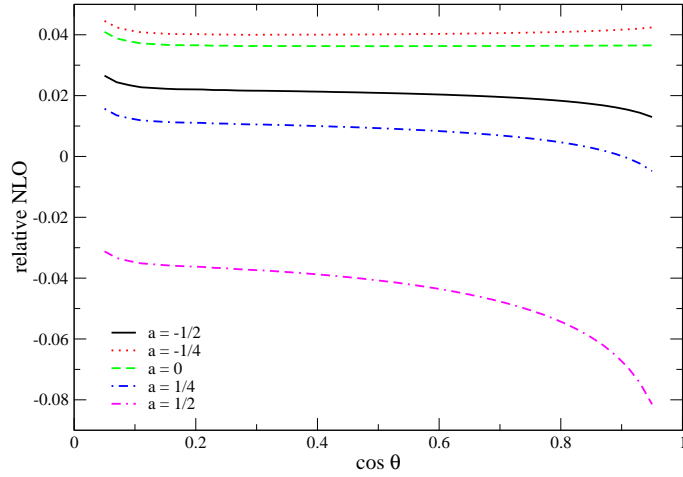


Figure 6.5: Angular dependence of the relative NLO corrections for S -type localization with different effective coupling a . We show only the $\cos \theta > 0$ part, since the result is symmetric. We leave out $\cos \theta = 0$, since at this angle the tree-level cross section (i.e. the denominator) is 0 and the numerical errors blow up. The center of mass energy was chosen as $\sqrt{S} = 0.01 M_{\text{pl}}$ and the particle mass $m = 10^{-16} M_{\text{pl}}$.

corrections are reached at nearly $\sqrt{S} = 0.02 M_{\text{pl}}$. This is roughly twice as high as in the pure scalar model, see fig. 5.7.

Performing variations of the clock and rod mass parameter m we see that there is no noticeable change in the relative NLO corrections. Even if the individual parts vary, their sum does not change. This property has been tested for masses in the range $m \in [10^{-20} M_{\text{pl}}, 10^{-4} M_{\text{pl}}]$. We see that the parts relevant at high energies are independent of the particle mass and only the irrelevant parts, which contribute with m^2/M_{pl}^2 show dependencies. This is a very nice property of the theory, since it leads to an universal high energy behavior, independent of the masses. Moreover the results are mass independent even if the effective coupling a is switched on. We conjecture that the mass independence is a consequence of the additional $\text{SU}(N)$ gauge invariance, since the mass dependencies cancel between different diagram types, in particular box and triangle contributions.

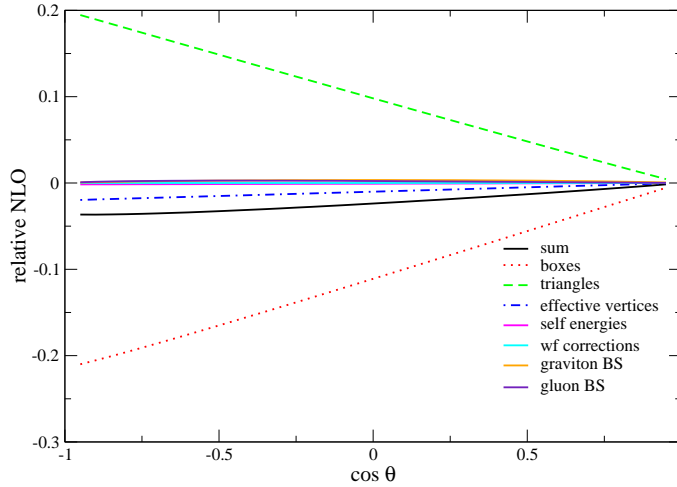


Figure 6.6: Angular dependence of the relative NLO corrections for T -type localization. The center of mass energy was chosen as $\sqrt{S} = 0.01 M_{\text{pl}}$. We have chosen the particle mass $m = 10^{-16} M_{\text{pl}}$.

Next we study the dependence on the effective graviton coupling parameter a . The results are shown in fig. 6.5 and show a strong dependence on a . This dependence is not as strong as in the case of the pure scalar model, but we see that we can even switch the sign of the relative NLO contributions by tuning the effective coupling to e.g. $a = 1/2$. Note that the absolute value of the NLO corrections stays of the same order of magnitude in presence of the effective coupling a . Thus the validity of the theory is not as much affected by the parameter a as in the pure scalar model.

Finally we have to mention that by varying the scalar-gluon effective vertices we can also switch the sign of the NLO corrections, but the results remain in the same order of magnitude for not too unnatural values of the effective coupling constants.

6.6.3 Relative NLO contributions for T -type localization

In this section we investigate T -type localization in the Yang-Mills model. As typical for a T -type model, the relative NLO corrections increase by increasing the scattering angle due to the decreasing tree-level cross section. This is shown in fig. 6.6 for a center of mass energy $\sqrt{S} = 0.01 M_{\text{pl}}$ and a particle mass $m = 10^{-16} M_{\text{pl}}$. The relevant contributions are again boxes, triangles and effective vertices and the remaining individual parts are only marginal, at least at the IR cutoff $m_{\text{grav}} = m_{\text{glu}} = 10^{-20} M_{\text{pl}}$. There are again cancellations between boxes and triangles.

The center of mass energy dependence of the NLO corrections is shown in figure 6.7 at a scattering angle of $\theta = \pi/2$ and particle mass $m = 10^{-16} M_{\text{pl}}$. It reaches 10% at $\sqrt{S} = 0.02 M_{\text{pl}}$, which is around twice as high as in the pure scalar model.

This natural bound is, as in the case of the S -type process, independent on the particle mass, and hence sets an universal bound for this model.

The dependence on the effective graviton coupling a is shown in fig. 6.8 and shows again a rather strong dependence, in particular at large angles. But the dependence is not as dramatic as in the case of the pure scalar model since in the Yang-Mills model the magnitude of the relative NLO corrections stays in the same range for natural values of a . This is an advantage of the Yang-Mills model since its validity does not get spoiled in the presence of a .

The dependence on the scalar-gluon effective couplings had been estimated analytically in section 6.5. We can change the sign of the effective vertex contributions by changing the sign of c_3 . This can lower the relative NLO corrections and prolong the validity of the theory. For example in the case of vanishing effective vertex contributions the 10% bound is reached at $\sqrt{S} = 0.04 M_{\text{pl}}$.

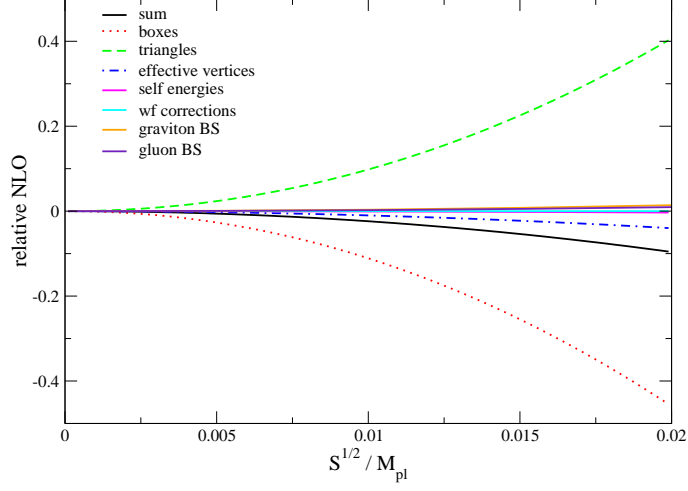


Figure 6.7: Center of mass energy dependence of the relative NLO corrections for T -type localization. The scattering angle was chosen as $\Theta = \frac{\pi}{2}$. We have chosen the particle mass $m = 10^{-16} M_{\text{pl}}$.

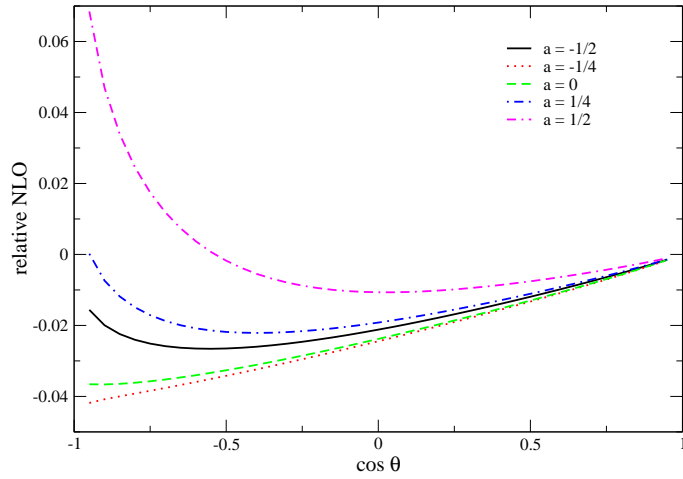


Figure 6.8: Angular dependence of the relative NLO corrections for T -type localization with different effective coupling a . The center of mass energy was chosen as $\sqrt{S} = 0.01 M_{\text{pl}}$. We have chosen the particle mass $m = 10^{-16} M_{\text{pl}}$.

6.6.4 Implications to localization and comparison to the pure scalar model

In the sections above we have obtained that the results of the Yang-Mills model have some advantages compared to the pure scalar model. Even if the maximal resolution is in general not considerably enhanced (approximately a factor of 2 for TeV particles) the results of this model are independent on the clock and rod field mass. Moreover the results are more stable under variations of the graviton effective coupling a . Altogether the Yang-Mills model leads to more universal results and is therefore a more sensible model for our purpose.

Chapter 7

Pseudo-local geometry observables with matter clocks and rods

In this section we will investigate a pure gravity observable, the pseudo-local curvature scalar induced by two crossing particles in small width wave packet states. The overlapping region of the particle wave packets will serve as clock and rod. The construction and calculation of this observable is performed in the in-in formalism. We will only study the effect of two high energetic particles on local curvature and we do not define an experimental realization of the experiment of measuring the local curvature, i.e. we only investigate the preparation of the experiment and not the execution itself. A full description of the quantum field theoretical measurement process is in this case a highly nontrivial task, since local curvature is not an operator which is easily measured by scattering. We would have to think about a different measurement if we would be interested in the phenomenology of this experiment. But in this section we only want to study the difference between the quantum field theoretical backreaction on local curvature and the classical one. We try to get insights into the nature of the backreaction induced by wave packet states. In particular we are interested in the question if the backreaction is dominated by classical or quantum geometry effects.

7.1 Definition of the pseudo-local curvature observable

Assume two free complex scalar quantum fields ψ_1 and ψ_2 on a generic background. If we fix the background to be flat Minkowski space and describe gravitons dynamically on it, we get the following action for the matter fields

$$S = \int d^4x \sum_{i=1}^2 \left(\partial_\mu \psi_i^\dagger \partial^\mu \psi_i - m^2 \psi_i^\dagger \psi_i - \frac{\kappa}{2} h^{\mu\nu} (2\partial_\mu \psi_i^\dagger \partial_\nu \psi_i - \eta_{\mu\nu} (\partial_\lambda \psi_i^\dagger \partial^\lambda \psi_i - m^2 \psi_i^\dagger \psi_i)) \right). \quad (7.1)$$

Assume the following state $|f_1, f_2\rangle$, where f_1 is a wave packet state of the particle ψ_1 and f_2 is a wave packet state of ψ_2 overlapping around the spacetime position 0. Moreover assume the following operator

$$O := \int d^4x \sqrt{-g} R(x) \psi_1^\dagger(x) \psi_1(x) \psi_2^\dagger(x) \psi_2(x) : , \quad (7.2)$$

which is the normal ordered spacetime integrated curvature scalar R together with a quartic scalar operator.

Now consider the following in-in matrix element in the Heisenberg picture

$$\langle f_1, f_2; \text{in} | O | f_1, f_2; \text{in} \rangle . \quad (7.3)$$

By switching off the coupling κ it is very easy to see that this matrix element is the expectation value of the curvature operator in the graviton state integrated over the overlapping region defined by the wave packets. This is of course 0 in the zero coupling limit since the gravitons will be always in their ground state. They can not be excited without scalar-graviton couplings.

If we now allow interactions between gravity and matter, the asymptotic graviton vacuum state will be filled with virtual gravitons due to emission of gravitons from the particles and the expectation value of the spacetime integrated curvature scalar will not vanish any longer. Therefore we can measure the local selfgravitation of two crossing wave packet state particles with this kind of observable. As mentioned above we will not attempt a dynamical description of the measurement of this value, since it is not required for our purposes.

We proceed by first giving a semiclassical computation of the pseudo-local curvature operator in the framework of quantum fields coupled to classical gravity by using the semiclassical linearized Einstein equations. Then after this calculation we compute this observable in the in-in formalism using quantum field theory for both, matter and gravity. We have chosen this particular order because the quantum calculation requires some low-energy data from the classical calculation in order to renormalize the occurring divergences.

7.2 Classical computation

As mentioned above we use semiclassical linearized Einstein equations in order to compute the classical backreaction induced by matter quantum fields. The equations of motion for the metric fluctuations read

$$\square\left(h_{\mu\nu} - \frac{\eta_{\mu\nu}}{2}h\right) = \langle T_{\mu\nu} \rangle, \quad (7.4)$$

where $\langle T_{\mu\nu} \rangle$ is the expectation value of the energy momentum tensor operator in the matter state defined above. It can be explicitly expressed through the wave packets by doing some algebra and is given by

$$\langle T_{\mu\nu} \rangle = -\kappa \sum_{i=1}^2 \left(\partial_{(\mu} f_i^* \partial_{\nu)} f_i - \frac{\eta_{\mu\nu}}{2} (\partial_\lambda f_i^* \partial^\lambda f_i - m^2 f_i^* f_i) \right). \quad (7.5)$$

The metric fluctuations now can be determined by using the retarded Green function of the equations of motion and are given by

$$h_{\mu\nu}(x) = P_{\mu\nu\alpha\beta} \int d^4y G_{\text{ret}}(x-y) \langle T^{\alpha\beta}(y) \rangle, \quad (7.6)$$

where $G_{\text{ret}}(x-y)$ is the scalar Green function of the box operator, and the tensor structure is given by

$$P_{\mu\nu\alpha\beta} := \frac{1}{2} (\eta_{\mu\alpha} \eta_{\nu\beta} + \eta_{\mu\beta} \eta_{\nu\alpha} - \eta_{\mu\nu} \eta_{\alpha\beta}). \quad (7.7)$$

With these ingredients we can express the induced curvature scalar through the energy momentum tensor. At lowest order it is given by

$$R(x) = \kappa (\square h - h_{\mu\nu}{}^{;\mu\nu}) = -\frac{\kappa}{2} \langle T(x) \rangle, \quad (7.8)$$

where we had to use the equations of motion for the Green function and the energy momentum conservation $\partial_\alpha \langle T^{\alpha\beta} \rangle = 0$.

By inserting (7.5) into the expression for the curvature we obtain

$$R = -\frac{\kappa^2}{2} \sum_{i=1}^2 \left(\partial_\alpha f_i^* \partial^\alpha f_i - 2m^2 f_i^* f_i \right). \quad (7.9)$$

For the further evaluation we assume $f_1(x)$ and $f_2(x)$ to be first order Gaussian wave packets with $\mathbf{q}_1 = (0, 0, q)$ and $\mathbf{q}_2 = (0, 0, -q)$, see appendix E.1. With this specific choice we can evaluate (7.9) and arrive at the following expression for the classical expectation value of the pseudo-local curvature observable

$$O_{\text{class}} = \frac{\kappa^2}{2} \int d^4x (\sigma^4 (x_1^2 + x_2^2) + m^2) (|f_1|^4 |f_2|^2 + |f_1|^2 |f_2|^4), \quad (7.10)$$

where x_i are the components of the spatial vector \mathbf{x} .

We see that only the densities $|f_i|^2$ enter this expression which is quite natural for a classical computation, since there are no interferences. This integral now can be evaluated by inserting the first order wave packets, see (E.6). The result in the limit $m \rightarrow 0$ and with the specific width $\sigma = q/2$ is given by

$$O_{\text{class}} = \frac{\kappa^2 q^4}{18432\sqrt{2}\pi^{\frac{5}{2}}}, \quad (7.11)$$

where we have used the first order normalization of the wave packets given by

$$N_{(q,\sigma)} = (4\sqrt{q}\pi^{\frac{9}{4}}\sigma^{\frac{3}{2}})^{-1}. \quad (7.12)$$

This normalization comes from the condition

$$(f_i, f_i)_{\text{cov}} = 1 \quad (7.13)$$

for the first order wave packets. It differs from the normalization of the non-approximated wave packets (E.3) by 5% for maximal width wave packets $\sigma = q/2$.

7.3 Quantum computation

For quantum backreaction we use the in-in formalism, see section 2.8. We will formulate the amplitudes by using position-space Feynman rules, since with this formalism we can better understand the vanishing of several terms.

The interaction vertex is given by the following bi-differential operator

$$\begin{array}{c}
 2 \\
 \nearrow \\
 1 \text{ --- wavy line --- } \bullet \\
 \searrow \\
 3
 \end{array}
 = \mp i \frac{\kappa}{2} (2\partial_{(\mu}^2 \partial_{\nu)}^3 - \eta_{\mu\nu} (\partial_\lambda^2 \partial^{3\lambda} - m^2)), \quad (7.14)$$

where the numbers on the partial derivatives indicate the leg they are acting on and $-$ is for the right and $+$ for the left vertex.

The graphical representation of the pseudo-local curvature scalar has the following analytical expression

$$\begin{array}{c}
 \nearrow \\
 \text{--- wavy line ---} \\
 \bullet \\
 \searrow
 \end{array}
 = \kappa (\eta_{\mu\nu} \square^h - \partial_\mu^h \partial_\nu^h), \quad (7.15)$$

where there is no distinction between left and right, since this operator is no interaction vertex. h indicates the action of the derivatives on the gravitons.

If we assume the vanishing of graviton tadpoles by either normal ordering the interaction or renormalizing the cosmological constant to zero, there are the following four leading order in-in diagrams contributing to our observable

$$\begin{array}{c}
 \nearrow \\
 \text{--- wavy line ---} \\
 \bullet \\
 \searrow
 \end{array}
 +
 \begin{array}{c}
 \nearrow \\
 \text{--- wavy line ---} \\
 \bullet \\
 \searrow
 \end{array}
 +
 \begin{array}{c}
 \nearrow \\
 \text{--- wavy line ---} \\
 \bullet \\
 \searrow
 \end{array}
 +
 \begin{array}{c}
 \nearrow \\
 \text{--- wavy line ---} \\
 \bullet \\
 \searrow
 \end{array}
 . \quad (7.16)$$

Note that the disconnected diagrams vanish because of the normal ordering of the operator O . It has to be mentioned that due to the in-in Feynman rules we have to sum up left and right vertices together with the corresponding anti-propagators and propagators.

Since all four diagrams are related by crossing we will compute the one where the graviton gets emitted from the f_1 particle in the ket-state explicitly in the following. Using the diagrammatic rules we arrive at

$$\mathcal{M} := \begin{array}{c} \text{---} \nearrow \bullet \searrow \text{---} \\ \text{---} \nwarrow \bullet \nearrow \text{---} \\ \text{---} \nearrow \bullet \searrow \text{---} \\ \text{---} \nwarrow \bullet \nearrow \text{---} \end{array} = -i \frac{\kappa^2}{2} \int_{-\infty}^{\infty} dx^0 \int_{-\infty}^{x^0} dy^0 \int d^3x d^3y f_1^*(x) f_2^*(x) f_2(x) \\ \left(f_1(y) \left(2 \overleftarrow{\partial}_{(\mu}^y \overrightarrow{\partial}_{\nu)}^y - \eta_{\mu\nu} \left(\overleftarrow{\partial}_{\lambda}^y \overrightarrow{\partial}^{y\lambda} - m^2 \right) \right) P^{\mu\nu\alpha\beta} \left(\Delta_{yx}^m \Delta_{yx}^0 - \bar{\Delta}_{yx}^m \bar{\Delta}_{yx}^0 \right) \left(\overleftarrow{\square}^x \eta_{\alpha\beta} - \overleftarrow{\partial}_{\alpha}^x \overleftarrow{\partial}_{\beta}^x \right) \right), \quad (7.17)$$

where Δ_{yx}^m is the Feynman propagator with mass m and $\bar{\Delta}_{yx}^m$ denotes the anti-Feynman propagator. Note that the y^0 integral is restricted by x^0 . Since we have the inequality $y^0 < x^0$, the time ordering is not required and we can use the equations of motion

$$\square^y \Delta_{yx}^0 = \square^x \Delta_{yx}^0 = \square^y \bar{\Delta}_{yx}^0 = \square^x \bar{\Delta}_{yx}^0 = 0, \quad \text{for } y^0 < x^0. \quad (7.18)$$

Therefore the box operators annihilate the (anti-) propagators.

If we substitute the spectral representations of the wave packets we can perform the required integrals for plane waves. We had to solve the energy integrals by using complex contour integration. Since our integrand falls off sufficiently fast in both, the positive and negative complex axis, we have chosen the contour which includes the lowest number of poles. At the end we arrive at the following expression

$$\mathcal{M} = \int \widetilde{d^3k_r} \widetilde{d^3p_r} \widetilde{d^3k_l} \widetilde{d^3p_l} \tilde{f}_1(\mathbf{k}_r) \tilde{f}_2(\mathbf{p}_r) \tilde{f}_1^*(\mathbf{k}_l) \tilde{f}_2^*(\mathbf{p}_l) \delta(k_r + p_r - k_l - p_l) \mathcal{I}(\mathbf{k}), \quad (7.19)$$

where the remaining integral is given by

$$\mathcal{I}(\mathbf{k}) := -\kappa^2 \pi \int d^3q \frac{E_q E_{q+k} + \mathbf{q}(\mathbf{q} + \mathbf{k})}{E_q E_{q+k} ((E_q + E_{q+k})^2 - E_k^2)} (E_k^2 E_q + \mathbf{k}\mathbf{q}(E_q + E_{q+k})). \quad (7.20)$$

Summing up the contributions from the four different graphs and transforming to position space we arrive at the following formula for the expectation value of the pseudo-local curvature observable

$$\langle O \rangle = \int \frac{d^4x}{(2\pi)^4} \left(f_1^{\text{mod}*} f_1 f_2^* f_2 + f_1^* f_1^{\text{mod}} f_2^* f_2 + f_1^* f_1 f_2^{\text{mod}*} f_2 + f_1^* f_1 f_2^* f_2^{\text{mod}} \right), \quad (7.21)$$

where f_i are the position space wave packets and f_i^{mod} the ‘‘modified’’ wave packets defined by

$$f_i^{\text{mod}}(x) := \int \widetilde{d^3k} \tilde{f}_i(\mathbf{k}) \mathcal{I}(\mathbf{k}) e^{-ikx}. \quad (7.22)$$

When we compare the structure of the result with the classical one, see (7.10), we see that as expected the quantum calculation affects the wave packets themselves, while the classical one only affects the densities $|f_i|^2$.

Next we have to calculate the integral (7.20), where we again restrict ourselves to the massless limit $m = 0$. The problem with this integral is that it is quadratically divergent, so that we have to renormalize its value. As a counterterm to the integrand we use the second order \mathbf{k} expanded integrand and subtract it. We will investigate below if there are some nonzero contributions from zeroth, first and second order in \mathbf{k} by matching the results to the classical one in the IR limit $\|\mathbf{k}\| \rightarrow 0$. In this limit we expect both results to agree.

Furthermore we use spherical coordinates and perform first the angular Ω_q integration and afterwards the radial one. The dependence of the spherically integrated integrand shows a sufficiently fast fall-off in the remaining variable $q = \|\mathbf{q}\|$ and it can be integrated analytically as well. After the angular Ω_q integration we see that the function $\mathcal{I}(\mathbf{k})$ is only dependent on the norm of \mathbf{k} .

The result is that $\mathcal{I}(\mathbf{k})$ is a polynomial in $k = \|\mathbf{k}\|$ given by

$$\mathcal{I}(k) = \alpha k^2 + \beta k^4, \quad (7.23)$$

where α has to be determined by the matching with the classical computation and

$$\beta = \frac{2\pi^2}{15}. \quad (7.24)$$

The modified wave packet is given by

$$f_i^{\text{mod}}(x) = (-\alpha\Delta + \beta\Delta^2)f_i(x) \quad (7.25)$$

and with it the expectation value is

$$\langle O \rangle = \kappa^2 \frac{187\beta q^4 + 96\alpha q^2}{16384\pi^5}, \quad (7.26)$$

where we have used the width $\sigma = q/2$.

Next we have to compare the classical and quantum result in order to determine α . Since we are interested in the relative difference between classical and quantum pseudo-local curvature, we have to relate their difference to some natural pseudo-local curvature. The problem is that the relation to the induced curvature itself is not sensible, since it is of the same order as the difference and vanishes in the IR. A more sensible natural quantity to which we can relate the difference is the pseudo-local Planck curvature defined by

$$O_{\text{pl}} := \kappa^{-2} \langle \int d^4x \psi_1^\dagger \psi_1 \psi_2^\dagger \psi_2 \rangle = \frac{\kappa^{-2}}{64\pi}, \quad (7.27)$$

where we have used $R = \kappa^{-2}$ as a natural curvature scale.

We now see that the relative difference between the quantum and classical result compared to the pseudo-local Planck curvature is given by

$$\frac{\langle O \rangle - O_{\text{class}}}{O_{\text{pl}}} = \kappa^4 q^4 \frac{561 - 10\sqrt{2}\pi}{5760\pi^2} \approx 0.0094\kappa^4 q^4, \quad (7.28)$$

where we have fixed $\alpha = 0$ by demanding the vanishing of the quadratic terms in the limit of $q \rightarrow 0$ and thus matching the quantum quadratic term to the classical one.

We see that in the limit $q \rightarrow 0$ the classical and quantum field theoretical result agrees and the quantum result receives relative corrections proportional to $(\kappa q)^4$. Furthermore the quantum pseudo-local curvature is larger than the classical one at every energy scale.

7.4 Comparison between the quantum and classical results and outlook

As we see from (7.28), the classical and quantum result for the pseudo-local curvature scalar are very similar compared to the Planck scale curvature for energies $q < M_{\text{pl}}$. Hence the original question of which effects contribute stronger to the breakdown of the perturbative treatment of quantum gravity can not be answered through this calculation. The problem is that the quantum fluctuations in the curvature scalar seem to be quite symmetric around the classical value, so that we can not estimate them from the expectation value of the local curvature alone.

In the remaining part of this section we define another observable which has good chances to give a deeper insight into the question of how quantum the backreaction effects are. Its evaluation requires further investigations and is not presented in this work. The remaining part is intended as an outlook on future work.

Assume the following second pseudo-local operator

$$O_2 := \int d^4x \sqrt{-g} R^2 \psi_1^\dagger \psi_1 \psi_2^\dagger \psi_2, \quad (7.29)$$

where now the quadratic scalar curvature enters. If we calculate the quantum expectation value of this operator in the the two-particle state defined above, we arrive at the pseudo-local squared curvature, which can be used to extract information from the relative fluctuation

$$\frac{\sqrt{\langle O_2 \rangle - \langle O \rangle^2}}{\langle O \rangle}. \quad (7.30)$$

This fluctuation is very sensitive to quantum effects, since in a classical calculation it is obvious zero and it becomes only nonzero in presence of quantum effects. If this ratio is larger than 1, it would indicate that the quantum effects are dominant. If it is smaller than one, the classical curvature effects would be more relevant. This means that if this ratio would be large, the perturbative description of quantum gravity breaks down because of quantum geometry effects and this breakdown can not be cured by e.g. adjusting a better suited classical background. In the case of a small ratio this would be different, since we could enhance the validity of the perturbative theory by adjusting the classical background if the energies are too high.

The evaluation of the expectation value of O_2 in the in-in formalism is rather demanding because of the appearance of two loop calculations with incomplete time integrations at the vertices. Because of this the standard Feynman integrals known from S -matrix calculations can not be used anymore and every integral has to be evaluated by hand. This requires further investigations, in particular whether one could automatize these calculations.

Chapter 8

Conclusions

We have studied several pseudo-local observables in effective quantum gravity. Based on the proposal of Giddings *et al.* [1] we have constructed Dirac observables in quantum gravity from local field theory observables by integration over the whole spacetime manifold. Afterwards we have used suitable wave packet states of the clock and rod variables in order to localize these nonlocal observables in the sense of relational locality.

The explicit calculations were performed using methods of perturbative quantum gravity. Therefore we have assumed geometry to be in a suitable semiclassical state, such that we can extract a smooth background geometry. This geometry was chosen to be a flat Minkowski spacetime for two reasons. First we assume that the basic features of dynamical localization are also present on a Minkowski spacetime and second this choice of background simplifies the application of perturbation theory in a dramatic manner. We have interpreted the breakdown of perturbation series as the limit on locality in this approach. This perturbative limit on locality is also related to our conceptional limit on locality, since most small scale experiments performed today involve scattering of particles. But the scattering of particles is nowadays only understood when performed on a fixed classical background.

The first explicit model we have investigated consists of one scalar field ϕ , which is localized with respect to four scalar clock and rod fields. The observable we were interested in was the two point correlation of the ϕ fields localized at a pair of points defined in a relational way by using the clock and rod fields. We used the proposal of [1] to define a diffeomorphism invariant observable from which we could extract this information by taking matrix elements between suitable states. These states were chosen to be in and out two-particle wave packet states of the clock and rod fields with carefully chosen overlap properties. We have used the overlap region of respectively two wave packets in order to localize the two spacetime points required for the correlator. We constructed the model in such a way that the information about the correlator is encoded in the two-particle wave packet scattering matrix element. This scattering process was calculated at tree and one loop level (together with soft real emissions). With the tree level result we proved that the desired information about the correlation is encoded in the scattering of two clock and rod fields. The NLO corrections were used in order to estimate the maximal spacetime resolution possible in this model. It was shown that the minimal length accessible by this model is about several hundred inverse Planck masses, dependent on the masses of the fields.

In order to check the universality of the results gained through the first model we defined a second model with similar properties. This model contains a $SU(N)$ Yang-Mills field localized with respect to colored scalar clock and rod fields. We could define a similar pseudo-local observable as in the model above and therewith extract information about the local Yang-Mills correlation function. In this model we have again calculated the NLO corrections and estimated the maximal resolution. The results agree with the ones from the pure scalar model, but there are some advantages of the Yang-Mills model. First, there is no dependence of the clock and rod field mass in this model, which leads to more universal results, and second the dependence of this model on the effective graviton-scalar couplings is weaker than in the first model.

In the last part we addressed the question if the backreaction of the quantum scalar wave packet states on geometry is more of a classical or a quantum effect. In order to answer this question we defined a pseudo-

local curvature observable which we localize using wave packets. We investigated the expectation value of the pseudo-local curvature observable in lowest order. We compared the result with the full classical evaluation of this observable and we found out that there is not much difference. Hence the curvature observable alone could not answer our question. We proposed a second operator which could be used to determine the fluctuations of the pseudo-local curvature. Its expectation value will require a two-loop calculation in the in-in (Schwinger-Keldysh) formalism and is left to future work.

Appendix A

General gauge fixed BRST invariant equations of motion

In this appendix we give the full expressions for the EOM of gravitons, ghosts and antighosts in a general linear gauge fixing. This gauge fixing is given by (4.29) and is parameterized by 10 parameters c_i .

The first and second time derivatives of the ghost fields are given by

$$\dot{\eta}^{(0)} = -\frac{1}{2}(c_1 + c_2 - c_3)\partial_i\eta^{(i)} + 2c_3\Delta\eta_s^{(0)} \quad (\text{A.1})$$

$$\dot{\eta}^{(i)} = -(c_4 - \frac{c_7}{2})\partial_i\eta^{(0)} + (c_5 + \frac{c_6}{2})\partial_i\partial_j\eta_s^{(j)} + \frac{c_6 - c_7}{2}\Delta\eta_s^{(i)} \quad (\text{A.2})$$

$$\dot{\eta}_s^{(0)} = -(1 + c_8)\eta^{(0)} + c_9\partial_i\eta_s^{(i)} \quad (\text{A.3})$$

$$\dot{\eta}_s^{(i)} = -(1 + \frac{c_{10}}{2})\eta^{(i)} - \partial_i\eta_s^{(0)} \quad (\text{A.4})$$

and

$$\begin{aligned} \ddot{\eta}_s^{(0)} &= -(2c_3(1 + c_8) + c_9)\Delta\eta_s^{(0)} + \left(\frac{1}{2}(c_1 + c_2 - c_3)(1 + c_8) - c_9(1 + \frac{c_{10}}{2})\right)\partial_i\eta^{(i)} \\ \ddot{\eta}_s^{(i)} &= -\frac{c_6 - c_7}{2}(1 + \frac{c_{10}}{2})\Delta\eta_s^{(i)} + \left(1 + c_8 + (1 + \frac{c_{10}}{2})(c_4 - \frac{c_7}{2})\right)\partial_i\eta^{(0)} \\ &\quad - \left(c_9 + (c_5 + \frac{c_6}{2})(1 + \frac{c_{10}}{2})\right)\partial_i\partial_j\eta_s^{(j)}. \end{aligned} \quad (\text{A.5})$$

Here we have omitted the second derivatives of the primary ghost fields, since we do not need them in this work.

Since the canonical momenta of the ghost fields $\bar{\eta}^a$ have their independent EOM we have to investigate them too. They are given by

$$\dot{\bar{\eta}}^{(0)} = (1 + c_8)\bar{\eta}_s^{(0)} - (c_4 - \frac{c_7}{2})\partial_i\bar{\eta}^{(i)} \quad (\text{A.6})$$

$$\dot{\bar{\eta}}^{(i)} = (1 + \frac{c_{10}}{2})\bar{\eta}_s^{(i)} - \frac{1}{2}(c_1 + c_2 - c_3)\partial_i\bar{\eta}^{(0)} \quad (\text{A.7})$$

$$\dot{\bar{\eta}}_s^{(0)} = -\partial_i\bar{\eta}_s^{(i)} - 2c_3\Delta\bar{\eta}^{(0)} \quad (\text{A.8})$$

$$\dot{\bar{\eta}}_s^{(i)} = -(c_5 + \frac{c_6}{2})\partial_i\partial_j\bar{\eta}^{(j)} - \frac{c_6 - c_7}{2}\Delta\bar{\eta}^{(i)} + c_9\partial_i\bar{\eta}_s^{(0)} \quad (\text{A.9})$$

and

$$\ddot{\bar{\eta}}^{(0)} = \left(-(1+c_8)2c_3 + \frac{1}{2}(c_4 - \frac{c_7}{2})(c_1 + c_2 - c_3) \right) \Delta \bar{\eta}^{(0)} - \left(1 + c_8 + (c_4 - \frac{c_7}{2})(1 + \frac{c_{10}}{2}) \right) \partial_i \bar{\eta}_s^{(i)} \quad (\text{A.10})$$

$$\begin{aligned} \ddot{\bar{\eta}}^{(i)} = & -(1 + \frac{c_{10}}{2}) \frac{c_6 - c_7}{2} \Delta \bar{\eta}^{(i)} + \left(\frac{1}{2}(c_1 + c_2 - c_3)(c_4 - \frac{c_7}{2}) - (1 + \frac{c_{10}}{2})(c_5 + \frac{c_6}{2}) \right) \partial_i \partial_j \bar{\eta}^{(j)} \\ & + \left((1 + \frac{c_{10}}{2})c_9 - \frac{1}{2}(c_1 + c_2 - c_3)(1 + c_8) \right) \partial_i \bar{\eta}_s^{(0)}. \end{aligned} \quad (\text{A.11})$$

The equations of motion for the graviton field and its conjugate momenta using the full Hamiltonian $H_{\text{BRST}} = H_{\text{min}} + \{\Omega_{\text{BRST}}, \Psi\}$ are given by

$$\dot{h}_{00} = -2c_2\pi^{00} - (c_1 - c_2)h_{0j,j} - c_3\pi^{jj} \quad (\text{A.12})$$

$$\dot{h}_{0i} = -c_7\pi^{0i} - \frac{1}{2}(c_4 + \frac{c_7}{2})h_{00,i} - \frac{1}{2}(c_5 - \frac{c_7}{2})h_{jj,i} - \frac{c_6 + c_7}{2}h_{ij,j} \quad (\text{A.13})$$

$$\dot{h}_{ij} = \pi^{ij} + c_{10}h_{0(i,j)} - \left(c_3\pi^{00} + \frac{1}{2}\pi^{kk} - (c_3 + \frac{1}{2})h_{0k,k} \right) \delta_{ij} \quad (\text{A.14})$$

$$\dot{\pi}^{00} = -c_4\Delta h_{00} + (1 + \frac{c_4 - c_5}{2} + c_8)\Delta h_{jj} - (1 + \frac{c_6}{2} + c_4 + c_8)h_{ij,i,j} - (c_4 + \frac{c_7}{2})\pi^{0i}_{,i} \quad (\text{A.15})$$

$$\dot{\pi}^{0i} = (\frac{1}{4} + c_1)h_{0j,j,i} - \frac{c_1 - c_2}{2}\pi^{00}_{,i} + \frac{1}{2}(\frac{1}{2} + c_3)\pi^{jj}_{,i} + \frac{c_{10}}{2}\pi^{ij}_{,j} - (1 + c_{10})\Delta h_{0i} \quad (\text{A.16})$$

$$\begin{aligned} \dot{\pi}^{ij} = & \Delta h_{ij} - (1 - c_5 - 2c_9)\Delta h_{kk}\delta_{ij} + (1 + c_8 + \frac{c_4 - c_5}{2})\Delta h_{00}\delta_{ij} \\ & - (1 + c_4 + c_8 + \frac{c_6}{2})h_{00,i,j} + (1 - c_9 - c_5 + \frac{c_6}{2})h_{kk,i,j} + (1 - c_9 - c_5 + \frac{c_6}{2})h_{kl,k,l}\delta_{ij} \\ & - 2(1 + c_6)h_{(ik,k,j)} - (c_5 - \frac{c_7}{2})\pi^{0k}_{,k}\delta_{ij} - (c_6 + c_7)\pi^{0(i}_{,j)} \end{aligned} \quad (\text{A.17})$$

and

$$\begin{aligned} \ddot{h}_{00} = & \Delta h_{00} \frac{1}{4} (2(c_1 + 3c_2)c_4 + (c_1 - c_2)c_7 - 2c_3(c_4 - 3c_5 - c_6 + 4c_8 + 4)) \\ & + \Delta h_{jj} \frac{1}{4} (c_1(2c_5 - c_7) + c_2(-4c_4 + 2c_5 + c_7 - 8c_8 - 8) - 2c_3(4c_5 + c_6 + 10c_9 - 2)) \\ & + h_{ij,i,j} \frac{1}{2} (c_1(c_6 + c_7) + c_2(4c_4 + c_6 - c_7 + 4c_8 + 4) + c_3(6c_5 + c_6 + 6c_9 - 2)) \\ & + \pi^{0j}_{,j} \left(2c_2c_4 + c_3(3c_5 + c_6 - \frac{c_7}{2}) + c_1c_7 \right) \end{aligned} \quad (\text{A.18})$$

$$\begin{aligned} \ddot{h}_{0i} = & \Delta h_{0i} (c_7 - \frac{1}{4}c_{10}(c_6 - 3c_7)) + \pi^{ij}_{,j} \frac{1}{2} (-c_6 - c_7(1 + c_{10})) + \pi^{jj}_{,i} \frac{1}{8} (2c_5 + 2c_6 - c_7 + 2c_3(2c_4 - c_7)) \\ & + h_{0j,j,i} \frac{1}{8} (4c_4(c_1 - c_2) - 2c_5(2c_{10} + 6c_3 + 3) - 2c_6(c_{10} + 2c_3 + 1) - c_7(6c_1 + 2c_2 - 2c_3 + 1)) \\ & + \pi^{00}_{,i} \frac{1}{4} (4c_2c_4 + c_3(6c_5 + 2c_6 - c_7) + 2c_1c_7) \end{aligned} \quad (\text{A.19})$$

$$\begin{aligned} \ddot{h}_{ij} = & \Delta h_{ij} - \Delta h_{kk}\delta_{ij} \frac{1}{8} (2c_5 + 2c_6 - c_7 - 2c_3(-2c_4 + c_7 - 4(c_8 + 1)) + 4c_9 + 4) \\ & + \Delta h_{00}\delta_{ij} \frac{1}{8} (2c_3(2c_4 - c_7) + 2c_5 + 2c_6 - c_7) - h_{00,i,j} \frac{1}{4} (2c_4(c_{10} + 2) + 2c_6 + c_7c_{10} + 4c_8 + 4) \\ & + h_{kk,i,j} \frac{1}{4} (2c_6 - 2c_5(2 + c_{10}) + c_7c_{10} - 4c_9 + 4) \\ & + h_{kl,k,l}\delta_{ij} \frac{1}{4} (2c_5 + 2c_6 - c_7 + 2c_3(2c_4 - c_7 + 2c_8 + 2) + 2c_9 + 2) - \pi^{0(i}_{,j)} (c_6 + c_7 + c_7c_{10}) \\ & - h_{(ik,k,j)} \frac{1}{2} (c_6(c_{10} + 4) + c_7c_{10} + 4) + \pi^{0k}_{,k}\delta_{ij} \frac{1}{4} (2c_3(2c_4 - c_7) + 2c_5 + 2c_6 - c_7). \end{aligned} \quad (\text{A.20})$$

Appendix B

BRST invariant states for effective quantum gravity coupled to classical matter

In this appendix we investigate the structure of the BRST operator when we include matter. Therefore we assume the following interaction term

$$S_{\text{int}} = -\kappa \int d^4x h_{\mu\nu} T^{\mu\nu}, \quad (\text{B.1})$$

where $T^{\mu\nu}$ is the energy momentum tensor of some matter and does not depend on h .

For this kind of single graviton emission the primary constraints remain the same as in the free case, since the graviton couples without derivatives to $T^{\mu\nu}$. But the secondary constraints change into

$$\tilde{\chi}_s^{(0)} = \chi_s^{(0)} - \kappa T^{00} \quad (\text{B.2})$$

$$\tilde{\chi}_s^{(i)} = \chi_s^{(i)} - \kappa T^{0i}, \quad (\text{B.3})$$

where the untilded constraints are the constraints from the free theory.

If there is energy momentum current conservation, i.e. $\partial_\mu T^{\mu\nu} = 0$, the time derivatives of the secondary constraints are given by

$$\dot{\tilde{\chi}}_s^{(0)} = -\partial_i \tilde{\chi}_s^{(i)} - \kappa \partial_\mu T^{\mu 0} + \mathcal{O}(\kappa^2) = -\partial_i \tilde{\chi}_s^{(i)} + \mathcal{O}(\kappa^2) \quad (\text{B.4})$$

$$\dot{\tilde{\chi}}_s^{(i)} = -\kappa \partial_\mu T^{\mu i} + \mathcal{O}(\kappa^2) = 0 + \mathcal{O}(\kappa^2). \quad (\text{B.5})$$

This means in particular that the constraint structure, i.e. the number of constraints and their algebra, is not changed by the introduction of this kind of interaction if we restrict ourselves to order κ^1 . Hence the BRST invariant extension of the Hamiltonian is equal to the free case, since it depends only on the algebra and the BRST charge is forminvariant, i.e.

$$\tilde{\Omega}_{\text{BRST}} = \tilde{\chi}^a[\eta^a] = \Omega_{\text{BRST}} - \kappa T^{0\mu}[\eta_{s\mu}] + \mathcal{O}(\kappa^2). \quad (\text{B.6})$$

Changing to interaction picture we can evaluate the free part of the BRST charge, i.e. Ω_{BRST} , as in the free case and arrive at

$$\tilde{\Omega}_{\text{BRST}} = i(\chi_\mu, \eta_s^\mu)_{\text{cov}} - \kappa T^{0\mu}[\eta_{s\mu}]. \quad (\text{B.7})$$

Because of the additional term in the BRST operator, we see that the only physical state of definite particle number is the Fock vacuum. This is clear, because in the presence of interactions it is not the free particle alone which is physical, but the particle together with its ‘‘quantum cloud’’ of gravitons and other particles.

Since the investigation of gravitons coupled to quantum matter is rather hard, we will study only the coupling of gravitons to classical matter. In this case we can construct closed expressions for physical states for given classical matter distributions. Even if the given assumptions of classical matter in the presence of quantized gravity has no direct application in our specific world, since there the quantum aspects of matter occur on larger scales than these of gravity, it is in principle interesting how the “graviton cloud” of a point particle would look like.

Before we give the closed expression of the graviton cloud, we first have to decompose our BRST operator into terms with specific domains and co-domains again. Since $T^{\mu\nu}$ is classical and therefore a \mathbb{C} -number, the following decomposition holds true

$$\tilde{\Omega}_{\text{BRST}} = \Omega_1 + \Omega_2 - \kappa T^{0\mu}[\eta_{s\mu}^+] - \kappa T^{0\mu}[\eta_{s\mu}^-], \quad (\text{B.8})$$

where $+/-$ denotes positive and negative frequency parts and Ω_i is defined as in (4.66). The individual domains and co-domains are

$$\Omega_1 : \mathcal{H}_{\text{graviton}}^n \otimes \mathcal{H}_{\text{ghost}}^m \otimes \mathcal{H}_{\text{antighost}}^l \rightarrow \mathcal{H}_{\text{graviton}}^{n+1} \otimes \mathcal{H}_{\text{ghost}}^m \otimes \mathcal{H}_{\text{antighost}}^{l-1} \quad (\text{B.9})$$

$$\Omega_2 : \mathcal{H}_{\text{graviton}}^n \otimes \mathcal{H}_{\text{ghost}}^m \otimes \mathcal{H}_{\text{antighost}}^l \rightarrow \mathcal{H}_{\text{graviton}}^{n-1} \otimes \mathcal{H}_{\text{ghost}}^{m+1} \otimes \mathcal{H}_{\text{antighost}}^l \quad (\text{B.10})$$

$$T^{0\mu}[\eta_{s\mu}^+] : \mathcal{H}_{\text{graviton}}^n \otimes \mathcal{H}_{\text{ghost}}^m \otimes \mathcal{H}_{\text{antighost}}^l \rightarrow \mathcal{H}_{\text{graviton}}^n \otimes \mathcal{H}_{\text{ghost}}^m \otimes \mathcal{H}_{\text{antighost}}^{l-1} \quad (\text{B.11})$$

$$T^{0\mu}[\eta_{s\mu}^-] : \mathcal{H}_{\text{graviton}}^n \otimes \mathcal{H}_{\text{ghost}}^m \otimes \mathcal{H}_{\text{antighost}}^l \rightarrow \mathcal{H}_{\text{graviton}}^n \otimes \mathcal{H}_{\text{ghost}}^{m+1} \otimes \mathcal{H}_{\text{antighost}}^l. \quad (\text{B.12})$$

We now make the following ansatz for the graviton cloud state

$$|\psi\rangle := G^\dagger|0\rangle := \sum_{n=0}^{\infty} w_n (A^\dagger)^n |0\rangle, \quad (\text{B.13})$$

where w_n are some weights and $A^\dagger := a_{\mu\nu}^\dagger(f^{\mu\nu})$ is the creation operator for some wave packet f , which we have to determine now.

Acting with $\tilde{\Omega}_{\text{BRST}}$ on the state $|\psi\rangle$ and demanding it to be invariant we get the following equation

$$0 = \tilde{\Omega}_{\text{BRST}}|\psi\rangle = (\Omega_2 - \kappa T^{0\mu}[\eta_{s\mu}^-])|\psi\rangle = ([\Omega_2, G^\dagger] - \kappa G^\dagger T^{0\mu}[\eta_{s\mu}^-])|0\rangle, \quad (\text{B.14})$$

which has the solutions

$$[\Omega_2, A^\dagger] = \kappa T^{0\mu}[\eta_{s\mu}^-] \quad \wedge \quad (n+1)w_{n+1} = w_n \quad (\text{B.15})$$

or

$$[\Omega_2, A^\dagger] = -\kappa T^{0\mu}[\eta_{s\mu}^-] \quad \wedge \quad (n+1)w_{n+1} = -w_n \quad (\text{B.16})$$

which are equivalent.

Choosing $w_0 = 1$ we arrive at a coherent state

$$|\psi\rangle = \sum_{n=0}^{\infty} \frac{1}{n!} (A^\dagger)^n |0\rangle = e^{A^\dagger} |0\rangle \quad (\text{B.17})$$

with the following condition for the spectrum of the wave packet

$$k_\nu \tilde{f}^{\mu\nu}(\mathbf{k}) = \int d^3x \kappa T^{0\mu} e^{ikx} \quad \forall \mathbf{k} \in \mathbb{R}^3. \quad (\text{B.18})$$

As an example we assume a point particle with mass m located at $\mathbf{x} = 0$. Then the energy momentum tensor is given by $T^{\mu\nu} = \delta_0^\mu \delta_0^\nu m \delta(\mathbf{x})$ and the condition for the wave packet (B.18) is for example fulfilled by using

$$\tilde{f}^{00}(\mathbf{k}) = \frac{\kappa m}{k^0} e^{ik^0 t}, \quad \tilde{f}^{\mu\nu}(\mathbf{k}) = 0 \text{ for } (\mu, \nu) \neq (0, 0). \quad (\text{B.19})$$

This spectrum leads to the following position space wave packet

$$f^{00}(x) = \int \widetilde{d^3p} \tilde{f}^{00}(\mathbf{p}) e^{-ipx} = \frac{\kappa m \pi^2}{r}, \quad (\text{B.20})$$

where $r = |\mathbf{x}|$ is the spatial distance. This result is in agreement with the classical result that nonrelativistic matter changes the 00 component of the metric by adding a Newtonian potential. The quantum state corresponding to the Newtonian potential is therefore given by a coherent state of h_{00} particle states with wave packets decreasing as $1/r$. This solution can be boosted in order to get the graviton cloud for a moving point mass.

It has to be mentioned that this state is only one representative of a whole equivalence class of states we get by adding exact states to it. Since our state is not of norm zero, it is not equivalent to the trivial state.

We now stop at this point without investigating, for example, the space of exact states or other physical states including physical gravitons. This is because our main goal was to show the similarity between the graviton cloud and Newton's potential. To understand this similarity we did not require a full understanding of the exact states as well as possible other physical states including physical gravitons. We also do not expect to gain much more insight by doing these additional investigations.

Appendix C

Renormalization of graviton induced tadpoles

Nonvanishing one point functions of massless particles generate serious divergences and render a theory inconsistent, if they can not be absorbed into the renormalization of some parameter. Therefore it must be checked that all one point functions behave like this.

In “standard theories” the only massless particles are vector bosons, such that the vanishing of one point functions is guaranteed by Lorentz covariance, since it holds that

$$\text{tadpole with wavy line} \sim \int d^4x e^{ipx} \langle 0 | j^\mu(x) | 0 \rangle = 0 . \quad (\text{C.1})$$

In the case of gravitons it looks quite different, since we have

$$\text{tadpole with wavy line} \sim \int d^4x e^{ipx} \langle 0 | T^{\mu\nu}(x) | 0 \rangle \neq 0 , \quad (\text{C.2})$$

because a general energy momentum tensor $T^{\mu\nu}$ has a trace nonequal zero and therefore scalar components.

Since such tadpoles come with a graviton propagator denominator $1/p^2$ in the on-shell limit $p^2 \rightarrow 0$, divergences will occur in some Feynman diagrams at NLO. But these divergences can be absorbed by renormalizing the cosmological constant as it has been shown in [25]. We will now briefly show how this works.

Since the most general action in general relativity also contains a cosmological constant term, we have in principle to include it. This additional action is of the form

$$S_\Lambda = \int d^4x \sqrt{-g} \Lambda = \int d^4x \frac{\kappa}{2} \Lambda h + \mathcal{O}(\kappa^2) , \quad (\text{C.3})$$

where we used the κ expansion on flat background and neglected the constant term in the action, since it does not contribute.

In terms of Feynman diagrams this additional action can be interpreted with the following “vertex”

$$\text{wavy line} \square = i \frac{\kappa}{2} \Lambda \eta_{\mu\nu} \quad (\text{C.4})$$

describing the “interaction” between graviton and the vacuum expectation value of the graviton trace h . This does not spoil Lorentz invariance, since the trace of h is a scalar.

Working now explicitly in the $\psi^2\phi$ model with the Feynman rules from fig. 5.2 the amplitudes for the one loop renormalization of the cosmological constant are given by

$$\begin{aligned} \mathcal{M}_{\mu\nu} &:= \text{wavy line} \square + \sum_{i=1}^4 \text{wavy line} \text{circle} + \text{wavy line} \text{dashed circle} \\ &= i \frac{\kappa}{2} \Lambda \eta_{\mu\nu} + 4 \frac{\kappa}{2} \int \frac{d^4 k}{(2\pi)^4} \frac{2k_\mu k_\nu - \eta_{\mu\nu}(k^2 - m_\psi^2)}{k^2 - m_\psi^2} + \frac{\kappa}{2} \int \frac{d^4 k}{(2\pi)^4} \frac{2k_\mu k_\nu - \eta_{\mu\nu}(k^2 - m_\phi^2)}{k^2 - m_\phi^2}. \end{aligned} \quad (\text{C.5})$$

Since the problematic part of this amplitude is its trace, we apply $\eta^{\mu\nu}$ and therefore get

$$\mathcal{M} = 2i\kappa\Lambda - \kappa \int \frac{d^4 k}{(2\pi)^4} \left(4 \frac{k^2 - 2m_\psi^2}{k^2 - m_\psi^2} + \frac{k^2 - 2m_\phi^2}{k^2 - m_\phi^2} \right). \quad (\text{C.6})$$

Next we have to evaluate \mathcal{M} in some regularization scheme. Since this is a trivial task, we assume that this had been done and simply demand the following renormalization condition

$$\Lambda_r := \mathcal{M} = 0, \quad (\text{C.7})$$

which relates the bare cosmological constant Λ to the renormalized one Λ_r . Therefore the additional bare cosmological constant action can be used as a counterterm for renormalizing the cosmological constant to 0 in order to avoid problems coming from graviton tadpoles.

With the cosmological constant counterterm it now holds true

$$\text{wavy line} \text{circle} \Big|_r = 0. \quad (\text{C.8})$$

Since the renormalized one point function does not depend on the external momenta (there is no incoming momentum) all Feynman diagrams containing graviton induced tadpoles as subdiagrams will vanish. Thus we will neglect them in our calculations.

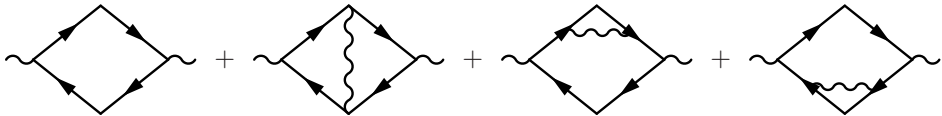
Appendix D

Colored processes, gluon Bremsstrahlung and IR finiteness in Yang-Mills theory

In this work we require rather untypical QCD cross sections, which are not averaged (summed) over color in the initial (final) state. Since the cancellation of IR divergences in QCD is usually discussed with summed and averaged color, we have to discuss the topic of fixed external color here in this work. We will make use of the Kinoshita-Lee-Nauenberg (KLN) theorem [20, 21], optical theorem and unitarity cuts in order to discuss the IR behavior of colored processes.

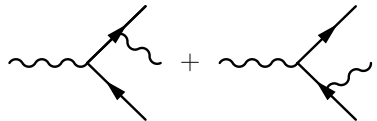
The KLN theorem guarantees by using unitarity that physical processes, i.e. processes summed (averaged) over all degenerate final (initial) states, are free of IR divergences. Since unitarity is related to the optical theorem and unitarity cuts, there is a diagrammatic formalism to check the IR finiteness. We will briefly explain this formalism by using the most simple IR divergent process of an off-shell photon decaying into electron and positron in QED.

The incomplete square of the sum of the tree-level and one loop diagrams is given by all cuts, which do not cut through the internal photon line, of the following diagrams



$$\text{Diagram 1} + \text{Diagram 2} + \text{Diagram 3} + \text{Diagram 4} \quad (\text{D.1})$$

But since the optical theorem requires all possible cuts, we have even to cut through the photon line and arrive at the diagrams of the final state Bremsstrahlung, i.e.



$$\text{Diagram 5} + \text{Diagram 6} \quad (\text{D.2})$$

Therefore we have also to include processes with degenerate final states, i.e. photon to electron, positron and soft photon in this case, in order to arrive at IR finiteness of the inclusive cross section.

In the case of massless matter or gauge bosons with self interaction there occur also collinear divergences. These divergences require an additional inclusive treatment of the initial state. This can be achieved by crossing all initial states to the final state. For a $n \rightarrow m$ process this would lead to $0 \rightarrow n + m$ amplitudes. Gluing these amplitudes together, i.e. performing an operation which is inverse to the cuts, we arrive at $0 \rightarrow 0$ amplitudes as a starting point for our investigations.

The problem with colored amplitudes in Yang-Mills theory is that if we construct the $0 \rightarrow 0$ amplitude from the color fixed tree and loop amplitudes, it does not agree with the full $0 \rightarrow 0$ amplitude, since

the matter legs are held at fixed color in the first case and the internal color is summed in the second case. This leads to the question if the KLN theorem applies to the case of color restricted processes and if they can be rendered IR finite by a physically sensible inclusive treatment of color. Now there are two possibilities. First it could happen that the KLN theorem does not apply to restricted $0 \rightarrow 0$ amplitudes, so that the treatment of colored cross section is not sensible at all. Second, it could be that applying all possible cuts to the restricted $0 \rightarrow 0$ amplitude will lead to an IR finite cross section. In this case it has to be checked if the cuts give rise to additional physically sensible inclusive cross sections, which cure the IR divergences. Independent of which of the two scenarios hold true, we will see that the straightforward definition of colored cross section is not possible in general. In the following we will, in particular, describe why the second possibility will not work either. We will use the example of scalar QED-QCD theory (or equivalently the Yang-Mills model from chapter 6), in which we investigate the one loop cross section for $\psi_1^{\text{red}} \bar{\psi}_1^{\text{blue}} \rightarrow \psi_2^{\text{red}} \bar{\psi}_2^{\text{blue}}$ scattering at order $e^2 g_s^4$.

From the tree and loop amplitudes we can, similar to the QED case described above, construct the restricted $0 \rightarrow 0$ amplitude. Performing all additional cuts, we recognize the expected photon Bremsstrahlung and the inclusive gluon Bremsstrahlung, which we expect by using physically motivated inclusive gluon processes. The physically motivated inclusive processes are those which we get by substituting consecutively every external particle of color i by a particle of color j plus a gluon performing the ij -transition. But there are also some additional contributions, which do not fit into this picture. To see this, consider the glued $0 \rightarrow 0$ amplitude constructed in the following way

(D.3)

We can cut the scalar lines in such a way that the following diagrams emerge

(D.4)

where the internal lines in the box diagram are held fixed at color red. The problem is that there are no cuts in the restricted $0 \rightarrow 0$ amplitude, which can be related to these diagrams with other internal colors. But a physical definition of the cross section is only possible if we do not restrict internal d.o.f..

There are now two “physical” possibilities. Either we take the exceptional processes into account by including also all other d.o.f. contributing to this kind of scattering, or we leave them out. Both methods lead to a non-vanishing of the IR divergences, because of either too much IR contributions from the additional inclusive processes or too little.

This shows that there is no consistent way of performing color fixed processes in general. We also have the conjecture that by a systematic completion of the incomplete processes followed by including the new additional cuts we would arrive at a initial and final state summed process in the end, if we built up the formalism on cuts of $0 \rightarrow 0$ amplitudes.

For our work we can use a trick in order to arrive at sensible cross sections for colored external particles. This trick only works if we have massive scalars, such that it is sufficient to include only the degenerate final states. In chapter 6 we are interested in $\psi_1^{\text{red}} \bar{\psi}_1^{\text{blue}} \rightarrow \psi_2^{\text{red}} \bar{\psi}_2^{\text{blue}}$ scattering in the framework of scalar gravity Yang-Mills theory. The trick now is to notice that in our desired order the color fixed non-inclusive process is given by the same diagrams as the non-inclusive $\psi_1^{\text{red}} \bar{\psi}_1^{\text{blue}} \rightarrow \psi_2^{\text{col1}} \bar{\psi}_2^{\text{col2}}$ process with summed

final state colors. But now for the final state color summed process we can construct the non-restricted $2 \rightarrow 2$ glued amplitude, which we can cut and cure the soft IR divergences in a consistent way. Because of the massive matter fields we do not require to work within cuts of the $0 \rightarrow 0$ amplitude. This leads to a well defined and IR finite inclusive process related to our tree and loop amplitudes.

It has to be mentioned that we can not use this approach to calculate fixed color processes with massless matter fields. This is because massless matter fields lead to collinear divergences and therefore require a summation over degenerate states of the final **and** initial state. But when using a summed initial and final state, no color information can possibly be left over. This subject requires further investigations.

Appendix E

Localized wave packet states

This appendix is devoted to localized wave packet states. First, we discuss the mathematical description of wave packet states. Therefore we use wave packets with Gaussian spectra and give approximations to study their spacetime representation. Second, we will discuss the problem of performing wave packet scattering processes. In particular the projection of the final state on wave packets will require a different setup than used in conventional colliders.

E.1 Gaussian wave packets

Throughout this work we frequently use wave packets localized in space for describing our particle states. A general wave packet for a scalar particle is given by

$$f(x) := \int \widetilde{d^3k} \tilde{f}(\mathbf{k}) e^{-ikx}, \quad (\text{E.1})$$

where $\tilde{f}(\mathbf{k})$ denotes the spectrum, which has to be normalized by the condition $(f, f)_{\text{cov}} = \int \widetilde{d^3k} \tilde{f}^*(\mathbf{k}) \tilde{f}(\mathbf{k}) = 1$. Obviously $f(x)$ is a solution to the Klein-Gordon equation.

Since we perform integrations involving wave packets we decided to use the most simple localized states given by the family of wave packets with a Gaussian spectrum, i.e.

$$\left\{ \tilde{f}_{(q,\sigma,\chi)}(\mathbf{k}) : \tilde{f}_{(q,\sigma,\chi)}(\mathbf{k}) = N_{(q,\sigma)} (2\pi)^3 2k^0 \exp\left(-\frac{(\mathbf{k}-\mathbf{q})^2}{2\sigma^2}\right) e^{ik\chi}, \mathbf{q} \in \mathbb{R}^3, \sigma \in (0, \infty), \chi \in \mathbb{R}^4 \right\}, \quad (\text{E.2})$$

where $N_{(q,\sigma)}$ is a normalization constant, σ the width, \mathbf{q} the central momentum vector and $k^0 = \sqrt{\mathbf{k}^2 + m^2}$ is on-shell. Furthermore χ is the spacetime position of the tightest spacelike wave packet, as we will see below.

The only drawback of the family of Gaussian wave packets is that it is not closed under Lorentz boosts, since $\tilde{f}_{(q,\sigma,\chi)}(\mathbf{k})$ receives some non-Gaussianities when boosted. But this problem is not too dramatic, since performing a boost the wave packet will still remain localized and therefore is applicable to our problems. In the following we will choose the wave packets to be Gaussian in the frame where we naturally perform our calculations and interpret the results, e.g. the center of mass system.

Next we are interested in the explicit value of $N_{(q,\sigma)}$. This can be derived for massless particles by a short calculation as

$$N_{(q,\sigma)} = \left\{ (2\pi)^3 \pi e^{-\left(\frac{q}{\sigma}\right)^2} \sigma^3 q \left(2\frac{\sigma}{q} + e^{\left(\frac{q}{\sigma}\right)^2} \sqrt{\pi} \left(2 + \frac{\sigma^2}{q^2} \right) \text{erf} \left(\frac{q}{\sigma} \right) \right) \right\}^{-\frac{1}{2}}, \quad (\text{E.3})$$

where $\text{erf}(x) := \frac{2}{\sqrt{\pi}} \int_0^x dt \exp(-t^2)$ denotes the error function and $q = \|\mathbf{q}\|$ is the norm of the \mathbf{q} vector.

Furthermore we are interested in the covariant overlaps $(f_{(q_1, \sigma_1, \chi_1)}, f_{(q_2, \sigma_2, \chi_2)})_{\text{cov}}$ among two wave packets $f_{(q_1, \sigma_1, \chi_1)}$ and $f_{(q_2, \sigma_2, \chi_2)}$, since they will give upper bounds on the width σ . For our problem we will always prepare two incoming particles (and also sometimes two outgoing particles), which, in the center of mass system, will be given by $f_{(q, \sigma, \chi)}$ and $f_{(-q, \sigma, \chi)}$, respectively. Note that we have chosen the width σ and offset χ to be equal for both wave packets. The width is constrained by the condition that we want to interpret one of the particles as left moving and one as right moving, i.e. the overlap $(f_{(q, \sigma, \chi)}, f_{(-q, \sigma, \chi)})_{\text{cov}}$ must be sufficiently small.

The overlap can be derived by a short calculation as

$$(f_{(q, \sigma, \chi)}, f_{(-q, \sigma, \chi)})_{\text{cov}} = 2N_{(q, \sigma)}^2 (2\pi)^4 e^{-\left(\frac{q}{\sigma}\right)^2} \sigma^4. \quad (\text{E.4})$$

By inserting (E.3) it can be shown that this overlap only depends on the ratio $\frac{q}{\sigma}$ and becomes smaller than 0.01 if $\sigma \leq \frac{q}{2}$. Therefore we will always set $\sigma = \frac{q}{2}$, which on one hand reduces the number of parameters by one and on the other hand gives the broadest momentum space wave packet, i.e. the narrowest position space wave packet, at given q , which is exactly the wave packet we require in the following.

For massive particles we have calculated the normalization numerically and found out that it differs less than 1% for $\frac{m}{q} \leq \frac{1}{2}$. This means that we can apply the massless normalization (E.3) in the following, since m will always be much smaller than q .

This concludes the discussion of the Gaussian wave packets in momentum space. But we also have to investigate the wave packets in position space in order to understand their dynamics and learn to control them. For this purpose we will construct the spacetime representation of the wave packets using some approximations and investigate products of different wave packets, since they always occur in problems of dynamical localization using wave packets.

The position representation (E.1) involves an integral which we can not solve directly, because of the exponentiated non-polynomial dispersion relation $k^0 = \sqrt{\mathbf{k}^2 + m^2}$ of the particles. As an approximation we have performed the Taylor expansion of the energy around $\mathbf{k} = \mathbf{q}$, which is given by

$$k^0 = E_q + \frac{\mathbf{q}(\mathbf{k} - \mathbf{q})}{E_q} + \frac{1}{2E_q} \left((\mathbf{k} - \mathbf{q})^2 - \frac{(\mathbf{q}\mathbf{k} - \mathbf{q}\mathbf{q})^2}{E_q^2} \right) + E_q \mathcal{O} \left(\left(\frac{k}{q} \right)^3 \right), \quad (\text{E.5})$$

where $E_q = \sqrt{\mathbf{q}^2 + m^2}$ and $\mathcal{O} \left(\left(\frac{k}{q} \right)^3 \right)$ represents some corrections which become small in the limit $\|\mathbf{k}\| \ll \|\mathbf{q}\|$. The zeroth order just leads to a phase, the first order fixes the velocity of the wave and the second order describes dispersion.

The position representation of the wave packet using the first order approximation is given by

$$f_{(q, \sigma, \chi)}(x) = \sqrt{2\pi}^3 \sigma^3 N_{(q, \sigma)} e^{-iq(x-\chi)} \exp \left(-\frac{\sigma^2}{2} \vec{\xi}^2 \right), \quad (\text{E.6})$$

where $\vec{\xi} := \mathbf{x} - \vec{\chi} - \frac{\mathbf{q}}{E_q}(t - \chi^0)$ is the time dependent spatial center of the wave packet. This wave packet describes a dispersion-free propagating Gaussian shape of width $1/\sigma$.

In second order approximation we get

$$f_{(q, \sigma, \chi)}(x) = \frac{\sqrt{2\pi}^3 N_{(q, \sigma)}}{\alpha \sqrt{\alpha - i(t - \chi^0) \frac{\mathbf{q}^2}{E_q^3}}} e^{-iq(x-\chi)} \exp \left(-\frac{\vec{\xi}^2}{2\alpha} - \frac{i(t - \chi^0)(\mathbf{q}\vec{\xi})^2}{2\alpha(\alpha E_q^3 - i(t - \chi^0)\mathbf{q}^2)} \right), \quad (\text{E.7})$$

where $\alpha := \frac{1}{\sigma^2} + i \frac{(t - \chi^0)}{E_q}$. This wave packet describes a propagating and dispersing Gaussian shape with a time dependent width. This time dependent width is given by

$$\sigma_{\perp}(t) = \frac{\sqrt{1 + \frac{\sigma^4 (t - \chi^0)^2}{E_q^2}}}{\sigma} \quad (\text{E.8})$$

for directions perpendicular to \mathbf{q} and

$$\sigma_{\parallel}(t) = \sigma_{\perp}(t) \left(1 + \frac{\mathbf{q}^2(t - \chi^0)^2(2E_q^2 - \mathbf{q}^2)}{\frac{E_q^6}{\sigma^4} + E_q^4(t - \chi^0)^2 + \mathbf{q}^4(t - \chi^0)^2} \right)^{-\frac{1}{2}} \quad (\text{E.9})$$

for the direction parallel to \mathbf{q} . It can be shown that this packet has its smallest width at $t = \chi^0$ and $\sigma_{\perp}(t) \geq \sigma_{\parallel}(t)$ because of length contraction. This shows that one can control the spacetime position at which the smallest width is reached by the parameters χ . This is the key to control the wave packets.

Next we are interested in products of crossing wave packets, since such expressions will always occur in problems where one performs dynamical localization using wave packets. We will investigate first and second order wave packets.

Using two first order wave packets (E.6) with $\|\mathbf{q}_1\| = \|\mathbf{q}_2\| = q$ crossing w.l.o.g. at $\chi = 0$, and using the relation $\sigma_1 = \sigma_2 = \frac{q}{2}$ for both of them, their product is given by

$$f_{(q_1, \frac{q}{2}, 0)} f_{(q_2, \frac{q}{2}, 0)} = (2\pi)^3 \left(\frac{q}{2}\right)^6 N_{(q, \frac{q}{2})}^2 e^{-2iE_q t} \exp\left(-\frac{q^2}{4}(\mathbf{x}^2 + \frac{q^2}{E_q^2}t^2)\right) \exp\left(\frac{q^2 t}{4E_q} \mathbf{x}(\mathbf{q}_1 + \mathbf{q}_2)\right), \quad (\text{E.10})$$

which is a nonsymmetric localized function on spacetime centered at $x = \chi = 0$ with a width proportional to q . For the special case of anti-parallel moving particles, i.e. $\mathbf{q}_2 = -\mathbf{q}_1$, the overlap is a spacelike symmetric Gaussian function with spatial width $\frac{\sqrt{2}}{q}$ and timelike width $\frac{\sqrt{2}E_q}{q^2}$. For sufficiently fast particles we have $E_q \approx q$, this means that the spatial and timelike width are nearly equal.

Products of crossing second order wave packets have a similar shape for the spatial coordinates with the time dependent width and non-Gaussian corrections to the time direction. We have investigated the product of two second order wave packets using *Mathematica* and found out that for sufficiently fast particles, i.e. $q \approx E_q$, the overlapping region does not differ too much from the first order result. In particular first and second order overlaps have nearly the same width. In this work we will use the compact result for the first order wave packets (E.10) in order to estimate the spacetime resolution due to two crossing wave packets.

E.2 Scattering of wave packets

Usual scattering experiments are performed by producing an initial state, which is approximately a four-momentum eigenstate. This state is transformed by the interactions into the outgoing state. Finally, the outgoing state is projected onto four-momentum eigenstates again by a detector.

The wave packets required for our kind of processes are widely spread over the momentum space and therefore can not be prepared and detected with today's colliders. The preparation and detection of these states is very important in order to resolve the positions of the correlation function.

The preparation of localized wave packet states can for example be performed by semiclassical acceleration in electric fields. We could first prepare some localized state in a trap and then accelerate it with electric fields. Since the electric force, $\mathbf{F} = e\mathbf{E}$, does not depend on the momentum of the particle, it accelerates a charged particle without projecting onto momentum eigenstates. As a note, this acceleration has to be performed in a linear accelerator, since ring accelerators would project out specific momentum eigenstates by the magnetic field, which forces the beam onto orbit motion.

The second step is to find a device projecting the final state onto wave packet states. This can not be done in conventional colliders too, since these resolve the momentum of the particle. This would destroy the information about locality in our case. From a mathematical point of view, we would have to find measurement devices which correspond to the projection operators $P_{\psi} = |\psi\rangle\langle\psi|$ on wave packet states $|\psi\rangle$. We can not give an experimental realization of such a device in this work and leave it as an open problem for e.g. experimentalists.

To conclude this section we explain why we can not extract our desired information by projecting the final state onto momentum eigenstates. Assume the matrix element of some Hermitian operator O in some desired states $|a\rangle$ and $|b\rangle$. We are interested in the square of the matrix element $|\langle b|O|a\rangle|^2 =$

$\langle a|O|b\rangle\langle b|O|a\rangle$. Now we insert the representation of the identity operator in terms of eigenstates of some operator which we know how to measure, e.g. the momentum operator. The result is

$$|\langle b|O|a\rangle|^2 = \sum_{n,n'} \langle a|O|n\rangle\langle n|b\rangle\langle b|n'\rangle\langle n'|O|a\rangle . \quad (\text{E.11})$$

We obtain that we can not extract the desired information about $|\langle b|O|a\rangle|^2$ by measuring the projected squared matrix elements $|\langle n|O|a\rangle|^2$, if the coefficient $\langle n|b\rangle\langle b|n'\rangle \neq \delta_{nn'}$. This shows that we really require a device projecting onto the wave packet states.

As a final remark, the purpose of our work is to perform a Gedankenexperiment in order to understand dynamical localization. We do not intend to describe the experimental realization of these Gedankenexperiments.

Appendix F

Implementation of gravitons in FeynArts and FormCalc

In order to perform our calculations using FeynArts and FormCalc we had to include the graviton field into the codes, since their field content is originally limited to scalars, fermions and vector bosons. In this chapter we briefly summarize which modifications have been performed in which parts of the code. The reason why we give this summary is to pass on the knowledge we have, such that it can be used by others who want to perform calculations including gravitons using FeynArts and FormCalc.

We have performed our changes using the versions FeynArts 3.2. and FormCalc 5.3..

Modifications in FeynArts

The first file we had to modify was the main file *FeynArts.m*. The line 907 which reads

```
P$Generic = F|S|V|U|SV
```

was extended to

```
P$Generic = F|S|V|U|SV|T
```

in order to define a generic field called *T* for tensor field.

The propagator, vertices and polarization of the new tensor field *T* can be defined in an extended generic model file, which we call *Gravity.gen*. This file contains the following source code

```
ReadModelFile["Lorentz.gen"]
```

```
KinematicIndices[ T ] = {Lorentz, Lorentz}
```

```
M$GenericPropagators = Flatten @ {M$GenericPropagators,  
  AnalyticalPropagator[External][ s1 T[j1], mom, {li1, li2} ] ==  
    PolarizationTensor[T[j1], mom, li1, li2],  
  
  AnalyticalPropagator[Internal][ s1 T[j1], mom, {li1, li2} -> {li3, li4} ] ==  
    I PropagatorDenominator[mom, Mass[T[j1]] ] *  
    (MetricTensor[li1, li3] MetricTensor[li2, li4] +  
     MetricTensor[li2, li3] MetricTensor[li1, li4] -  
     MetricTensor[li1, li2] MetricTensor[li3, li4])/2  
}
```

```
M$GenericCouplings = Flatten @ {
```



```

DeleteCases[M$GenericCouplings, _[_S, _S, _S] == _],

(* S-S-S: *)

AnalyticalCoupling[ s1 S[j1, mom1], s2 S[j2, mom2], s3 S[j3, mom3] ] ==
G[1][s1 S[j1], s2 S[j2], s3 S[j3]] .
{ 1,
  ScalarProduct[mom1, mom2],
  ScalarProduct[mom2, mom3],
  ScalarProduct[mom1, mom3],
  ScalarProduct[mom1, mom1],
  ScalarProduct[mom2, mom2],
  ScalarProduct[mom3, mom3]},

(* T-S-S *)

AnalyticalCoupling[ s1 T[j1, mom1, {li1, li2}], s2 S[j2, mom2],
s3 S[j3, mom3] ] ==
G[1][s1 T[j1], s2 S[j2], s3 S[j3]] .
{ FourVector[mom2, li1] FourVector[mom3, li2] +
  FourVector[mom2, li2] FourVector[mom3, li1] -
  MetricTensor[li1, li2] ScalarProduct[mom2, mom3],
  -MetricTensor[li1, li2] ScalarProduct[mom1, mom1]
+ FourVector[mom1, li1] FourVector[mom1, li2],
  MetricTensor[li1, li2] },

(* T-S-S-S *)

AnalyticalCoupling[ s1 T[j1, mom1, {li1, li2}], s2 S[j2, mom2],
s3 S[j3, mom3], s4 S[j4, mom4] ] ==
G[1][s1 T[j1], s2 S[j2], s3 S[j3], s4 S[j4]] .
{ MetricTensor[li1, li2] } ,

(* T-V-V *)

AnalyticalCoupling[ s1 T[j1, mom1, {li1, li2}], s2 V[j2, mom2, {li3}],
s3 V[j3, mom3, {li4}] ] ==
G[1][s1 T[j1], s2 V[j2], s3 V[j3]] .
{- ScalarProduct[mom2, mom3] (MetricTensor[li1, li3] MetricTensor[li2, li4]
+ MetricTensor[li1, li4] MetricTensor[li2, li3]
- MetricTensor[li1, li2] MetricTensor[li3, li4])
- FourVector[mom2, li4] FourVector[mom3, li3] MetricTensor[li1, li2]
- (FourVector[mom2, li1] FourVector[mom3, li2]
+ FourVector[mom2, li2] FourVector[mom3, li1]) MetricTensor[li3, li4]
+ FourVector[mom2, li1] FourVector[mom3, li3] MetricTensor[li2, li4]
+ FourVector[mom2, li2] FourVector[mom3, li3] MetricTensor[li1, li4]
+ FourVector[mom2, li4] FourVector[mom3, li1] MetricTensor[li2, li3]
+ FourVector[mom2, li4] FourVector[mom3, li2] MetricTensor[li1, li3],
  MetricTensor[li1, li2] (FourVector[mom2, li3] FourVector[mom1, li4]
+ FourVector[mom2, li3] FourVector[mom3, li4]
+ FourVector[mom1, li3] FourVector[mom3, li4])
+ MetricTensor[li1, li4] FourVector[mom2, li2] FourVector[mom2, li3]}

```

```

+ MetricTensor[li1,li3] FourVector[mom3,li2] FourVector[mom3,li4]
+ MetricTensor[li2,li4] FourVector[mom2,li1] FourVector[mom2,li3]
+ MetricTensor[li2,li3] FourVector[mom3,li4] FourVector[mom3,li1] },

```

```
(* T-S-S-V *)
```

```

AnalyticalCoupling[ s1 T[j1, mom1, {li1, li2}], s2 V[j2, mom2, {li3}],
s3 S[j3, mom3], s4 S[j4, mom4] ] ==
G[1][s1 T[j1], s2 V[j2], s3 S[j3], s4 S[j4]] .
{ FourVector[mom3-mom4, li3] MetricTensor[li1,li2]
- FourVector[mom3-mom4,li2] MetricTensor[li1,li3]
-FourVector[mom3-mom4,li1] MetricTensor[li2,li3]}
}

M$LastGenericRules = Flatten @ {M$LastGenericRules,
PolarizationTensor[p_, __. mom:FourMomentum[Outgoing, _], li__] :=
Conjugate[PolarizationVector][p, mom, li]
}

```

In this file we have defined the required interaction vertices for graviton couplings to scalars and vectors.

Together with this generic model file we have used several specific model files for our different models. For example the source code for the $\psi^2\phi$ model is given by

```

M$ClassesDescription = {
S[1] == {
SelfConjugate -> True,
Mass -> Mpsi,
PropagatorLabel -> "psi1",
PropagatorType -> Straight,
PropagatorArrow -> None },
S[2] == {
SelfConjugate -> True,
Mass -> Mpsi,
PropagatorLabel -> "psi2",
PropagatorType -> Straight,
PropagatorArrow -> None },
S[3] == {
SelfConjugate -> True,
Mass -> Mpsi,
PropagatorLabel -> "psi3",
PropagatorType -> Straight,
PropagatorArrow -> None },
S[4] == {
SelfConjugate -> True,
Mass -> Mpsi,
PropagatorLabel -> "psi4",
PropagatorType -> Straight,
PropagatorArrow -> None },
S[5] == {
SelfConjugate -> True,
Mass -> Mphi,
PropagatorLabel -> "phi",
PropagatorType -> ScalarDash,
PropagatorArrow -> None },
T[1] == {

```

```

    SelfConjugate -> True,
    Mass -> 0,
    PropagatorLabel -> "g",
    PropagatorType -> Sine,
    PropagatorArrow -> None }
}

M$CouplingMatrices = {
  (* T-S-S *)
  C[ T[1], S[1], S[1] ] == I kap/2 {{1}, {2 bbb}, {-Mpsi^2}},
  C[ T[1], S[2], S[2] ] == I kap/2 {{1}, {2 bbb}, {-Mpsi^2}},
  C[ T[1], S[3], S[3] ] == I kap/2 {{1}, {2 bbb}, {-Mpsi^2}},
  C[ T[1], S[4], S[4] ] == I kap/2 {{1}, {2 bbb}, {-Mpsi^2}},
  C[ T[1], S[5], S[5] ] == I kap/2 {{1}, {2 aaa}, {-Mphi^2}},

  (* S-S-S *)
  C[ S[1], S[2], S[5] ] == I lam {{1}, {-kap^2 ccc }, {0}
    , {0}, {-kap^2 ddd/2}, {-kap^2 ddd/2}, {-kap^2 eee}},
  C[ S[3], S[4], S[5] ] == I lam {{1}, {-kap^2 ccc }, {0}
    , {0}, {-kap^2 ddd/2}, {-kap^2 ddd/2}, {-kap^2 eee}},

  (* T-S-S-S *)
  C[ T[1], S[1], S[2], S[5] ] == I kap/2 lam {{1}},
  C[ T[1], S[3], S[4], S[5] ] == I kap/2 lam {{1}}
}

M$LastModelRules = {}

```

These (generic) model files now can be used in order to deal with internal gravitons. External gravitons require some changes in FormCalc, to be discussed now.

Modifications in FormCalc

The modifications in *FormCalc.m* are much more complicated than these in FeynArts, so that a complete listing of all modifications is not sensible. The reason for this is that FormCalc uses the symbolic programming language *form*, which requires a precise declaration of the variables and therefore has problems with the new variable *PolarizationTensor*. The main task was to declare the new variable and perform the necessary manipulations, like for example polarization sums over graviton polarizations. The source code of *FormCalc.m* has over 4000 lines and hence it was too for us to find the required sections to be modified. Therefore we convinced its inventor Thomas Hahn to help us to modify FormCalc. A copy of the modified version of FormCalc is made available in the internet [26] as download.

The second file to be modified was the file *PolarizationSum.frm*, where we have defined the sum over graviton polarizations.

With these modifications we could use FeynArts and FormCalc in order to calculate amplitudes including internal as well as external gravitons.

Bibliography

- [1] S. B. Giddings, D. Marolf, and J. B. Hartle, “Observables in effective gravity,” *Phys. Rev.* **D74** (2006) 064018, [hep-th/0512200](#).
- [2] T. Thiemann, “Introduction to modern canonical quantum general relativity,” [gr-qc/0110034](#).
- [3] T. Hahn and J. I. Illana, “Excursions into FeynArts and FormCalc,” *Nucl. Phys. Proc. Suppl.* **160** (2006) 101–105, [hep-ph/0607049](#).
- [4] M. Nakahara, “Geometry, topology and physics,”. Taylor & Francis (2003) 573 p.
- [5] P. Dirac, “Lectures on Quantum Mechanics,”. Dover Publications Inc. (2001) 96 p.
- [6] M. Henneaux and C. Teitelboim, “Quantization of gauge systems,”. Princeton Univ. Pr. (1992) 520 p.
- [7] T. Ohl, “Die BRS-Invarianz in der kanonische Quantisierung von Eichtheorien,”. Diploma thesis, (1987) Technische Hochschule Darmstadt.
- [8] N. Nakanishi and I. Ojima, “Covariant operator formalism of gauge theories and quantum gravity,” *World Sci. Lect. Notes Phys.* **27** (1990) 1–434.
- [9] A. Ashtekar and R. S. Tate, “An Algebraic extension of Dirac quantization: Examples,” *J. Math. Phys.* **35** (1994) 6434–6470, [gr-qc/9405073](#).
- [10] S. Waldmann, “Deformation quantization: Observable algebras, states and representation theory,” [hep-th/0303080](#).
- [11] M. Maggiore, “A Modern Introduction to Quantum Field Theory,”. Oxford Univ. Pr. (2005) 310 p.
- [12] T. Kugo and I. Ojima, “Local Covariant Operator Formalism of Nonabelian Gauge Theories and Quark Confinement Problem,” *Prog. Theor. Phys. Suppl.* **66** (1979) 1.
- [13] S. Weinberg, “Quantum contributions to cosmological correlations,” *Phys. Rev.* **D72** (2005) 043514, [hep-th/0506236](#).
- [14] C. P. Burgess, “Quantum gravity in everyday life: General relativity as an effective field theory,” *Living Rev. Rel.* **7** (2004) 5, [gr-qc/0311082](#).
- [15] J. F. Donoghue, “General relativity as an effective field theory: The leading quantum corrections,” *Phys. Rev.* **D50** (1994) 3874–3888, [gr-qc/9405057](#).
- [16] F. A. Berends and R. Gastmans, “On the High-Energy Behavior in Quantum Gravity,” *Nucl. Phys.* **B88** (1975) 99.
- [17] G. ’t Hooft and M. J. G. Veltman, “One loop divergencies in the theory of gravitation,” *Annales Poincare Phys. Theor.* **A20** (1974) 69–94.
- [18] M. Henneaux and C. Teitelboim, “BRST cohomology in classical mechanics,” *Commun. Math. Phys.* **115** (1988) 213–230.

- [19] H. van Dam and M. J. G. Veltman, “Massive and massless Yang-Mills and gravitational fields,” *Nucl. Phys.* **B22** (1970) 397–411.
- [20] T. D. Lee and M. Nauenberg, “Degenerate Systems and Mass Singularities,” *Phys. Rev.* **133** (1964) B1549–B1562.
- [21] T. Kinoshita, “Mass singularities of Feynman amplitudes,” *J. Math. Phys.* **3** (1962) 650–677.
- [22] T. Hahn, “The CUBA library,” *Nucl. Instrum. Meth.* **A559** (2006) 273–277, [hep-ph/0509016](https://arxiv.org/abs/hep-ph/0509016).
- [23] S. Weinberg, “Phenomenological Lagrangians,” *Physica* **A96** (1979) 327.
- [24] R. Kleiss and W. J. Stirling, “Massive multiplicities and Monte Carlo,” *Nucl. Phys.* **B385** (1992) 413–432.
- [25] B. de Wit and R. Gastmans, “On the induced cosmological term in quantum gravity,” *Nucl. Phys.* **B128** (1977) 294.
- [26] <http://theorie.physik.uni-wuerzburg.de/~aschenkel/FormCalc-5.3.tar.gz>.

Acknowledgements

The author wants to thank the following persons for supporting him during the university education and diploma thesis.

- PD Dr. Thorsten Ohl for the opportunity to write my thesis in his group and the various discussions.
- Prof. Dr. Reinhold Rückl for fascinating me for quantum physics during his lectures on quantum mechanics and quantum field theory.
- Dr. Thomas Hahn for helping me to modify FeynArts and FormCalc.
- Tim Koslowski for various mathematical discussions.
- Laslo Reichert and Julian Adamek for several professional and also personal discussions.
- Julian Adamek for a careful reading of this work.
- And last but not least my family for supporting me during my studies.

Erklärung

Hiermit erkläre ich, dass ich die vorliegende Arbeit selbständig verfasst und keine anderen als die angegebenen Hilfsmittel verwendet habe.

Würzburg, den 21. Mai 2008

Alexander Schenkel